An Investigation into Adopting Different Piling Systems for Integral Abutment Bridges

by

Jitesh Harripershad

Submitted in partial fulfilment of the academic requirements of

Master of Science in Civil Engineering

School of Engineering

College of Agriculture, Engineering and Science

University of KwaZulu-Natal

Howard Campus

South Africa

March 2016

PREFACE

The research contained in this dissertation was completed by the candidate while based in the discipline of Civil Engineering, School of Engineering and of the College of Agriculture, Engineering and Science, University of KwaZulu-Natal, Howard Campus, South Africa. The research was financially supported by the student and eThekwini Municipality.

The contents of this work have not been submitted in any form to another university and, except where the work of others is acknowledged in the text, the results reported are due to investigations by the candidate.

_____

Signed: Supervisor - Mrs Christina McLeod

Date: 24 March 2016

DECLARATION

I, Jitesh Harripershad, declare that:

(i) the research reported in this dissertation, except where otherwise indicated or acknowledged, is my original work;

(ii) this dissertation has not been submitted in full or in part for any degree or examination to any other university;

(iii) this dissertation does not contain other persons' data, pictures, graphs or other information, unless specifically acknowledged as being sourced from other persons;

(iv) this dissertation does not contain other persons' writing, unless specifically acknowledged as being sourced from other researchers. Where other written sources have been quoted, then:

a) their words have been re-written but the general information attributed to them has been referenced;

b) where their exact words have been used, their writing has been placed inside quotation marks, and referenced;

(v) where I have used material for which publications followed, I have indicated in detail my role in the work;

(vi) this dissertation is primarily a collection of material, prepared by myself, published as journal articles or presented as a poster and oral presentations at conferences. In some cases, additional material has been included;

(vii) this dissertation does not contain text, graphics or tables copied and pasted from the Internet, unless specifically acknowledged, and the source being detailed in the dissertation and in the References sections.

_____

Signed: Mr Jitesh Harripershad

Date: 24 March 2016

ABSTRACT

In recent years the use of integral abutment bridges has become increasingly popular, globally. These bridges have many advantages because the super-structure and sub-structure are monolithic in nature, no bearings and expansion joints are required and maintenance is minimal. However these bridges are uncommon in South Africa. The behavioural performance of this type of integral structure is influenced by the movement requirements of the foundations and steel H-piles are generally preferred but H-piles are very rarely used in South Africa due to the high costs. This research work investigates the behaviour and possibility of adopting other commonly used types of piles in South Africa for integral abutment bridges instead of steel H-piles. The research also provides commonly used techniques that are used in practice such as pile sleeving which inherently increases the slenderness of the pile, so the pile can absorb the deck movements. Some of the common challenges regarding integral bridges are considered and appropriate concepts are also presented. The purpose of the research work is also to enlighten the practical bridge designer about integral abutment bridges so important aspects are considered in the design phase. The investigation of different pile types proposed for the integral bridge structure was based on empirical formulae and a desktop study was done. The outcome from the work recommends that steel H-piles on the weaker axis are a superior choice of pile that should be used. Other pile types are also possible such as precast piles, however the designer needs to ensure they perform well under cyclic loading. The work also recommends that a pile sleeve or similar of over 3m long is beneficial to reduce the bending moment and shear force at the point of virtual fixity of the pile. Integral abutment bridges have numerous advantages over conventional bridges, however a carefully thought-out concept of the integral structure must be considered. One important aspect is the length of the integral bridge; to ensure that the structure performs well over its anticipated life span, integral bridges should only be used for short to medium spans.

ACKNOWLEDGMENTS

I would like to thank God, Almighty for blessing me with the strength, courage, wisdom, good luck and guidance for helping me successfully complete my MSc dissertation and MSc course work modules. Indeed, “God is Great”!

My sincere appreciation and thanks to my supervisor, Mrs Christina McLeod for the assistance and positive motivation throughout this research. My gratitude is also expressed to Mr Malcolm Jaros for his expert guidance and teachings provided in the field of foundation engineering.

A big thank you to one of the countries bridge sages, Mr Peter G. Fenton (from eThekwini Municipality) for also supervising, checking, brainstorming and helping me over the many challenges faced in this research project.

I would like to express my sincere gratitude to Dan and Usha Harripershad, my father and mother, for always providing me with the very best in my life, the loving support and the continuous encouragement to achieve the best.
Thank you to my sister, Natisha & brother, Vikash and my friends for your inspiration and support.

Thank you to Luke Jabulani Reid (from eThekwini Municipality) for helping with the steel calculations, checking of the final draft, providing constructive ideas and valuable information.

Thank you to the following helpful individuals for providing me with their time to interview them and also for providing me with valuable information that was used in my research project:

- Mr Bruce Durrow (Royal Haskoning DHV, Pietermaritzburg)
- Mr Darryl Klassen (Royal Haskoning DHV, Pietermaritzburg)
- Mr Gons Poonan (BPH Engineers, Durban)
- Mr Pieter Boorsma (BPH Engineers, Durban)
- Ms Sarah Skorpen (University of Pretoria)

I acknowledge eThekwini Municipality for the partial funding for my MSc post-graduate studies.

TABLE OF CONTENTS

LIST OF FIGURES

LIST OF TABLES

CHAPTER 1

1 INTRODUCTION

1.1 General Overview

Integral bridges are generally structures where the superstructure and substructure are monolithic in nature. These bridges could be single or multiple spans with a continuous concrete deck and approach slabs, integral with the abutments which are supported on flexible foundations (Husain & Bagnariol 1996). Bridges that were constructed in the 1960s and 1970s in the United Kingdom were articulated with expansion joints and bearings to separate the superstructure from the substructure and the surrounding soil interaction, which is also generally the norm for bridge construction in South Africa. However in the 1980s and 1990s, most of these required maintenance due to serviceability problems associated with the joints. As a result of the high rehabilitation costs, the form of integral bridges became more popular and are likely to become much more widespread in the future (O'Brien & Keogh 1999, p.121).

1.2 Hypothesis Statement

A wider selection of pile types could be adopted for integral abutment bridges.

1.3 Aims and Objectives

The concept of integral bridges is well established and is very popular in certain countries, however the use of integral bridges is almost non-existent in South Africa. The probable reason for this could be due to the issues surrounding the soil-structure interaction. In addition, the piling system generally adopted for the integral bridge abutments in other countries are driven H-section steel piles whilst in South Africa this is not a commonly used pile. Owing to this limitation, it is proposed to investigate various possibilities for the foundations for this type of structure. In particular, the foundation type to be investigated will be various pile types.

The following are the key objectives:

I. Understand the typical behavioural performance of various types of piles used in integral bridges, with particular focus on the abutments.
II. Investigate the varying of the piles' effective height.
III. Understand the benefits of isolating the top few meters of the piles and predicting the most appropriate isolation length.

1.4 Layout of Thesis

Chapter 1: Provides a brief introduction to integral bridges and highlights the objective of this study. The focus is on pile performance of integral bridge abutments.

Chapter 2: Provides a literature review of some of the important aspects of integral bridges that are related to this research study.

Chapter 3: This chapter discusses the issues surrounding integral abutment bridges and is an extension of the literature review in Chapter 2. Different concepts and various commonly implemented solutions from practice are presented.

Chapter 4: The method for investigation is discussed in order to obtain the results and outcomes. All assumptions are noted.

Chapter 5: Gives the results and discussion. Comparisons are made with the literature review.

Chapter 6: Concludes the dissertation and summarises some of the critical aspects concerning the piling for integral abutment bridges. This chapter also provides recommendations on issues that require further research work to be carried out.

CHAPTER 2

2 LITERATURE REVIEW

2.1 Introduction

This chapter reviews some of the fundamental concepts and principles regarding integral bridges. Integral bridges have a number of advantages as well as some disadvantages. Bridge designers should generally consider three important aspects relating to the design of a new bridge: it should be safe (fit for the intended purpose), economically viable and aesthetically pleasing (Arsoy et al 1999).

It is important to note that the application of integral bridges in South Africa is very rare thus the research and literature regarding integral bridges in South Africa is limited. The literature reported in this chapter is mostly based on research work from the United States as they are well advanced in this field and were perhaps the first to promote the use of integral bridges.

Most of the bridges constructed before the 1960s in the United States included expansion joints at piers and the abutments. The expansion joints did not behave as well as anticipated thus considerable maintenance was required and ultimately undermined the economical operation of these structures. Malfunctioning of expansion joints led to safety concerns and thus a widespread interest in the construction of jointless bridges in the early 1960s (Arsoy et al 1999).

2.1.1 Integral Bridges

> *"Building in piers and abutments and eliminating bearings and expansion joints should be a major aim of the bridge designer"*
>
> (Benaim 2008, p227)

Research work carried out by Wolde-Tinsea and Klinger (1987, cited in Arsoy et al. 1999) classified jointless bridges into four basic categories;

- flexible arch bridges,
- slip joint bridges,
- abutmentless bridges, and
- Integral bridges.

In the United States integral bridges are defined as bridges with short stub-type abutments rigidly fixed to the bridge deck without any joints. The abutments and superstructure act as a single structural unit and the abutments are founded on a single row of piles (Arsoy et al 1999).

Integral bridge structures are concrete or composite structures such that the superstructure and substructure are monolithic or "integral" in nature thus providing a structure acting as one unit. Integral bridges are also referred to as jointless bridges or frame bridges. These type of bridges generally don't have bearings and expansion joints unless they are semi-integral bridges. These types of bridge are not new since masonry arches are a typical early example of integral structures (Concrete Bridge Development Group, 2013).

Semi-integral bridges generally have sliding bearings but no expansion joints (Sisk & Terzaghi 2009). Semi-integral abutment bridges are similar to integral abutment bridges as the deck is continuous with the approach slabs and expansion joints are eliminated at the end of the deck however, semi-integral bridges differ from integral bridges because the superstructure is not continuous with the abutments. Semi-integral abutment bridges allow for the use of bearings to allow for horizontal movements between deck and superstructure. This concept is adopted in circumstances not suitable for fully integral abutments (Husain & Bagnariol 1999).

Benaim (2008) states that in an integral abutment bridge, the abutment structure behaves more like a pier when it is fixed to the superstructure. This form eliminates costly mechanical expansion joints and greatly simplifies the abutment structure. The abutment either rocks or slides back and forth to accommodate thermal effects on the bridge thus settlement of the backfill behind the abutment may lead to slight deformations at the road surface. This matter is overcome either by bridging the deformed area with a short transition (approach) slab or regular maintenance of the road surface. The approach slab is generally fixed to the abutment and follows its movement by sliding on a prepared substrate (Benaim, 2008).

The design of integral abutment bridges aims to ensure that the abutments (including the piles) have sufficient flexibility to absorb thermal movements of the bridge superstructure but should also have adequate stiffness to resist secondary forces on the deck such as braking and skidding (Card & Carder 1993). Figure 1 shown below illustrates the basic components of an integral abutment bridge, essentially there is the bridge and the approach arrangement.

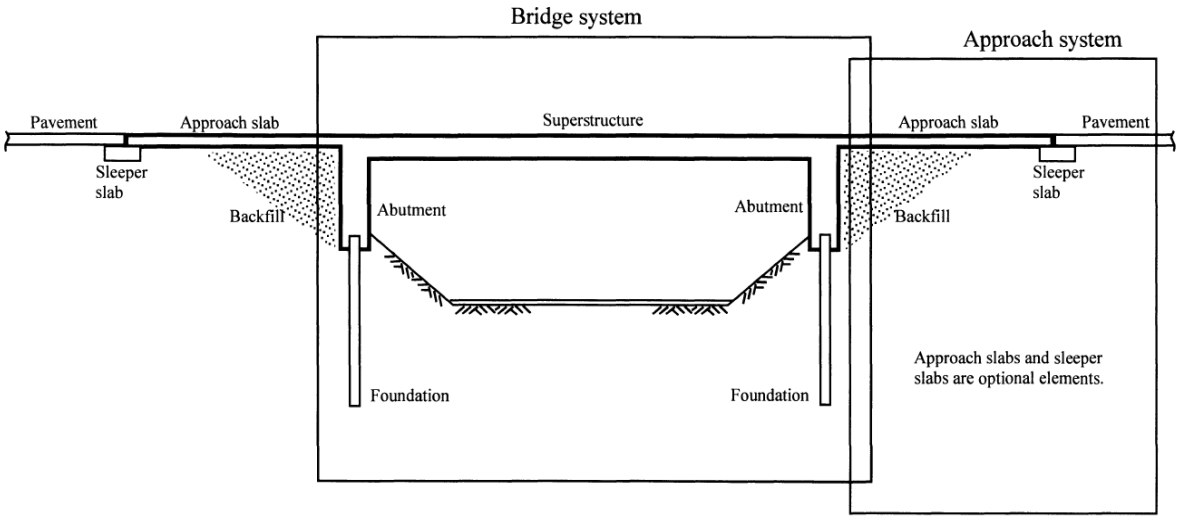

Figure 1: General arrangement of a typical integral abutment bridge (Arsoy et al 1999)

2.1.2 The Advantages of Integral Bridges

Some of the advantages of integral bridges are listed below as discussed by Arsoy et al (1999);

- Construction costs are lowered due to the removal of expansion joints.
- There are lower maintenance costs since in conventional bridges most of the maintenance costs arise from the repair or in some cases replacement of joints.
- Integral bridges provide enhanced seismic performance.
- A smaller number of piles are required for the foundation supports and generally battered piles are not required.
- Construction is simple.
- Due to the fixity of the superstructure and abutment, greater end span ratios are achievable.
- Integral bridge deck surfaces are smooth and uninterrupted thus improving the vehicular riding quality.
- The continuity of the integral bridge improves the aesthetic appearance however this is subjective and depends on the engineer's perspective.

The cost of an expansion joint in South Africa is dependent on the anticipated movement of the bridge deck. An approximate cost for an expansion joint ranges from R 2,500-00 /m to R 15,500-00 /m, the lower cost is for joints such as asphalt plug joints and the higher cost is indicative of proprietary joints such as armoured nosing. This cost covers the supply of material and initial installation, the joints are generally installed by approved specialist subcontractors with Agrément certification. Presently there are a limited number of specialists with this certification in South Africa. Maintenance on bridges depends on the bridge authority but generally after 5 years bridge inspections are done. One of the highest costs contributing to maintenance of joints on bridges is lane closures. This depends on the road authority and as an indicative value a lane closure could cost from R 1,500-00/lane/hour to R 2,800-00/lane/hour.

Burke (2009, p. 4-13) describes how in certain geographical regions which experience very low seasonal temperatures and an abundance of snow and freezing rain, the pavements are kept dry throughout the winter season by using de-icing chemicals. These chemicals have a significantly adverse effect on the durability and integrity on the structures constructed with movable bridge deck joints. Some of the joints such as open joints, sliding plate joints and finger joints allow drainage from the road surface which is contaminated with de-icing chemicals to infiltrate below the roadway surfaces and wash over supporting beams, bearings and bridge seats. This previously resulted in such severe corrosion and wearing that some bridges collapsed while others have been closed to traffic to prevent collapse and some have remained in service but required almost continuous maintenance to remedy the deck drainage impacts. Due to the high maintenance costs, many road authorities strongly motivate for the use of integral bridge structures.

2.1.3 The Problems and Challenges

Some aspects regarding limitations and challenges with regard to design and construction of integral bridges are discussed below.

- One of the most important issues regarding integral bridges, which has attracted a lot of attention, is related to the analysis of the soil-structure interaction of the abutment walls and the supporting piles (David & Forth 2013).
- According to Sisk & Terzaghi (2009), integral bridges present challenges regarding load distribution calculations because the superstructure (deck), substructure (piers and abutments), foundations (piles), embankments and soil must be considered as a single compliant system. Considering the supports behind abutments and adjacent foundation piles as a series of spring supports is a common modelling method. However the difficulty arises in deriving appropriate spring constants.
- Integral bridges are generally adopted for short to medium span structures. Bridge overall lengths from 100m to 150m are generally considered for integral abutment design (Husain & Bagnariol 1996).
- The types of superstructure to be adopted with an integral abutment are limited and generally includes a design of (Husain & Bagnariol 1996);
    i. Steel girders with a concrete slab deck
    ii. Pre-tensioned concrete girders with a concrete slab deck
    iii. Prestressed box girders with concrete deck
    iv. Concrete slab bridge decks
- Cast-in-place, post-tensioned deck type structures are not common with integral abutments due to the movements resulting from (Husain & Bagnariol 1996);
    i. Creep,
    ii. Shrinkage
    iii. Elastic shortening due to prestress forces
- Skew decks are permitted but it is advised that a skewness of 30^{o} is not exceeded due to the complexities created in the analysis especially in the foundation piles (Burke 2009).
- Research has shown that various bridge authorities from different countries have self-imposed limitations on the lengths of integral bridges and heights of abutments. This is based on their own experience with the performance of their structures and lessons learned (Tlustochowicz 2005). It is recommended that abutment heights and abutment lengths are limited to reduce the soil pressures that are generated. Abutment heights should also be balanced because varying abutment heights leads to unbalanced lateral loads thus resulting in side sway. (Husain & Bagnariol 1996)
- The piles need to carry vertical loads from the abutments as well as being relatively flexible to accommodate temperature induced displacements. Piles can fail if the induced lateral forces are higher than the elastic buckling load (Arsoy et al 1999). Figure 2 shown below illustrates the cyclic movement of the abutment and deck due to changes in temperature.
- Integral abutment bridges should be avoided in cases where the soil is prone to;
    i. Liquefaction
    ii. Slip failure
    iii. Boiling
- Most integral bridges in the United States have been designed by using steel H-piles since they can tolerate a considerable amount of deflection without failure (Burke 2009, p13). In some countries such as South Africa, steel H-piles are not widely used due to the fact that the cost of steel is relatively high and so is normally an uneconomical solution (Byrne et al 1995, p89).

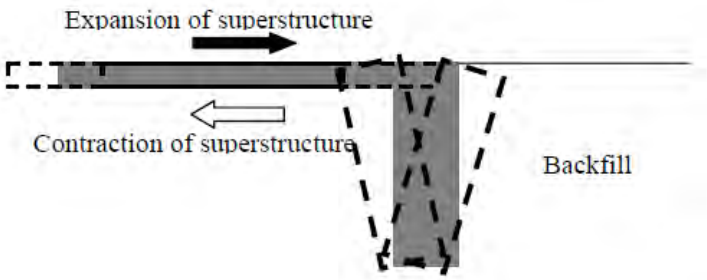

Figure 2: Cyclic loading induced by thermal displacements (David & Forth 2011)

2.2 The South African Bridge Loading Code – TMH7 (1988)

The current loading requirements for road bridges and culverts in South Africa are governed by Technical Methods for Highways TMH7 (1988) *Code of Practice for the Design of Highway Bridges and Culverts in South Africa*. This code was issued by the former Committee of State Road Authorities (CSRA) and forms part of the series of Technical Methods for Highways (FitzGerald & Steyn 1998).

The TMH7 consists of three parts:

Part 1: General Statement

Part 2: Specification for Loads

Part 3: Design of Concrete Bridges

According to the current TMH7, as amended in 1988, the South African bridge code is based on limit state design principles guided by the commendations of the CEP-FIB Model Code for Concrete Structures published in 1978. The semi-probabilistic procedure adopts the use of partial safety factors for determining design action effects and resistance at the ultimate limit state and the serviceability limit state. The code is based strongly on the British code of Practice BS 5400, Parts 1, 2 and 4, published by the British Standards Institution in 1978.

The integral bridge example used in this dissertation will adopt the TMH 7 loading regime, as amended in 1988. The traffic loadings according to TMH 7 comprise of three independent load models NA, NB and NC (FitzGerald & Steyn 1998).

NA Loading - represents the *normal traffic* loading which comprises of uniformly distributed loads and concentrated loads.

NB Loading - represents a single *abnormal* vehicle and is defined by NB 36.

NC Loading - represents *super loading* which refers to a multi-wheeled trailer which could have various combinations carrying very heavy indivisible loads.

TMH7 also covers a number of non-traffic loads. The non-traffic loads for bridges governed by TMH 7 are earth pressure, wind, hydraulics, seismic, accidental loads and thermal loads.

2.3 Bridge Deck Movements

Conventional design of bridges allow for the substructure and superstructure to be independent from each other and are merely “connected”, generally by bearings and expansion joints.

Reid et al (2008) states that the expansion joint serves to join the gap and form a seal between the two elements of a structure whilst accommodating for relative movements between them. Bridge deck joints are specified when the bridge deck movements are quantified. There are a number of movements to consider such as;

- Temperature movements
- Irreversible movements such as creep and shrinkage of the concrete
- Lateral joint movements on skew decks and curved bridges
- Settlement of supports
- Longitudinal movements due to longitudinal forces causing a sway on the bridge from braking and traction loads
- Superstructures with deep or flexible decks are prone to significant rotation thus causing movements under the live loads.

2.3.1 Temperature Effects

Thermal loading on bridge decks is a serviceability concern and results in flexural stresses being developed in the concrete bridge superstructures due to the heating and cooling of concrete. The distribution of temperature through the superstructure is nonlinear and is a function of the superstructure depth. This can be computed by using one-dimensional heat flow analysis (Radolli & Green 1976).

Hambly (1991) discusses how when the temperature increases in an element such as concrete, it causes the element to expand if it is unrestrained as depicted in Figure 3. The unrestrained thermal strains are given by;

Expansion: $\boldsymbol{\varepsilon = \alpha \Delta T}$

Where $\boldsymbol{\alpha}$ is the coefficient of thermal expansion and is generally given as 12 x 10^{-6} $^{o}C^{-1}$ for concrete.

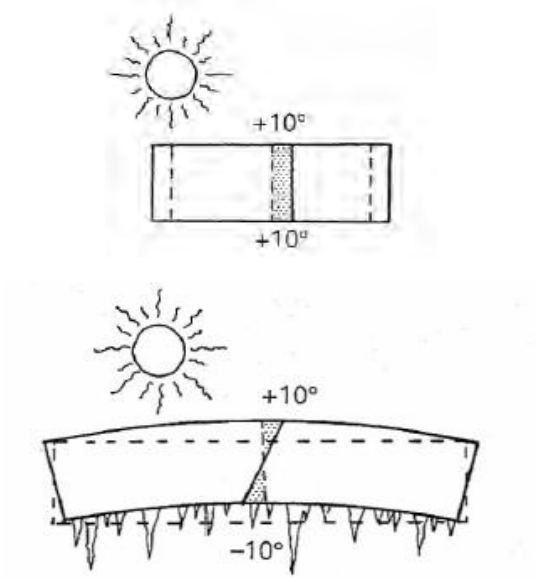

Figure 3: Temperature effect on an unrestrained element of a bridge deck (Hambly 1991)

If the element is prevented from expanding as depicted in Figure 4 below, with plane sections remaining plane, then the locked-in stresses are given by;

Compression: $\boldsymbol{\sigma = \alpha E \Delta T}$

Where $\mathbf{E}$ is the Young's modulus of the concrete.

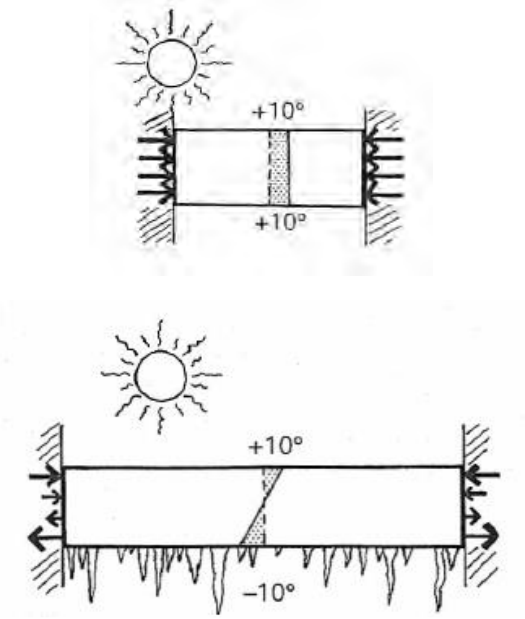

Figure 4: Temperature effect on a restrained element of a bridge deck (Hambly 1991)

2.3.2 Creep and Shrinkage Effects

The effects of differential creep and shrinkage in a structure is similar to that of temperature. One of the differences is that the creep and shrinkage strain diagram is generally stepped (Hambly 1991). The creep and shrinkage influences on integral bridges are often assumed to have opposite effects, and are particularly difficult to evaluate accurately. Thus creep and shrinkage are often ignored in the design of integral bridge structures (VTrans - State of Vermont Agency of Transportation, 2002).

Thippeswamy and GangaRao, as cited in a report by VTrans (2002), suggests that integral bridges with steel or prestressed concrete girders undergoes non-uniform shrinkage through the depth of the superstructure. The steel or prestressed concrete girders restrain the *free shrinkage* of the concrete slab deck thus resulting in compressive stresses in the steel or prestressed concrete girders (at midspan) and tensile stresses develop in the concrete deck slab.

2.4 Nature of Piles in Integral Abutment Bridges

2.4.1 Types of Piles

The research work done by Tlustochowics in 2005 discussed how there were a limited number of published papers regarding typical pile types used in integral bridges. The research done revealed that steel H-piles are the most commonly used pile.

The use of precast, prestressed concrete (PC) piles for integral bridges are also used by some bridge authorities and designers such as the Iowa Department of Transportation (Abendroth et al 2007).

Research conducted by Arsoy et al (1999) stated that the main concern is the pile deflections which arise from the cyclic movements generated from the temperature variations. Their results show that the steel H-pile is most suitable for integral bridge abutments. Their conclusion is that further research in this area is required. Figure 5 below shows the cross sections of various types of piles.

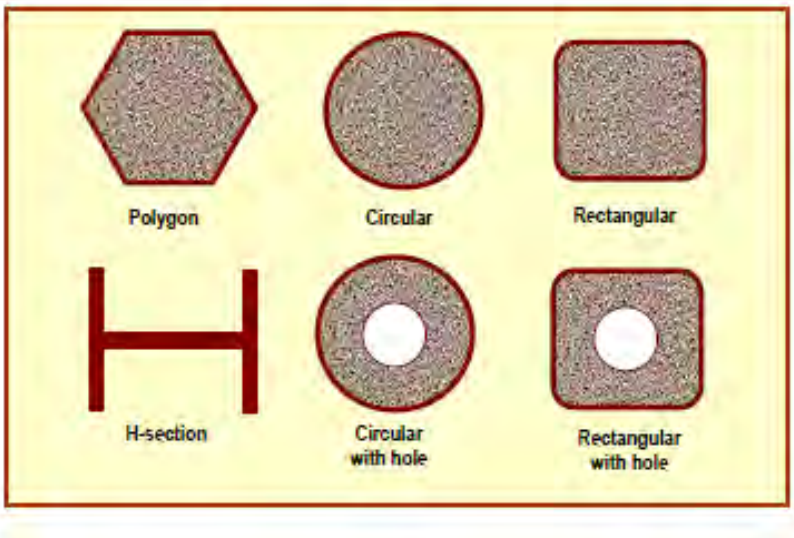

Figure 5: Different type of pile cross sections (Jaradat 2005)

2.4.1.1 Steel H-Piles

These piles have shown that they are capable of undergoing a substantial amount of distortion without failure, thus steel H-piles are generally favoured for integral bridge applications (Burke 2009). The research work conducted by Tlustochowics (2005) revealed that steel H-piles are able to withstand loads induced by thermal changes (expansion and contraction effects) and so can withstand cyclic loading provided the maximum pile stresses are within the limits of the yield stress of the pile.

Steel H-piles are manufactured in South Africa and are available but due to the cost of steel being relatively high, they are not widely used since they are not economically viable compared to the conventional cast insitu or precast concrete piles. (Byrne et al 1995, p89). Steel H-piles for integral bridges are often isolated by sleeving the top few meters of the pile as shown in Figure 6.

Figure 6: Sleeved H-piles for an integral abutment bridge (Tlustochowics 2005)

2.4.1.2 Prestressed Concrete Piles

The research conducted by Abendroth et al (2007) revealed that these piles are not commonly used, due to the concerns relating to the pile flexibility and the probability of cracking thus causing exposure of the pre-tensioned strands to moisture and overall durability concerns. The authors discuss that where sand and gravels are present, the use of prestressed concrete (PC) piles may be more economical than steel H-piles. The conclusion from this research also recommends that further work needs to be done regarding the use of PC piles for integral bridges. Figure 7 below shows an isometric view of an integral abutment bridge with precast concrete piles.

> *"the available literature presents divergent conclusions regarding the suitability of PC piles of this application"*
>
> (Abendroth et al 2007)

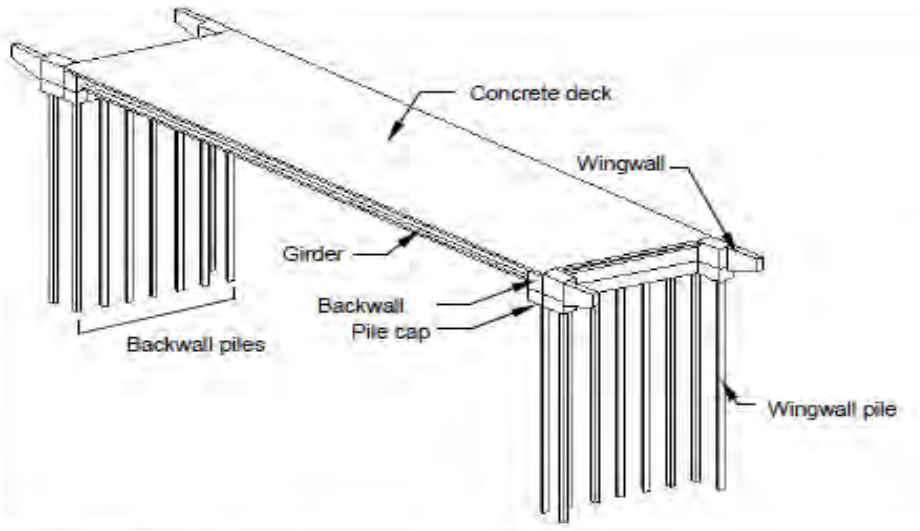

Figure 7: Isometric view of the integral bridge with precast prestressed piles investigated by Abendroth et al (2007)

Table 1 shown below provides typical working loads for precast piles that are often used in South Africa.

Table 1: Square precast pile working loads (Byrne et al 1995)

Pile Size	250mm Square	350mm Square
Typical working load (kN)	1000	2000
Maximum depth (m)	Unlimited	Unlimited

Precast pile lengths of up to 30 meters are possible by using prestressing technology but these are not very common in South Africa (Byrne et al 1995). A typical example of the usage of prestressed piles in South Africa are for the foundations for the ocean terminal in Durban, built in the late 1950s as shown in Figure 8. This type of piles was predominantly used for the foundation to the jetties (Zakrzewski 1962).

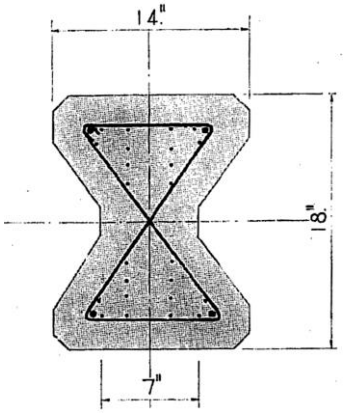

Figure 8: Section of prestressed precast concrete pile adopted for the foundations for the ocean terminal in Durban (Zakrzewski 1962)

2.4.2 Configuration of Piles

The configuration of piles for integral abutment bridges varies in many States in the USA and generally depends on the particular Department of Transportation guidelines.

The recommendations by the Ontario Ministry of Transportation suggest that the abutment wall should be supported on a single row of vertical H-piles. These guidelines also advise that the end piles at each abutment could be battered to a minimum of 1:10 in the transverse direction for additional lateral resistance (Husain & Bagnariol 1996).

The Tennessee Department of Transportation as well as many other states recommend the use of one row of piles driven vertically. This causes the abutment to move in the longitudinal direction, thus increasing the degree of flexibility to accommodate for cyclic movements. (Tlustochowics 2005).

Other references such as Burke (2009) also suggest that design engineers should provide a single row of slender vertical piles under each abutment.

2.4.3 Pile Orientation

The Ontario Ministry of Transportation recommends that if the structure's movement and loading requirements are such that piles are designed within the boundaries of the elastic range, then it is suggested that the connection should be considered as fixed and the piles should be orientated such that the strong axis is normal to the direction of the movement. When the loading and movements are such that the pile resistance exceeds the elastic range, the connection should be assumed as pinned and the piles weak axis orientated such that they are normal to the direction of movement (Husain & Bagnariol 1996).

> According to Burke (2009), suggests that engineers generally orientate the *"weak axis of H-piles normal to the direction of pile flexure"*.

The literature review by Tlustochowics (2005) revealed that various States in the USA have different opinion and practice regarding pile orientation for integral abutment bridges. The work reveals that according to a survey done in 1983, fifteen states in the USA orientate the piles so that the direction of thermal movement causes bending actions about the strong axis of the pile whilst thirteen other states orientate the piles such that the direction of movement causes bending about the weak axis of the pile. The piles orientated such that bending is about the strong axis is due to perhaps some degree of stiffness required to carry supplementary loads such as skidding and braking forces on the deck. The research also discussed that the most common recommendation is to orientate piles such that bending is about the weak axis of the pile. According to the research for *stub* abutments the pile axis of bending has a negligible effect regarding the displacement capacity for integral stub abutments.

The research done on this topic also often advises that both pile axes should be checked so the most economic and safe design could be done. Figure 9 shown below illustrates the two bending direction of H-piles.

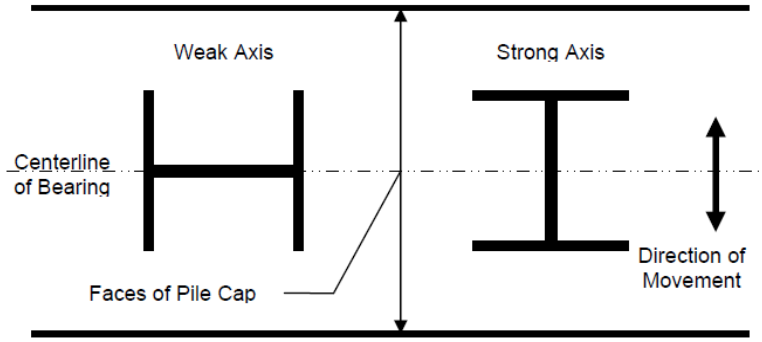

Figure 9: Typical orientation of H-piles (VTrans 2009)

2.4.4 Pile-Abutment Connection

The various States and bridge authorities generally have their own guidelines and advice regarding the connection between integral bridge piles and the abutment. The recommendations by the Ontario, Ministry of Transportation suggest that the top of piles should be embedded at least 600mm into the abutment wall and sufficient reinforcement provided to transfer bending forces (Husain & Bagnariol 1996). The guidelines also suggest;

> *"the connection between the superstructure and the abutment is normally assumed pinned for girder design and analysis".*

It is advantageous and economical to consider the frame action in the design by considering some degree of fixity but this requires careful engineering judgement and advanced girder analysis programmes. If the frame action is considered in the design then a consistent connection detail must be used (Husain & Bagnariol 1996).

There are various commonly used connection methods that could govern the design and analysis process such that the abutments could be pinned or fixed at the connections to the deck. Figure 10 shown below provides typical connection details of an integral abutment bridge showing the connection of pile, concrete stub abutment, beam girder, concrete top slab and approach slab fixity. Figure 10 (a, b, & c) from different states also shows that the girder is fixed into the concrete stub abutment with continuity reinforcement from the top slab into the stub abutment.

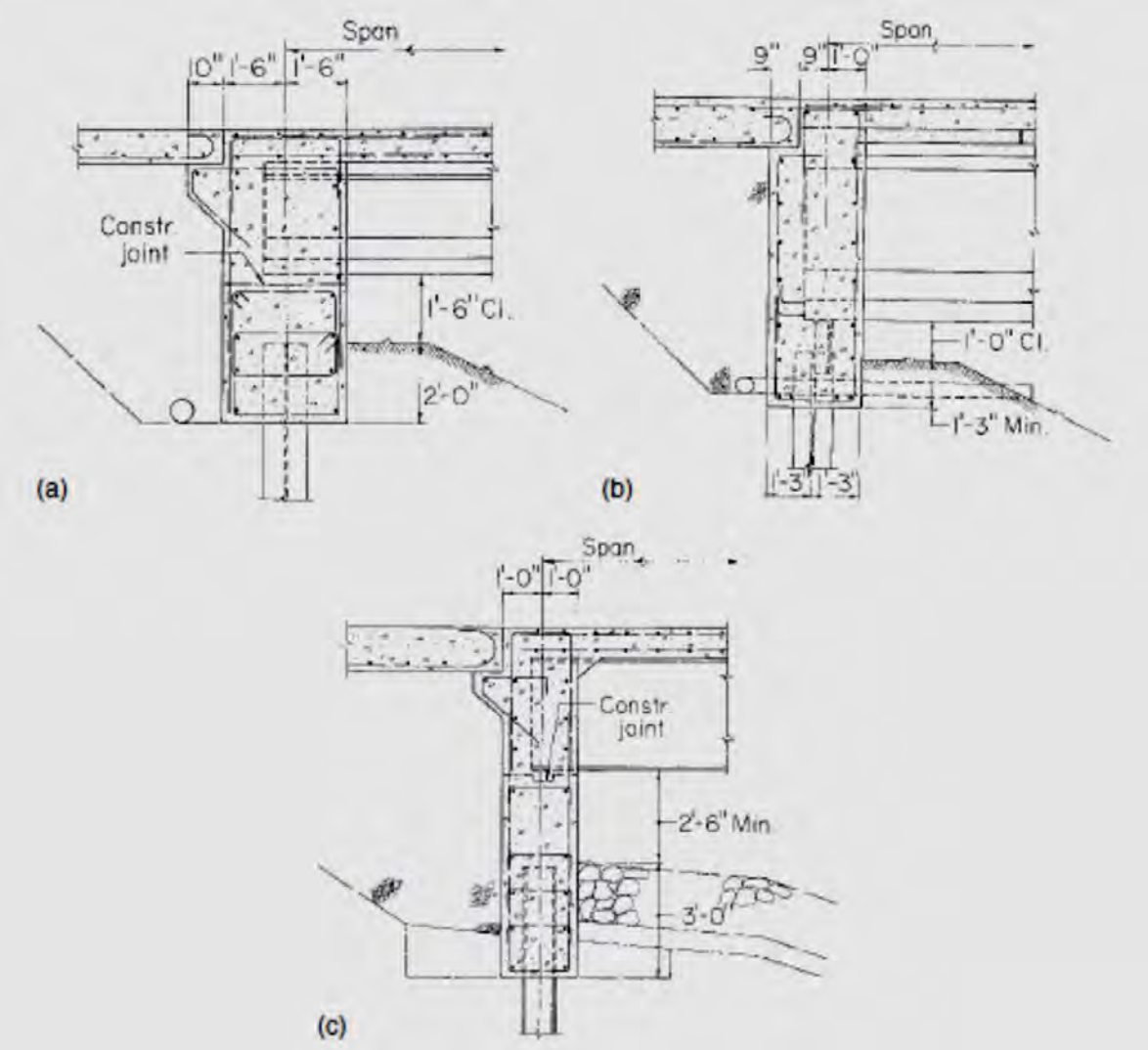

Figure 10: Integral abutment details for different States :(a) Iowa DOT (Department of Transportation); (b) Pennsylvania DOT and (c) North Dakota DOT (Burke 2009)

Using a rubber bearing under the girder creates a “pinned” condition to a certain extent and is contentious. The rubber bearing will be permanently fixed and would be impossible to replace as shown in the Figure 11 below. Figure 11 also shows the 600mm pile embedment into the concrete stub abutment. The stub abutment concept is very common with integral bridges as they essentially reduce the potential active and passive soil pressures behind the wall. This abutment concept also allows greater flexibility rather than a high abutment wall which generally has to be stiffened by counterforts.

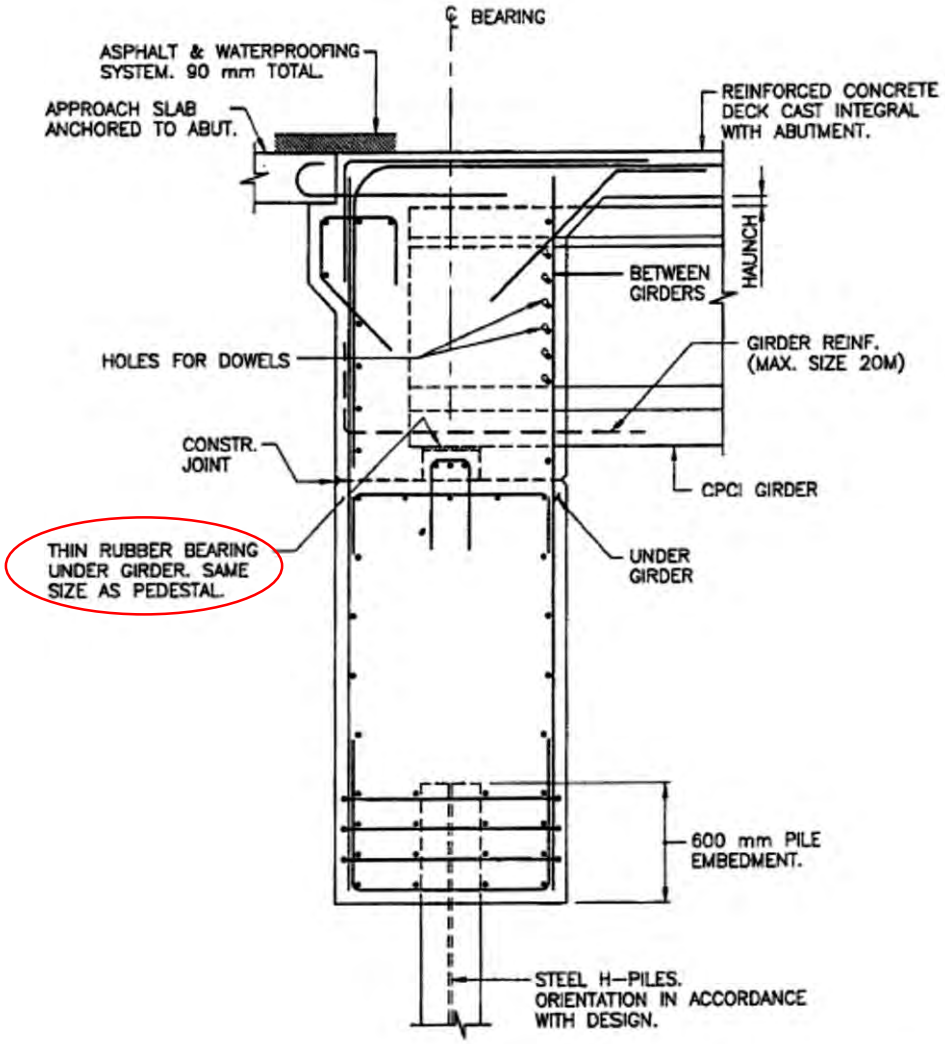

Figure 11- Integral abutment with CPCI girder and concrete deck - Ontario Ministry of Transportation (Husain & Bagnariol 1996)

Figure 12 shown below is similar to the concept presented in Figure 11. To create the pinned connection at deck and abutment interface a continuous strip of thin rubber bearing is placed under each girder as shown.

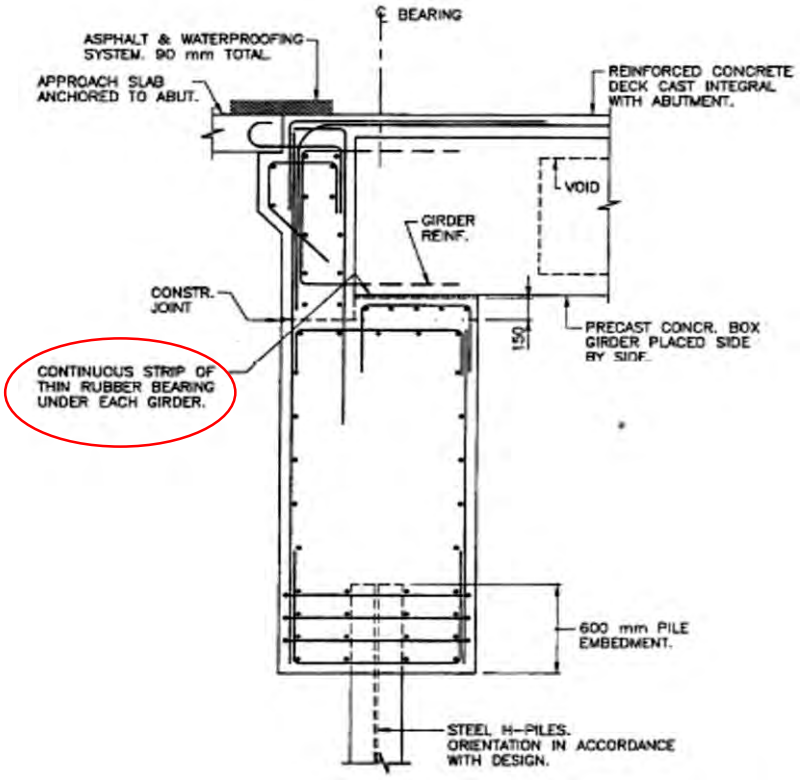

Figure 12: Integral abutment with precast concrete box girder and concrete deck - Ontario Ministry of Transportation (Husain & Bagnariol 1996)

The research and testing done by Abendroth et al (2007) adopted the use of “carpet wrap” at the top ends of the prestressed concrete piles supporting the abutment as shown in Figure 13. The carpet rap is a padding material that is installed (wrapped) around the pile that is embedded in the concrete stub abutment. The aim of this was to reduce rotational restraint at the tops of the abutment piles and create conditions of a “pinned type connection” between the piles and abutment. Carpet wrap is common practice and is often used in such applications. The results from the pile strain data did not reveal how much freedom of rotation was available for this type of connection and the researchers suggested that carpet wrapping at the top of piles should not be assumed to be a fully pinned-end condition.

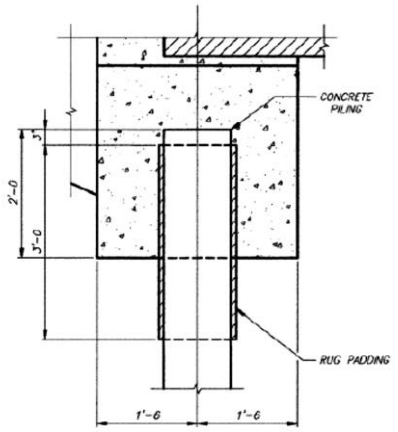

Figure 13: Precast PC pile wrapping detail for the research done by Abendroth et al (2007)

2.4.5 Length and Skew Limits for Integral Bridges

2.4.5.1 Length Limitations

The length limit is an important consideration in the design of integral bridges. Some of the recommended lengths are discussed below. Table 2 below summarises the length limits for integral steel and concrete bridges used in various states.

Table 2: Recommended maximum length limits for Integral Bridges (Tlustochowics 2005)

Department/state of Transportation	Concrete Integral Bridge length (m)	Steel Integral Bridge length (m)
Colorado	240	195
Illinois	125	95
New Jersey	140	140
Ontario, Canada	100	100
Tennessee	244	152
Washington	107	91

The literature review conducted by Card & Carder (1993) revealed that composite (steel-concrete) bridges undergo about 20% greater movement ranges in effective bridge temperature than concrete decks whilst steel box girders could experience 50% greater movement ranges. The table 2 above, thus shows smaller bridge lengths for steel integral bridges than concrete integral bridges. The table also shows that there is no common limit for integral bridge lengths as there is high variation in the values presented in the table.

The Ontario Ministry of Transportation suggests where the overall length of a bridge structure is over 100m but less than 150m, it may be designed as an integral bridge (Husain & Bagnariol 1996). The Design Manual for Roads and Bridges – The Design of Integral Bridges (BA 42/96) suggests that bridge decks of up to 60m in length are generally required to be designed as an integral bridge. In Switzerland the largest possible concrete integral bridge length is 108m, this transpires from national codes and based on the limitations of accepted deformations (Dreier et al 2010).

The Tennessee Department of Transport (DOT) is generally leading in integral bridge development. For example, The Happy Hollow Creek Bridge is a seven span prestressed concrete curved integral bridge with a total length of over 358m as shown in Figure 14. A single row of steel H-piles were used to support each abutment (Burke, 2009).

Figure 14: Aerial view of Happy Hollow Creek Bridge (Burke 2009)

The research by Tlustochowics (2005) discusses how as the integral bridge length increases, the lateral cyclic displacements in the piles due to temperature variations also increase. The piles may not perform within their elastic limits and may deform within the plastic range resulting in a reduction in their service life.

2.4.5.2 Skew Limitations

The Ontario, Ministry of Transportation suggests that if a rigorous analysis is carried out to account for skew effects, skews greater than 20^{o} but not exceeding 35^{o} may be considered. The reasons for the limitation on skew are primarily due to the non-uniform distribution of loads and complexities in establishing the movements in its associated direction (Husain & Bagnariol 1996). The Design Manual for Roads and Bridges – The Design of Integral Bridges (BA 42/96) advocates that integral bridge skews should not exceed 30^{o}.

The Project Report by Card and Carder (1993) recommends that the skew angle for integral bridge abutments should be minimised, usually between 10^{o} to 15^{o} but typically not greater than 30^{o}. The research also discusses how skews are limited to minimise the pile deflection in both longitudinal and transverse planes. When the skews are large, raked piles have been used to resist rotation caused by the earth pressures.

Figure 15 below shows the bridge length and skew limits for integral, semi-integral and conventional abutment designs. Figure 15 shows that for an integral abutment bridge the length limit is 61m and the maximum skew angle permitted is 30^{o} as per the literature. The semi-integral abutment bridges is permitted to have lengths up to 125m and thereafter conventional abutment design is governed for higher lengths.

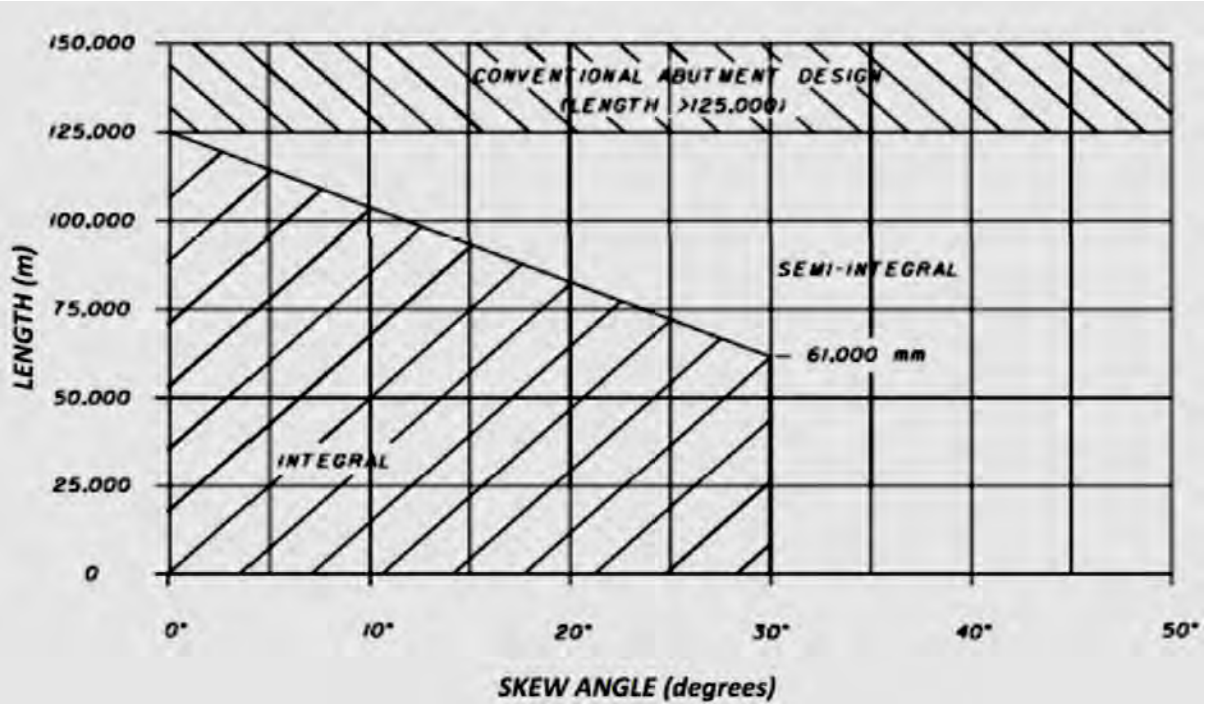

Figure 15: Skew angle limitations of Integral and Semi-Integral abutment bridges versus bridge length (Ohio, Department of Transportation 2003)

2.5 Chapter Summary

The main aim of this chapter was to understand the benefits of adopting integral abutment bridges. This chapter introduced the various fundamental requirements for integral abutment bridges. The numerous advantages of integral bridges are coupled with limitations such as the length and skew limits. The literature review showed there exists a wide spectrum regarding the integral bridge length limit and varies in different states. The types of piles were described and details provided; the steel H-pile is the preferred choice according to the literature reviewed. The soil-structure interaction is perhaps the biggest challenge concerning integral abutment bridges and is discussed in the forthcoming chapter.

CHAPTER 3

3 ISSUES CONCERNING INTEGRAL BRIDGE ABUTMENTS

3.1 Design Methods

3.1.1 General Issue

Integral bridges have numerous advantages, however the main difficulty from a designer's perspective is the soil-structure interaction. The interaction between abutment walls, supporting piles and soil media are essential for the analysis and understanding the structural behaviour (David & Forth 2011).

A commonly used modelling method is to postulate a series of spring supports along the foundation piles and behind the abutment walls. The main challenge with the spring type model is the derivation of the spring constant. Ideally the aim is to simulate actual site conditions (Sisk & Terzaghi, 2009).

3.1.2 Calculation Methods

There are several methods and models for analysing integral abutments. One of the most common methods is by adopting complex finite element models. However such detailed analysis is seldom adopted in practice as most states apply the simple length and skew rules with their typical state designed details. Research conducted at the Iowa State University has led to two fundamental types of *equivalent cantilever pile* analysis alternatives, one for elastic stresses and a second that considers plastic stress (Dunker & Liu 2007).

According to David and Forth (2011), there are six modelling approaches generally adopted by researchers for analysis of soil structure interactions;

I. Winkler spring approach
II. Finite element analysis
III. Integrated modelling
IV. Partitioned analysis
V. Staggered approach and
VI. Iterative coupling

Some of the common methods and models are briefly discussed below.

3.1.2.1 Equivalent Cantilever Method

The equivalent cantilever method is a simplified model presented by Abendroth and Greimann in the late 1980s. The pile and surrounding soil is modelled as a column with a fixed base at some distance below the ground surface. This method is based on finite element and analytical studies and can consider the elastic or plastic behaviour of piles. Both these alternatives are conservative when compared to finite element simulations. The concept is illustrated in the Figure 16 and Figure 17 shown below. However this method does not simulate the abutment wall and approach fill interaction (Tlustochowicz 2005; Bagnariol & Husain 1996).

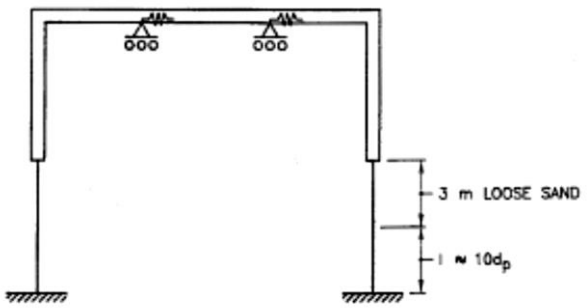

Figure 16: Equivalent cantilever concept (Bagnariol & Husain 1996)

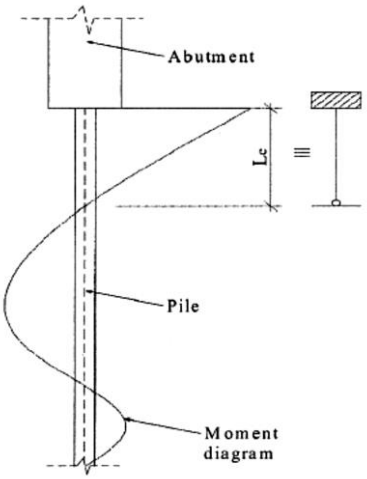

Figure 17: Equivalent cantilever concept (Tlustochowicz 2005)

This model is commonly used by the Ontario, Ministry of Transportation - Structural Office to design integral bridges, and is widely adopted by many bridge designers and authorities (Bagnariol & Husain 1996). The equivalent cantilever method was also successfully used to design the piles for the bridge on the M50 Freeway in Ireland (Wagle & Watt 2011). Figure 18 below is the grillage model of the M50 Freeway Bridge showing the piles as equivalent cantilevers providing fixed support conditions at the bottom end.

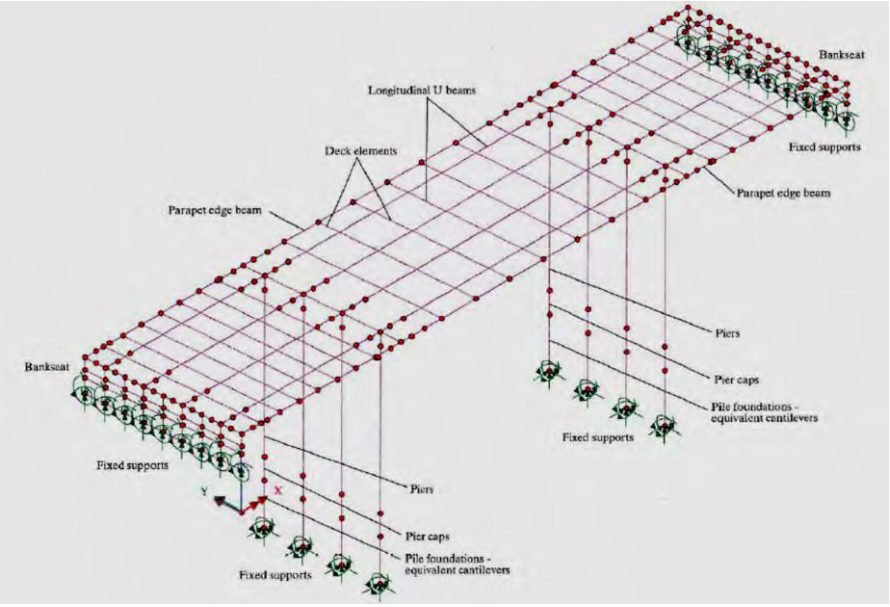

Figure 18: Idealised grillage model of M50 Bridge in Ireland showing equivalent cantilever concept for the pier piles (Wagle & Watt 2011)

3.1.2.2 Finite Element Method

The Finite Element Method (FEM) is perhaps one of the most commonly used methods to model complex structures today. Modern computer capacity provides reasonable accuracy, which is governed by the size of the element mesh and accurate modelling of material properties. FEM subdivides a complex structure into a finite number of individual components called elements whose behavioural characteristics can be assumed. The displacements, strains, stresses and resulting nodal forces for each element can be determined by their shape functions and their derivatives. The individual elements are connected by nodes and the *stiffness matrices of the individual elements* $[\mathbf{K}]^e$ are added to form the *global stiffness matrix* [**K**], from which the unknown *deformations or displacements* {***u***} can be determined (Rombach 2011, p 4-7).

$$[\mathbf{K}].\{\boldsymbol{u}\} = \{\boldsymbol{F}\}$$

Where:

[**K**] is the global stiffness matrix

{***u***} is the vector of nodal displacements

{***F***} is the vector of nodal forces

According to Rombach (2011) rigid piles can be modelled as *"linear elastic supported truss elements"*. The bedding modulus K_s and the stiffness of the horizontal springs may vary along the pile shaft and the circumference.

The spring analogy is derived from the Winkler spring type model. The challenge of FEM analysis of integral bridges is again deriving appropriate spring constants (Sisk & Terzaghi, 2009).

3.1.2.3 P-Y Curve Method

The *"p-y method"* originates from the initial work by Cox and Reese (1974) using the finite-difference method for laterally loaded pile solutions which involved using ***springs p*** and ***lateral node displacements y***. Each node has its own *p-y curve* and there are different soil node springs along the pile shaft. The product of node spring **p** and the node displacement **y** yields ***p.y = node force*** similar to spring forces computed in the common form of;

$$[\mathbf{K}].\{\boldsymbol{u}\} = \{\boldsymbol{F}\}$$

(Bowles 1996).

The p-y analysis is suitable for heavily loaded piles causing yielding to the soil or where considerable cyclic loading is experienced. The p-y curves may be chosen to closely model the data from experiments which could be correlated to other designed piles adopted in similar soil conditions. The p-y curves do not have a firm theoretical background and reference should be made to the original papers. The challenge with this type of method is to establish a set of p-y curves for each site (Elson 1984). The American Petroleum Institute (API) adopted proposed p-y curves for sand in 1974 by Cox and Reese (Bezgin 2010).

3.2 Theoretical Background: Subgrade Reaction Modulus

The pile foundations supporting an integral abutment bridge need to resist the lateral loads generated. The ultimate lateral capacity of the piles is not of major concern but the maximum deflection of the piles is important. In the past, design practice made use of empirical pile information from fully scaled lateral pile load tests; however since the late 1970s theoretical approaches for predicting lateral pile behaviour have developed significantly (Poulos & Davis 1980, p 163-174).

Some of the approaches are briefly discussed in the forthcoming sections.

3.2.1 Winkler Soil Model

In 1867 Winkler proposed a model that portrayed soil as springs, which were known as "Winkler Springs" as illustrated in Figure 19 and are often used to model the soil-pile interaction (Rajapakse 2008). This subgrade reaction approach characterises the soil as an independent series of linearly elastic springs thus deformation or deflection occurs only where loads exist.

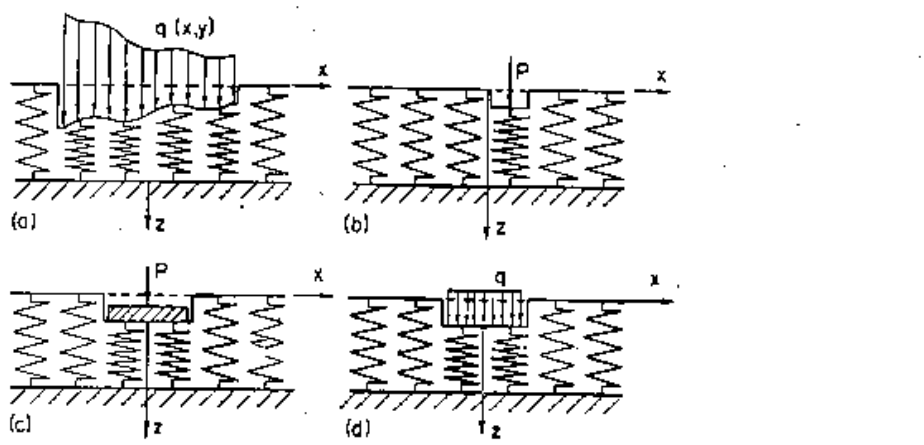

Surface displacements of the Winkler model due to (a) a non-uniform load, (b) a concentrated load, (c) a rigid load, (d) a uniform flexible load.

Figure 19: Illustration of the Winkler Spring concept for Foundations (Chandra 2013)

The concept of the Winkler soil model of a beam on an elastic foundation can be idealized to predict the behaviour of piles. This model could be used to model the vertical forces along the length of a pile (skin friction) as well as the laterally loaded piles as demonstrated in Figure 20 and Figure 21 shown below.

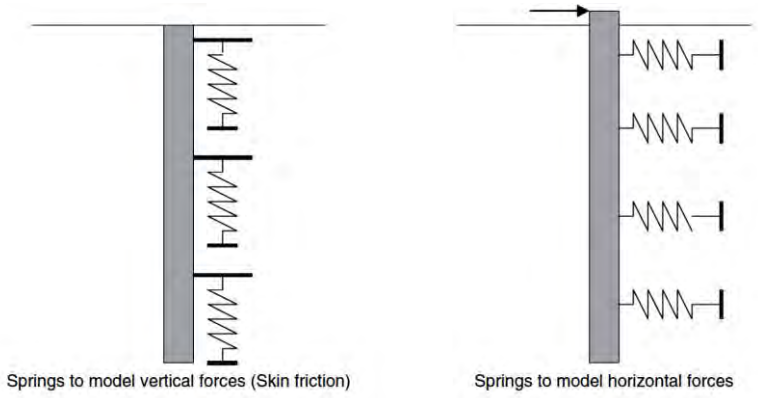

Figure 20: Winkler Soil Model for vertical and horizontal forces on a pile shaft (adapted from Rajapakse 2008, p247)

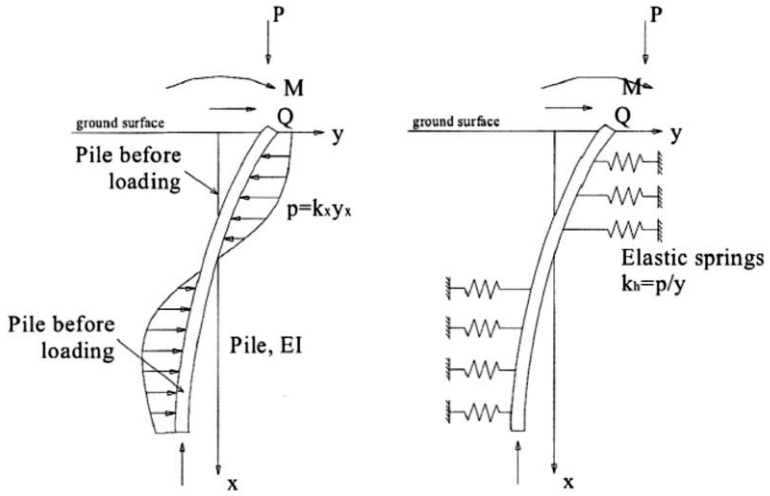

Figure 21: Winkler's idealization for laterally loaded piles (Tlustochowicz 2005)

There are some disadvantages of this model such as a lack of continuity amongst springs that does not model the true behaviour of soil, which has a degree of continuity interaction. Another disadvantage is that the spring modulus of the Winkler model (the modulus of subgrade reaction) is based on the overall size of the foundation. Despite these disadvantages the subgrade reaction approach is widely used since it is a simple means of analysis and considerable amount of experience with reasonable results and empirical data have been collated (Davis & Poulos 1980). One of the challenges of using this model is the difficulty in deriving an appropriate spring constant for the soil mass under consideration. However this difficulty is also a concern when other methods are used.

The basic theory of the Winkler Model is presented below as shown by Davis and Poulos (1980);

The **pressure** $\boldsymbol{p}$ and **deflection** $\boldsymbol{\rho}$ at a point are assumed to be related through a **modulus of subgrade reaction,** $\mathbf{k_h}$ ($\mathbf{h}$ denotes horizontal loading). Thus,

$$\boldsymbol{p} = \mathbf{k_h} \,.\, \boldsymbol{\rho}$$

Where $\mathbf{k_h}$ has the units of **force / length** $^{\mathbf{3}}$. The above equation is often written as;

$$\mathbf{w} = \mathbf{K}.\, \boldsymbol{\rho}$$

Where:

$\mathbf{w}$ = soil reaction per unit length of pile

$\mathbf{K}$ = subgrade reaction modulus, units of force/length^2 ($\mathbf{K} = \mathbf{k_h d}$)

$\mathbf{d}$ = diameter or width of the pile

The pile is assumed to act as a beam whose behaviour is governed by the following equation;

$$\boldsymbol{E_p I_p} \left(\frac{\boldsymbol{d^4 \rho}}{\boldsymbol{dz^4}}\right) = -\boldsymbol{pd}$$

Where:

$\boldsymbol{E_p}$ = modulus of elasticity of the pile

$\boldsymbol{I_p}$ = moment of inertia of pile section

$\boldsymbol{z}$ = depth in soil

$\boldsymbol{d}$ = width or diameter of pile

From a combination of the equations above, the governing equation for a laterally deflected loaded pile is;

$$\boldsymbol{E_p I_p} \left(\frac{\boldsymbol{d^4 \rho}}{\boldsymbol{dz^4}}\right) + \mathbf{k_h} \,.\, \boldsymbol{d}.\, \boldsymbol{\rho} = \mathbf{0}$$

The solutions to the above equation may be solved by either numerical or analytical methods.

3.2.2 Modulus of Subgrade Reaction

The pile shown in Figure 22 below is held by soil which is modelled as springs. The spring constant or the modulus of subgrade reaction (sometimes referred to as the coefficient of subgrade reaction) generally increases with depth. The coefficient of subgrade reaction may be assumed for a simplified analysis for laterally loaded piles and maybe taken as being constant for the entire pile shaft. The inaccuracy of this assumption is not substantial in most scenarios (Rajapakse 2008). However a more accurate analysis of pile behaviour using the subgrade-reaction approach considers the variation of $\mathbf{k_h}$ along the pile shaft. Many researchers have proposed distributions of $\mathbf{k_h}$ and some of them will be discussed below.

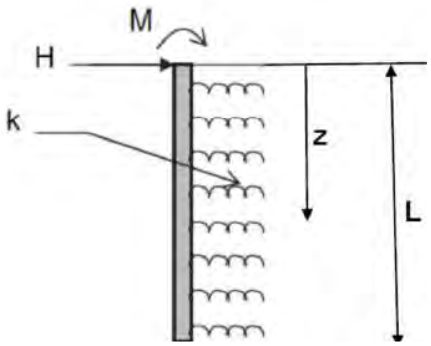

Figure 22: Laterally loaded pile supported by soil springs (Rajapakse 2008)

In 1948 Palmer and Thompson presented the commonly used formulae below;

$$\mathbf{k_h} = \mathbf{k_L}\left(\frac{\mathbf{z}}{\mathbf{L}}\right)^{\mathbf{n}}$$

Where:

z = depth below surface

L = length of pile

$\mathbf{k_L}$ = is the value of $\mathbf{k_h}$ at the pile tip (z = L)

n = an empirical index equal to or greater than zero

A common assumption is that $n = 0$ for clay. This implies that the spring constant is same throughout the pile. Another assumption is that $n = 1$ for granular soils, thus the modulus increases linearly with depth. In 1963, Davisson and Prakash suggested that for clays a more realistic value to consider for undrained conditions will be $n = 0.15$. The undrained conditions are considered since the clay particles are surrounded by a nearly incompressible layer of fluid such as water.

For the case of $n = 1$;

$$\mathbf{k_h} = \mathbf{n_h}\left(\frac{\mathbf{z}}{\mathbf{d}}\right)$$

Where:

$\mathbf{n_h}$ = coefficient of subgrade reaction (units of force/ length^3)

d = pile width or diameter

The true behaviour of soils is such that soil pressure and deflection are non-linear, with soil pressure approaching a limited value when deformations are high. The range of limiting values is essentially based on the soil type. The p-y approach developed by Reese may be the most satisfactory method to carry out a non-linear analysis. If linear theory is to be adopted then appropriate secant values of the subgrade modulus must be chosen (Poulos & Davis 1980). However the work done by Tlustochowicz (2005) also states that the formulae by Palmer and Thompson proposed in 1948 is widely used. The work done by Tlustochowicz (2005) as shown in Table 3 below, summarises proposed coefficients of reactions by Davisson in 1970. Table 3 provides subgrade reaction modulus ranges for the different soil types. For cohesive soils the subgrade reaction modulus is dependent on the undrained shear strength of the soil.

Table 3: Estimated values of coefficient of subgrade reaction modulus (Davisson 1970 cited by Tlustochowics 2005)

Soil type	Values
Granular	n_h ranges from 0.408 to 54.4 MN/m^3, is generally in the range from 2.72 to 27.2 MN/m^3, and is approximately proportional to relative density
Normally loaded organic silt	n_h ranges from 0.1088 to 0.816 MN/m^3
Peat	n_h is approximately 0.0544 MN/m^3
Cohesive soils	k_h is approximately 67 C_u, where C_u is undrained shear strength of the soil

Rombach (2011) suggested that rigid piles can be modelled by linear elastic supported truss elements. The bedding modulus $\boldsymbol{k_s}$ and the stiffness of horizontal springs around the pile shaft may vary along its length and circumference. The Figure 23 shown below illustrates this concept. The work done presents a proposed method by Timm and Bladauf (1988) which suggests the formulae below;

$$\boldsymbol{k_s(z) = k_s(d).\left(\frac{z}{d}\right)^n}$$

Where:

$n = 0$ for cohesive soils under small loads, similar to Palmer and Thompson (1948)

$n = 0.5$ for medium cohesive soil and non-cohesive soil above ground water table

$n = 1.0$ for non-cohesive soil below the ground water level or under greater loads

$n = 1.5\ to\ 2.0$ for loose non-cohesive soil under very high loads.

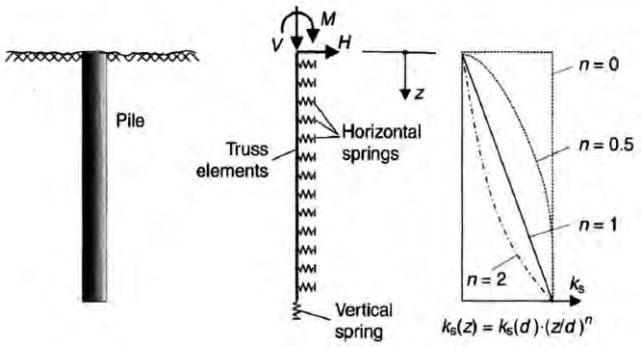

Figure 23: Distribution of bedding modulus k_s and numerical model for a laterally loaded pile (Rombach 2011)

Rombach (2011) recommends that if no results are available from actual pile tests then the bedding modulus k_s may be estimated from the following expression;

$$k_s = E_s/d$$

Where:

k_s is the bedding modulus

E_s is the stiffness modulus of the ground

d is the diameter of the pile where d is less than or equal to 1000 mm

Further guidelines provided suggest that the stiffness modulus for non-cohesive soil varies between E_s = 100 to 200 MN/m^2 for gravel whilst E_s varies between 10 to 100 MN/m^2 for sand (Rombach 2011). The modulus of subgrade reaction has also been proposed by various other researchers and some of them are discussed below.

Terzaghi in 1955 proposed that the modulus for subgrade reaction is the same horizontally and vertically for clays and is actually independent of depth. Typical values for the over-consolidated clays are show in the Table 4 below;

Table 4: Values of k_{sl} (tons/ft^3) for square plates, 1 x 1 ft., on overconsolidated clays (Terzaghi 1955 cited in Poulos & Davis 1980)

Consistency of Clay	Stiff	Very Stiff	Hard
Undrained shear strength c_u ton/ft^2	0.5-1	1-2	2
Range for $\bar{k}_{s1}$	50-100	100-200	200
Proposed values of $\bar{k}_{s1}$	75	100	300

[a] After Terzaghi (1955).

Vesic (1961) compared results from an infinite horizontal beam on elastic foundation to results obtained from subgrade reaction theory and found the following relationship;

$$k = \left(\frac{0.65}{d}\right)\sqrt[12]{\frac{E_S d^4}{E_P I_P}}\left(\frac{E_S}{1-\nu_S^2}\right)$$

Where:

$E_P I_P$ = pile stiffness

d = pile diameter

Broms (1964) proposed the empirical correlation, that k_h for clays is related to the secant modulus E_{50} at half the ultimate stress in an undrained test;

$$k_h = 1.67.E_{50}/d$$

Whilst Skempton (1951) suggested using an E_{50} value equal to 50 to 200 times the undrained shear strength, c_u thus obtaining the relationship;

$$k_h = (80 - 320)c_u/d$$

A more conservative reaction of subgrade modulus was suggested by Davisson (1950);

$$k_h = 67c_u/d$$

Although many researchers propose that for clay, the k_h value could be considered constant along the length of a pile shaft, some researches assume that k_h increases linearly with depth;

$$k_h = n_h.\left(\frac{z}{d}\right)$$

Typical values are presented in Table 5 below;

Table 5: Typical values for n_h in cohesive soils (Davis & Poulos 1980)

Soil Type	n_h (lb/in.^{3})	Reference
Soft N/C clay	0.6-12.7	Reese and Matlock, 1956
	1.0-2.0	Davisson and Prakash, 1963
N/C organic clay	0.4-1.0	Peck and Davisson, 1962
	0.4-3.0	Davisson, 1970
Peat	0.2	Davisson, 1970
	0.1-0.4	Wilson and Hilts, 1967
Loess	29-40	Bowles, 1968

For sands, Terzaghi (1955) assumed that the modulus of elasticity depends on the density of the sand and overburden pressure thus found the following correlation;

$$n_h = \frac{A.\gamma}{1.35}\ (tons/(ft^3\ )$$

Typical values of A and n_h are shown in the Table 6 below;

Table 6: Values of n_h (ton/ft^3) for sand (Terzaghi 1955 cited in Davis & Poulos 1980)

Relative Density	Loose	Medium	Dense
Range of values of A	100-300	300-1000	1000-2000
Adopted values of A	200	600	1500
n_h, dry or moist sand	7	21	56
n_h, submerged sand	4	14	34

[a] After Terzaghi, 1955.

Research by Sisk and Terzaghi (2009) suggests that different methods for obtaining the spring constants along a pile give widely varying results, which could lead to over or under designing the piles. The use of conventional springs is thus discouraged and the combining of the structural geotechnical models is promoted.

3.2.3 Laterally Loaded Piles

Research work done by Broms (1965) suggested that the ultimate lateral resistance of a laterally loaded pile is governed by;

I. *The ultimate lateral resistance of soil surrounding the pile*
II. *The moment resistance of the pile section*

The ultimate lateral resistance of piles can be calculated from graphs that were presented by Broms (1965). The work carried out showed that for short piles, the ultimate lateral resistance was dependent on the depth of the pile and independent of the resistance offered by the pile section. The ultimate lateral resistance for a long pile was found to be governed by the ultimate lateral resistance of the pile section and independent of the pile penetration depth.

The method presented by Broms (1965) was based on the concept of a coefficient of subgrade reaction and assumed that for cohesion-less soils, it increases linearly with depth whilst for cohesive soils it remains constant with depth. When plastic hinges develop along the length of a steel, timber or reinforced concrete pile, collapse occurs as a form of failure mechanism. Broms (1965) assumed that the rotational capacity of these plastic hinges is enough to develop the passive lateral soil resistance, allowing full redistribution of bending moments along the length of the piles.

Local buckling may occur for relatively thin walled pipe piles. In this case, Broms' (1965) proposed analysis would not apply. It is suggested that the local buckling can be easily prevented if the steel pipe piles are filled with sand or concrete. The wall thickness of pipe piles as well as the web and flange thickness of H-pile sections should be chosen such that local buckling does not occur, generally local buckling is not likely to occur if conventional sections are adopted. When the stress at the sections of maximum bending moment reaches the yield strength of the pile material, plastic hinges are formed in steel piles. The plastic moment of resistance of the section, $\boldsymbol{M_{yield}}$ can be calculated based on ultimate strength analysis.

For a cylindrical steel pipe section;

$$\boldsymbol{M_{yield} = 1.3 f_y W}$$

And for an H- section pile;

$$\boldsymbol{M_{yield} = 1.1 f_y W_{max}}$$

Where:

f_y is yield strength of pile material

W is section modulus of the pile

And coefficients of 1.3 and 1.1 are plastic moment shape factors for the respective sections.

It is important to note that in the literature presented by Broms (1965), the axial loads that are likely to be present in reality are now ignored because axial loads decrease the ultimate bending resistance strength of steel H-piles and pipe piles, whilst in the case of precast and cast in-situ piles it is increased. The reason for such behaviour depends on the type of material and the degree of buckling resistance provided, which essentially depends on the buckling mode of failure.

The Figure 24 and Figure 25 shows the soil reaction and bending moment of short piles in cohesive and cohesionless soil respectively.

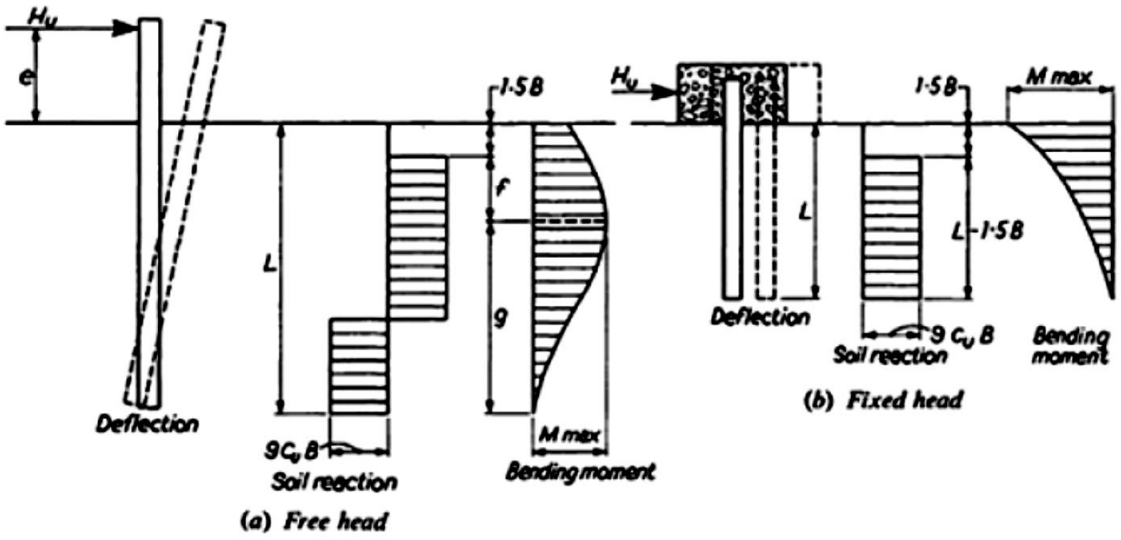

Figure 24: Cohesive soil – short pile under horizontal loads (Broms 1964 cited in Tomlinson 1994)

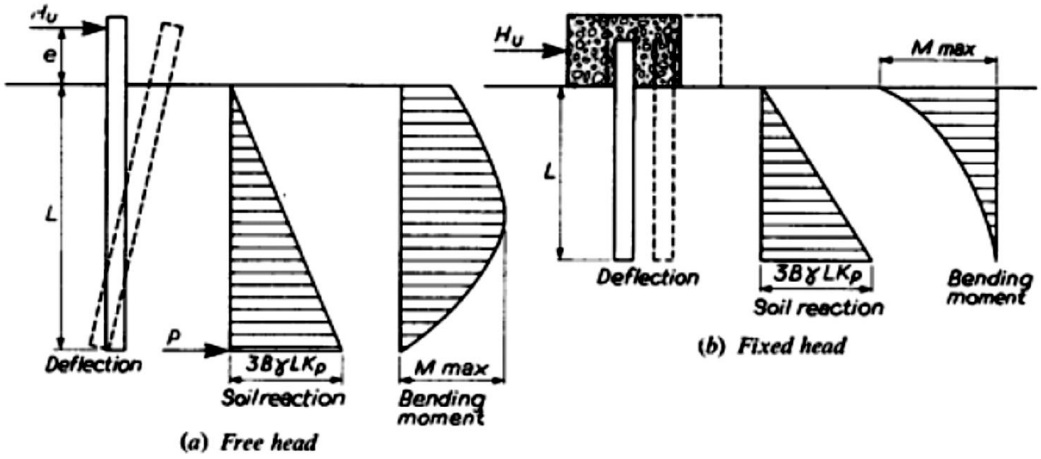

Figure 25: Cohesionless soil – short pile under horizontal loads (Broms 1964 cited in Tomlinson 1994)

The Figure 26 and Figure 27 shows the soil reaction and bending moment of long piles in cohesive and cohesionless soil respectively.

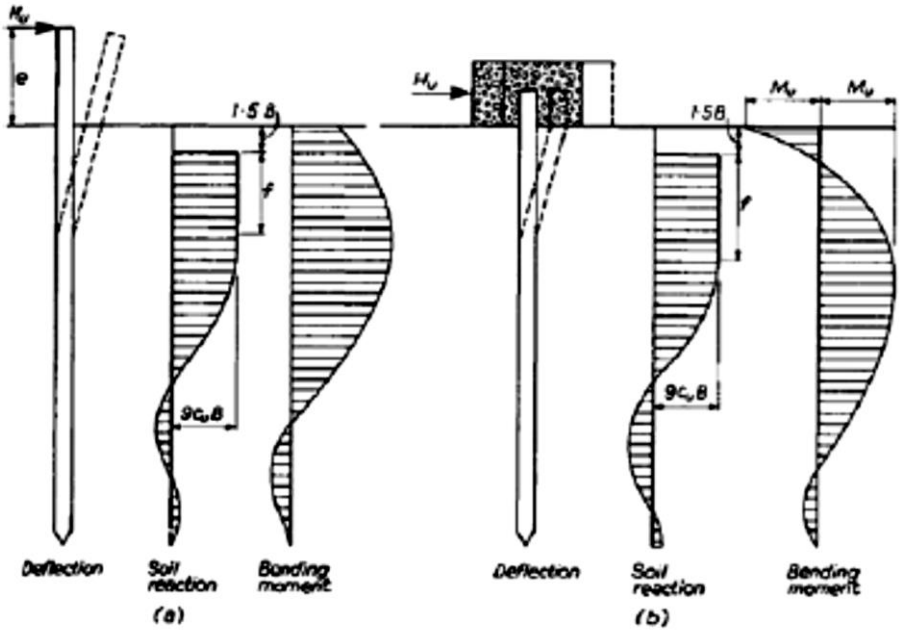

Figure 26: Cohesive soil – long pile under horizontal loads (Broms 1964 cited in Tomlinson 1994)

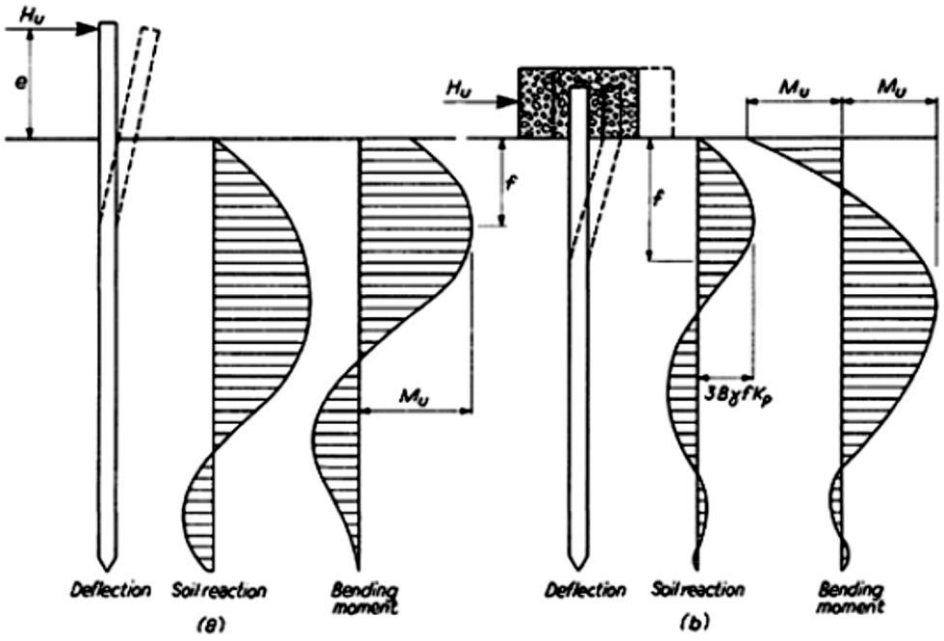

Figure 27: Cohesionless soil – long pile under horizontal loads (Broms 1964 cited in Tomlinson 1994)

3.3 Geotechnical Problems and Solutions Using Materials to Absorb Lateral Stresses Behind Integral Bridge Abutments

3.3.1 General Overview

Integral bridge abutment concept has many advantages as previously discussed but as historically implemented can have its own inherent post-construction flaws. The problems are fundamentally of a geotechnical nature and not structural. Thus, for an improved and better long-term performance of an integral bridge, it is imperative the designer considers the soil-structure interaction of the bridge abutments (Horvath 2005). One of the fundamental flaws of integral abutment bridges is that the concept fails to demonstrate how the relative displacement between the cyclic movement of the superstructure (and /or substructure) and ground is to be accommodated. This has actually led to integral bridge abutments still requiring maintenance when in actual service, although many authors argue that the cost for this maintenance is less than that for conventional bridges with joints and bearings (Horvath 2005).

3.3.2 Thermal Effects on Integral Abutment Bridges

> *"Thus IABs (integral abutment bridges) as currently designed still have maintenance costs as did their jointed predecessors which inflates the true life-cycle cost of an IAB"*
>
> (Horvath 2005)

Figure 28 below describes the abutment behaviour of an integral bridge. As Horvath describes, the abutment primarily undergoes rigid-body rotation about the bottom of the abutment but there is also a certain degree of rigid-body translation of the abutment. Since rotation of the abutment is dominant, the magnitude of the horizontal displacement at the top will be greatest.

Due to seasonal temperature changes, the bridge superstructure experiences corresponding seasonal length changes, i.e,

i. In winter the integral abutments move inwards and away from the soil mass they are retaining.
ii. In summer the integral abutments move outward and push into the soil mass

The magnitude of these thermal movements depend on the length of bridge, coefficient of thermal expansion of material and the corresponding temperature range as discussed in Chapter 2 (2.3.1).

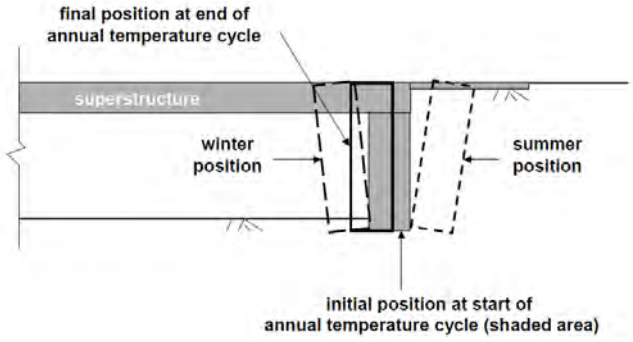

Figure 28: Thermal effects on Integral Abutment Bridges and Displacements (Horvath 2005)

Horvath (2005) explains that as a result of the cyclic behaviour, at the end of each annual thermal cycle, there is often a net displacement of each abutment inwards toward each other and away from the retained soil mass as shown in Figure 28. This inward displacement of the abutment as a result of the winter season is of sufficient magnitude to cause active earth pressure conditions behind the wall thus resulting in a "soil wedge" to develop adjacent to each abutment and follow the abutment wall inwards, with the soil slumping downwards behind the abutment wall. Since the soil is inelastic in nature, the inward and downward movement of the soil mass is not fully recovered during the summer season when the abutment is pushed outwards. The author also emphasises that this inward and downward displacement of the soil will occur, irrespective of the type of soil and degree of compaction adopted during construction. One should also note that, the net inward movement of the abutment is intensified when the superstructure is concrete due to the inherent shrinkage of concrete. There are two significant consequences that result from the seasonal thermal effects

3.3.2.1 Ratcheting Failure

The first was discovered as early in the 1960s (Broms 1971, Card 1993 & Sandford 1993 cited in Horvath 2005) and is the relatively large lateral earth pressures that develop on the abutment wall during the annual summer expansion of the superstructure. These lateral earth pressures can approach the theoretical passive pressure especially towards the upper part of the abutment where horizontal displacements are generally the greatest. If the abutments are not designed for these high pressures, structural distress and even failure of an abutment can occur. The summer-seasonal increase in lateral earth pressure, which is not necessarily constant over time, can increase significantly.

> *"The reason is that not only is one seasonal cycle of inward-outward displacement nonlinear, but each succeeding season is nonlinear with respect to the proceeding one."*
>
> (Horvath 2005)

In simple terms, this implies that each winter the abutment moves slightly inward more than the preceding winter and each summer it moves slightly outwards to a lesser degree than the preceding summer. There is a "consistent" net soil displacement inward towards the abutments yet the bridge superstructure still expands each summer season the same amount as the preceding year. As a result, the lateral earth pressures increase over the summer season as the soil mass directly behind the abutment wall becomes increasingly wedged in over many cycles. This complex overall soil mechanics behaviour is termed ***ratcheting*** (Horvath 2005).

The *ratcheting effect* results in each summer's lateral earth pressures being higher in magnitude than those of the preceding year. This essentially implies that structural distress at abutments and failure of the abutments are likely after a few decades or even years, and represents a potentially serious "long-term" problem for integral bridge abutments. This also implies that the full design service life of the bridge may not be achieved (Horvath 2005).

3.3.2.2 Void Subsidence

The second significant problem associated with integral abutment bridges is the void that develops behind the abutment face as illustrated in the figure 29 below;

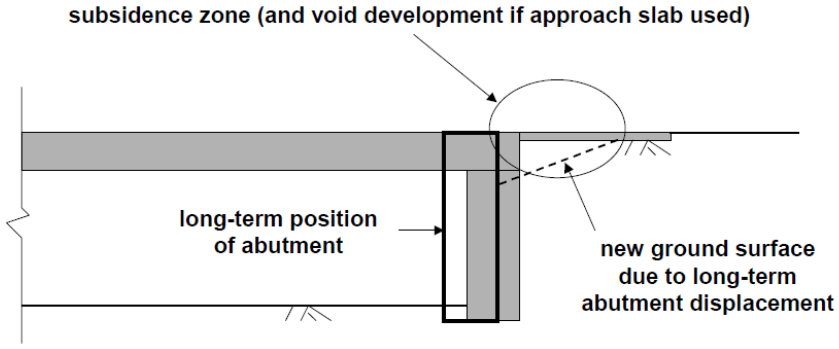

Figure 29: Subsidence of the ground surface behind integral abutment bridges (Horvath 2005)

Due to the irreversible slumping of the soil-wedge behind each abutment, a subsidence pattern forms adjacent to each abutment as shown in Figure 29. This subsidence pattern is also a result of the overall net inward displacement of the abutment. The subsidence pattern (gap) depends on whether or not a transition slab (approach slab) was constructed as part of the abutment. If no approach slab is used, there will be a difference in road surface elevation over a short distance, creating the typical "bump" at the end of the bridge. If a transition slab is adopted, then it will initially span over the gap/void created underneath by the subsided soil mass (Horvath 2005). The research by Reid, as cited by Horvath (2005) reveals that from a field survey of 140 IAB's (integral abutment bridges) approach slabs in the state of South Dakota, USA, a void was found under practically every approach slab, the void depths varied from 13mm to 360mm and the void length under the approach slab extended as much as 3m.

3.3.3 Proposed Solutions Using Stress Absorbing Materials

Recent work related to finding solutions to some of the problems with regard to integral bridge abutments include the study of different types of compressible materials. In concept these compressible materials are intended to serve as a *sacrificial cushion* between the abutment and adjacent soil mass thus reducing the lateral earth pressures caused by seasonal thermal movements (Horvath, 2005).

> *"Because of the current extensive use of IABs, there is a critical need to develop solutions to correct the behavioural deficiencies inherent in all IABs as they are typically designed and constructed at the present time"*
>
> (Horvath, 2005)

Horvath (2005) based solutions on the following considerations and concepts;

I. The natural phenomenon of expansion and contraction of the bridge superstructure due to seasonal temperature variation is *inevitable and unavoidable* and the displacement will occur regardless of concept adopted in the design phase. The displacement between the IAB and soil mass is thus unavoidable and must be addressed in the design.
II. Horvath also suggests the soil mass behind the IAB abutment must be made "inherently self-stable" for all seasonal cycles thus preventing the development of subsidence (gap) during the winter seasons.
III. A specialised material or structural element (compressible layer) must be provided between the "inherently self-stable" soil mass and the moving IAB concrete abutment to reliably accommodate for the horizontal displacement between them. In the past voids have been left between the ground and abutment but experience has shown that this is difficult to construct and the reliability of the gap for long term effects is uncertain.

Horvath (2005) presents two different concepts, the details are provided below and illustrated in Figure 30.

Concept 1: (as shown in Figure 30(a))

The concept makes use of geosynthetic tensile reinforcement to create a mechanical stabilised earth (MSE) mass behind the concrete abutment thus achieving an "inherently self-stable" soil mass for the design life of the bridge.

Figure 30(a) below is most likely to be cost effective and appropriate in most conditions with some of the key features:

- Figure (a) below is appropriate were the insitu soils have no issues regarding compressibility or stability
- A relatively thin (typically in the order of 150mm) layer of compressible material such as resilient- EPS (expanded polystyrene) geofoam would be adopted to serve as a compressible inclusion between the soil mass and abutment wall.
- The durable compressible material functions as the desired "expansion joint" between the concrete abutment and MSE soil mass.
- The compressible material layer also thermally insulates the retained soil from winter freezing and insulates the geosynthetic tensile reinforcement from the summer heat which can increase the geosynthetic creep.
- The compressible inclusion can also be designed to serve as a drain for ground water flow.
- The most important function of the compressible inclusion layer is to allow the reinforcement within the soil mass to strain in tension thus preventing the soil from moving inwards towards the abutment back-face and downwards during each winter season. In addition it allows the abutments to move seasonally (expanding and contracting) either way with minimal restraint. In summer seasons the lateral earth pressures are reduced to relatively smaller magnitudes, this advantage could result in cost savings for the structural design of the abutment.

Concept 2: (as shown in Figure 30(b))

The other alternative is shown Figure 30(b) below, some of the features of this proposal are listed below;

- As an alternative to the MSE soil mass, one could adopt a self-stable wedge of geofoam such as EPS blocks.
- The use of lightweight fill material also has many advantages such as reducing the loads imposed onto the abutment and the underlying ground layers. This alternative is thus appropriate for sites where the insitu soils underlying the approach embankment are compressible and soft.
- The compressible material forming the inclusion serves the same purpose as described above.

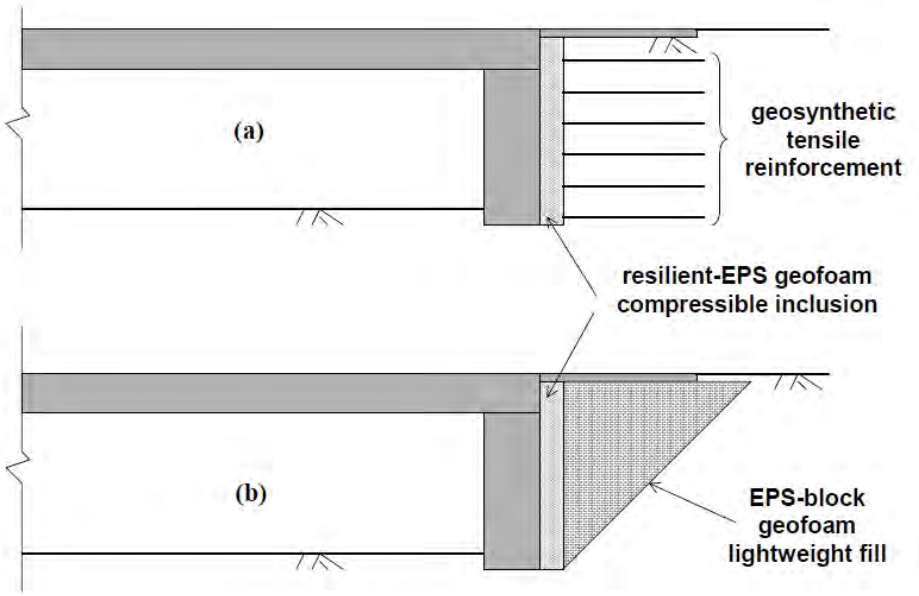

Figure 30: Schematic Proposal of New IAB Design Alternatives by Horvath (2005)

The new IAB design alternatives, as shown in Figure 30 above, aims to isolate the structure from the surrounding soil mass and simplify the complex soil-structure interaction. The scheme shown in Figure 30(a) would be more practical for construction in South Africa as the concept of using geosynthetic tensile reinforcement or similar material in mechanically stabilized earth retaining walls is popular, with the resources and expertise for such an application readily available.

SUMMARY OF RESEARCH WORK BY CARDER, BARKER & DARLEY (2002)

Stress-absorbing layers between the backfill and abutment by use of various innovative materials have been identified and a testing regime was set up to primarily assess their fitness for purpose. The authors above selected a product from each generic type of material and set up a testing programme.

The testing programme was aimed at investigating;

I. Potential fitness for purpose of a specific type of material and
II. Refine the testing procedures

The test procedures proposed included;

I. Determination of modulus at strain levels expected in the field
II. Shear strength
III. Permanent compression set, locked-in when the loading applied was released
IV. Thereafter actual trials were undertaken to assess the effect of compacting granular fill against some of the materials

The suitably identified materials investigated were;

I. Polyethylene foam
II. Expanded polystyrene
III. Extruded polystyrene
IV. Geocomposite
V. Voided rubber
VI. Rubber-soils
VII. Shredded tyres
VIII. Rubber crumb

The results of the investigation showed that some of the materials prove to have good potential for use as layers to absorb lateral stresses behind the IAB concrete abutment. The main concern was that some materials exhibited a compression set on the release of the load. This phenomenon in practice would result in excessive void formation when subjected to cyclic loading. The solution that the authors proposed was to adopt thicker material layers to limit the in-service strains and thus in turn reduce the compression set.

The tests were in accordance with the recommended engineering properties of the stress-absorbing layer behind an integral bridge abutment published by Carder and Card (1997). The properties were derived on the basis of typical requirements for a continuous deck with the following properties;

I. Deck span of 60m. Note 60m is also the limit of integral bridge length in many states in the USA.
II. Assuming a coefficient of thermal expansion of 12×10^{-6} per ^{o}C.
III. The effective deck temperature range was based on that which is experienced in the United Kingdom (UK).

The figures below are a typical example of the results obtained from tests performed on the expanded polystyrene. Similar tests were performed on the other type of materials. The figure below shows the results from compression testing to determine the horizontal modulus. The figures show typical stress-strain plots on compression of expanded polystyrene at strain limits of 2% and 6% in Figure 31 and Figure 32 respectively. From these tests performed by the researchers, the tangent modulus values were obtained from a series of three tests and are tabulated next to the figures. These values were determined after accommodating for initial seating effects due to friction between the specimen sides and the box used for testing. From Figure 31 the expanded polystyrene proved to be elastic in nature up to approximately 2% of strain, yielding a mean modulus of 6.6 MPa for the first loading. Due to effects of the specimen being confined in the test box, the values were higher than the manufacturer's conservative value of 4.5 MPa.

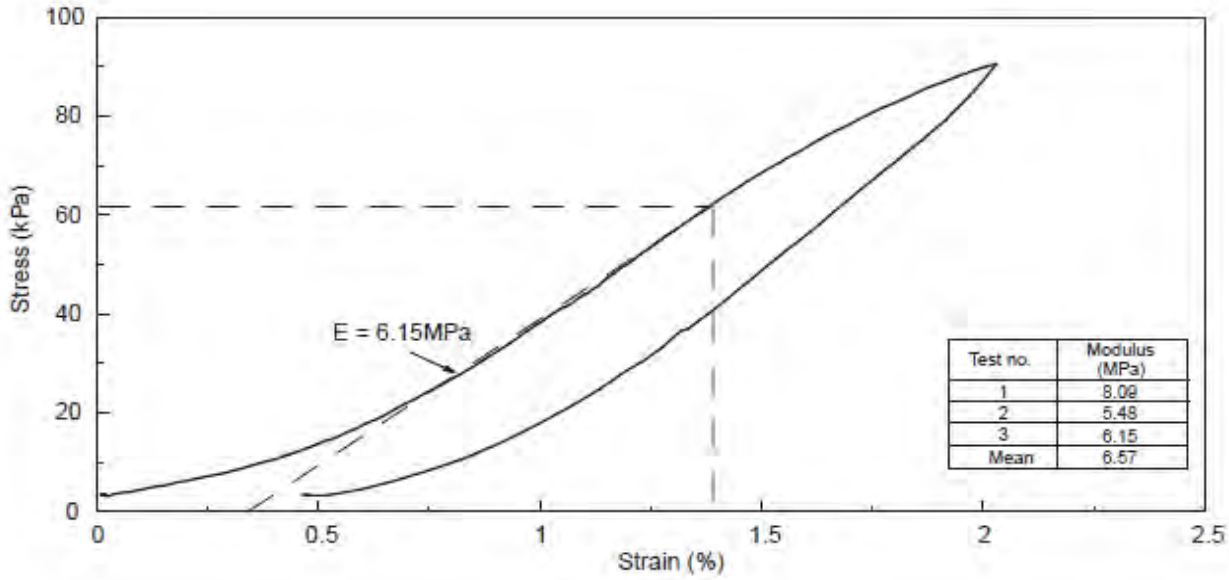

Figure 31: Modulus testing of expanded polystyrene (first load cycle of 2% strain) – (Carder et al 2002)

In Figure 32 shown below, testing up to 6% strain was carried out on the expanded polystyrene. A small change in the modulus was measured but significant plastic deformation was observed when the strains above 2% occurred. A distinct increase in permanent deformation was recorded after unloading was done. This indicated that the need to control the working strain of expanded polystyrene to less than 2% was required if it were to be adopted behind integral bridge abutments to avoid the formation of voids.

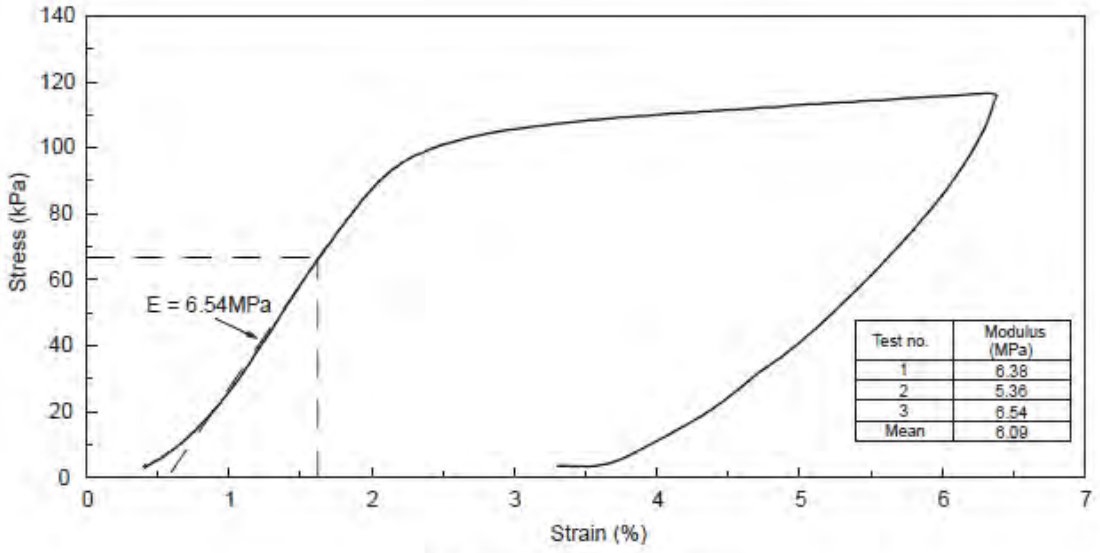

Figure 32: Modulus testing of expanded polystyrene (second load cycle of 6% strain) - (Carder et al 2002)

Figure 33 shows results from the shear tests performed on the expanded polystyrene material layer. The shear strength calculated was 120 KPa which exceeded the vertical strength requirement. A minimum horizontal shear strength of 150 KPa would be required if a 300mm thick layer was adopted. The reason for this test was to check the minimum layer thickness required to avoid shearing of the material when installed behind an integral abutment bridge. The un-notched and notched specimen values shown in the table are merely an adjustment to the testing regime.

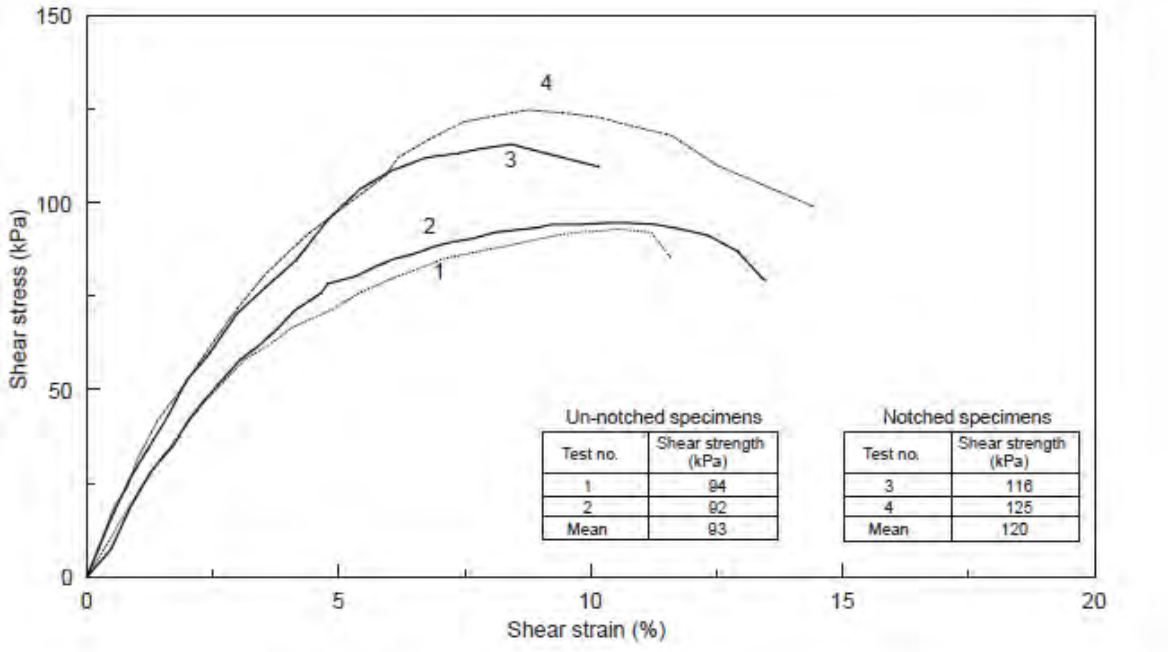

Figure 33: Results from shear test of expanded polystyrene (Carder et al 2002)

The Table 7 below shows the results from the compression tests performed on the expanded polystyrene. The material was removed from the test box before measuring its recovery after the sustained loading. The mean compression set of 75.8% was recorded after three days and a small further recovery of 74.0% measured after seven days. The lack of recovery of this material after compression to 10% was not unexpected as it corresponds to Figure 31 and Figure 32 above.

Table 7: Results for expanded polystyrene – compression set (Carder et al 2002)

	Thickness (mm)			*Compression set (%)*		
Specimen	*1*	*2*	*3*	*1*	*2*	*3*
Initial height	300.34	298.77	300.03	–	–	–
Immediately after release	276.27	274.40	274.47	79.3	84.7	85.1
3 days after release	278.69	276.35	276.54	71.4	77.9	78.2
10 days after release	279.07	276.95	277.21	70.1	75.8	76.0

Percentage compression set is defined as $100(h_0-h_f)/(h_0-h_s)$ *where* h_0*=initial thickness,* h_f*=recovered thickness, and* h_s*=compressed thickness.*

In summary, expanded polystyrene is a good stress absorbing material but is not competent in terms of recovery when the lateral stresses are large and cyclic in nature since plastic deformation occurs after about 2% strain. If the strains are limited to 1% then it may be suitable for use behind integral abutment bridges. Generally a minimum layer thickness of 1m would be required for a 60m span bridge, based on the results of the laboratory investigation. The high compression set would indicate respective void sizes of 1.8mm for 300mm thick material and void size of 0.5mm for 1m thick material. These void sizes are comparable to the proposed acceptability limit of 2mm. Durability must also be considered when using expanded polystyrene and encasement is often used to prevent contact with accidental fuel or chemical spillage during service life of the bridge.

Table 8 shown below is a summary of the different type of potential material types that were tested to investigate their potential use behind integral abutment bridges. Table 8 also provides a summary of product details, compression modulus at 1% strain, shear strength and the void size from the compression set at three and ten days after release of load. The test results of expanded polystyrene were presented above as an example. The expanded polystyrene showed high compression set after release of load. The table below shows polyethylene foam with favourable void sizes i.e. good recovery after the removal of the load compared to expanded polystyrene. The shear strength of polyethylene foam is fairly high but the compression modulus is low. The material chosen to isolate the abutment and soil as a stress-absorbing layer must be carefully chosen such that all minimum required parameters are achieved.

Table 8: Summary of results based on the testing of the different type of materials that could potentially be adopted behind an integral bridge abutment (Carder et al 2002)

Generic material type	*Particular product*	*Mean compression modulus at 1% strain (MPa)*	*Mean shear strength (kPa)*	*Void size[1] (mm)*	
				0.3m layer	*1m layer*
Polyethylene foam	Aerofil 2	1.6	279	0.32 (0.18)	0.10 (0.05)
Expanded polystyrene	Fillmaster 100	6.6	120	1.64 (1.60)	0.49 (0.47)
Extruded polystyrene	Styrofoam IB	14.0 (h) 11.7 (v)	> 245 (h) > 245 (v)	1.84 (1.80)	0.54 (0.53)
Geocomposite	Geofin	1.7 (h)	n/a	~0.97 (~0.91)	~0.29 (~0.27)
Voided rubber	Natural rubber	10.8 (h)	n/a	n/a	n/a
Rubber-soil	Well graded sand + 35% rubber	0.2	68[2]	n/a	n/a
	Sandy clay + 35% rubber	0.2	58[2]	n/a	n/a
Shredded tyres	15mm to 20mm particle size	0.2	64[2]	n/a	n/a
Rubber crumb sheet	Regupol 6010 PL	0.4	n/a	0.55 (0.47)	0.17 (0.14)
Recommended properties for 60m bridge span	0.3m thick layer	1 to 2 (h) >3 (v)	>150 (h) > 20 (v)	2 (Proposed revision to 1)	
	1m thick layer	3 to 6 (h) >3 (v)	> 50 (h) > 20 (v)		

[1] *Void size calculated from mean compression sets measured 3 days after release; numbers in brackets are calculated from sets measured 10 days after release.*

[2] *At vertical load of 60kPa, ie. load at mid-height of 6m high abutment.*

Compaction Trials

The research work conducted by Carder et al (2002) also carried out experimental trials to understand the effect of;

- The compaction of free draining granular fill behind some of the suitable materials that were identified as stress-absorbing layers.
- Investigate if there was any damage of the stress-absorbing materials due to compaction.
- The effect on the stress absorbing materials due to initial structure moving away from the material, which would occur in the winter season due to contraction. This behaviour was simulated by carefully hand-excavating the backfill from behind the stress-absorbing layers and analysing the impact on the material layer.

Figure 34 below shows the experimental setup for the testing.

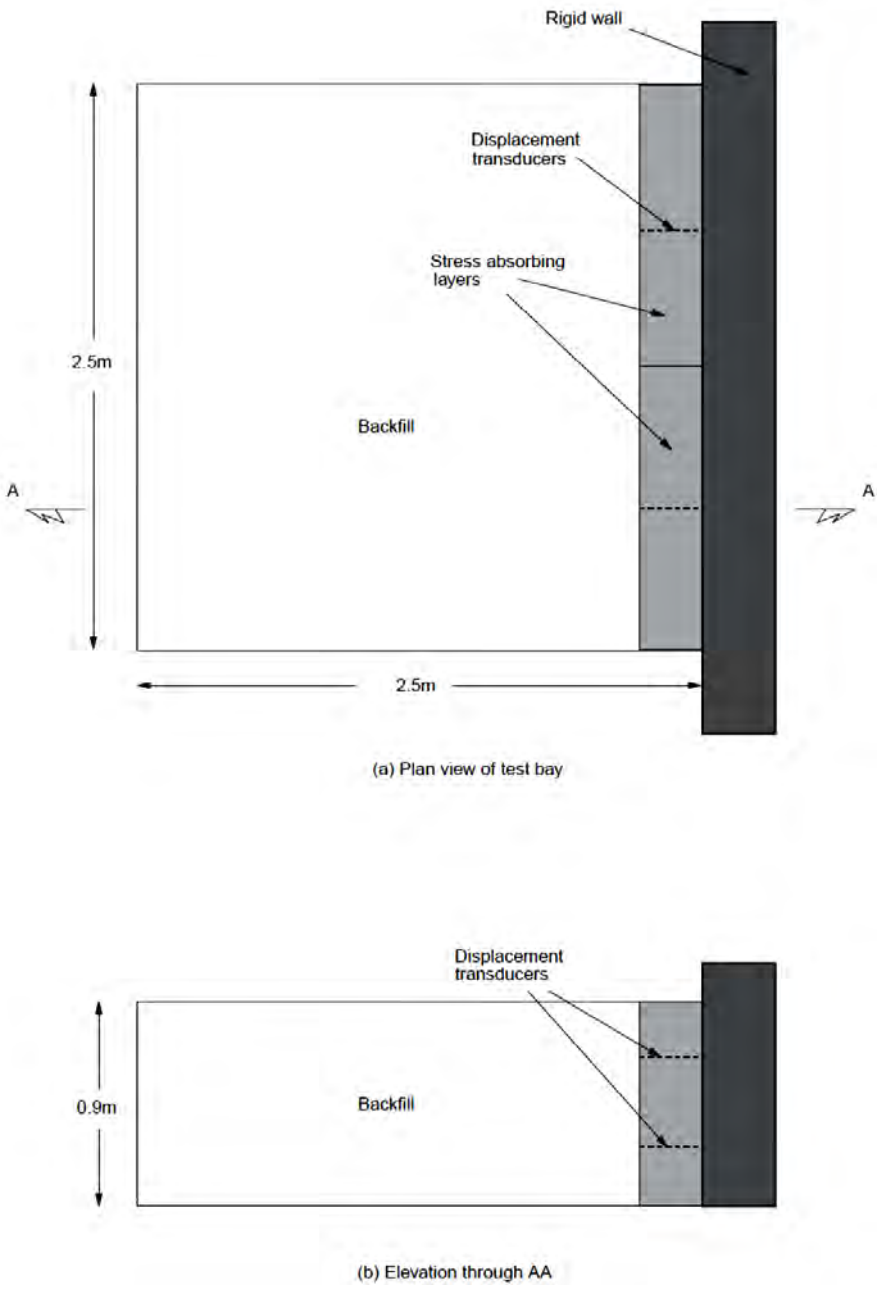

Figure 34: Plan and elevation of the experimental test bay (Carder et al 2002)

Carder et al (2002) suggested that from this experiment, all the materials investigated had an acceptably rebounding nature. The expanded and extruded polystyrenes had some localised damage due to the indentation of the soil particles (< 5mm) onto the material, which can be considered as relatively insignificant. For most of the materials tested, the displacements recorded during compaction were greater than when the backfill was removed. The reason for this was because of small seating effects. The polyethylene foam, rubber crumb sheet and voided rubber shown good elastic recovery and minimal compression set. The authors also suggested that these types of material can be more effectively used by varying the overall thickness of the layers (decreasing from bottom to top) used behind integral bridge abutments. The results are shown in the Table 9 below.

Table 9: Summary of results from compaction experiment (Carder et al 2002)

Generic material type	*Layer thickness, t (mm)*	*Horizontal modulus, E (MPa)*	*t/E (mm/MPa)*	*Displacement during compaction (mm)*		*Displacement during excavation (mm)*	
				Lower level	*Upper level*	*Lower level*	*Upper level*
Voided rubber	200	10.8	18.5	3.6	2.3	0.1	0.5
Extruded polystyrene	600	14.0	42.9	2.7	3.5	0.6	1.2
Expanded polystyrene	600	6.6	90.9	5.9	4.1	0.9	0.5
Polyethylene foam	300	1.6	187.5	8.1	4.4	0.8	0.9
Rubber crumb sheet	150	0.4	375.0	7.3	6.7	4.0	1.9
	300	0.4	750.0	11.6	7.3	5.1	2.0

3.3.4 Cost of Proposed Solutions

The revised conceptual designs presented above will increase the overall construction cost of IABs but the high quality post-construction benefits and overall performance coupled with reduction in future maintenance and repair costs may make the above proposals feasible and economical. Similarly, if these concepts are adapted to suit existing IABs, it should be cost effective by reducing future repair and maintenance costs. Where the geofoam is going to serve as a self-stable block, the benefits of faster construction by using geofoam materials should also be taken into consideration (Horvath, 2005). The cost of the generic stress-absorbing materials provided in the test regime described above range from approximately R 150-00/m^2 to R 450-00/m^2, for a 300mm thick layer. However based on the material and compression set the layer could be more than 300mm thick.

3.4 Expansion Joints for Integral Bridge Abutments

The *Alberta Transportation Board's (2003) guidelines on the design of integral abutments* suggests that integral abutment bridges do not completely eliminate bridge deck joints. Integral bridges inherently still need to undergo thermal contraction and expansion movements due to temperature changes. To accommodate cyclic thermal movements, joints are provided, however these joints are shifted to the end of the approach slab or roof slab. The joint location at these parts of the structure allow for minor leakage to be tolerated or handled much better. According to the guidelines, the magnitude of the movements are reduced due to passive pressure on the abutment end diaphragms and the pier/abutment stiffness. However the approach slab is structurally connected to the end of the deck superstructure, thus adding to the overall length of the superstructure contributing to the cyclic temperature variations. The *Alberta Transportation Board's (2003) guidelines on the design of integral abutments* collates information from Ontario, the FHWA, various DOT's and the UK Highways Agency and accommodates for thermal movements. Some of the standard details for integral abutment joints are presented below.

Joint Type 1 – Figure 35 and Figure 36 shows the type of joint adopted for many short integral abutment bridges. The only evidence of movement was shown in the form of a crack at the end of the approach slab. The cracks are generally of a minor nature and do not appear to present any problem. A simple pavement joint with bitumen-impregnated soft board and an approved hot asphaltic joint sealant generally works well according to *Alberta guidelines for design of integral abutments* (2003).

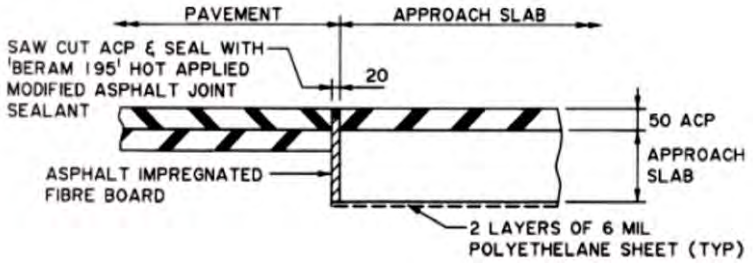

Figure 35: Cycle Control Joint Type 1 – Short Integral Abutment Bridges to Alberta guidelines for design of integral abutments (2003)

Figure 36 (below) is a standard detail from the Ontario Bridge Office and similar to figure 35 (above). This joint shown works well as an isolation joint where the total length of the integral bridge is less than 75m for structural steel bridges and 100m for concrete bridges (Bagnariol et al, 1999).

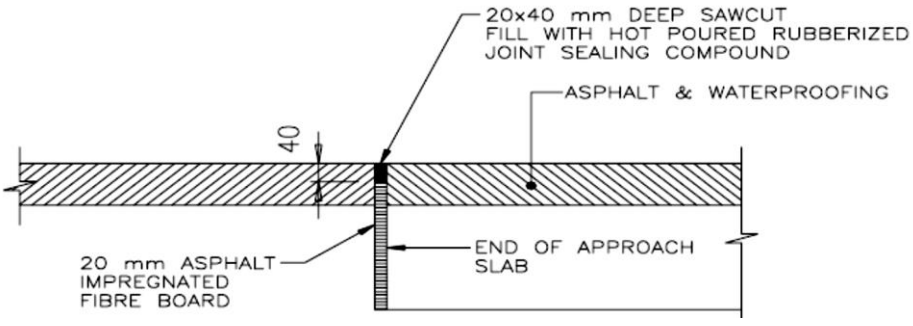

Figure 36: Expansion Joint at End of Approach Slab (maximum movement of 25mm) to Bagnariol & Husain (1999)

The gap inevitably opens up or widens in the winter season due to contraction and the edges of the asphalt pavements shows signs of separation from the sealing compound. During the summer months the gap closes up again and does not result in any loss of riding quality. The Figure 37 shows a typical joint showing separation from the sealing compound (Husain, 2000).

Figure 37: Separation of joint sealant from asphalt premix during winter (Husain et al 2000)

Where the overall bridge length exceeds the above limitations, there is generally evidence as seen in Figure 38, of a wider gap at the joint location. There is a much more discrete separation of the sealant during contraction of the bridge structure (Husain et al, 2000).

Figure 38: Distinct separation of joint sealant from asphalt surface due to limits being exceeded (Husain et al 2000)

Joint Type 2- The joint shown in Figure 39 presents a simple yet cost effective design for an intermediate length integral bridge with *light traffic* as suggested by the Alberta guidelines (2003). The joint sealant can de-bond during bridge contraction thus causing the joint to be opened. The opened joint can allow for debris accumulation and roadway drainage water to penetrate the joints and ultimately cause them to malfunction. The roadway drainage can also cause pavement pumping. The subgrade is protected by providing a sleeper slab under the end of the approach slab as shown above including weeping drains to facilitate movement of any water.

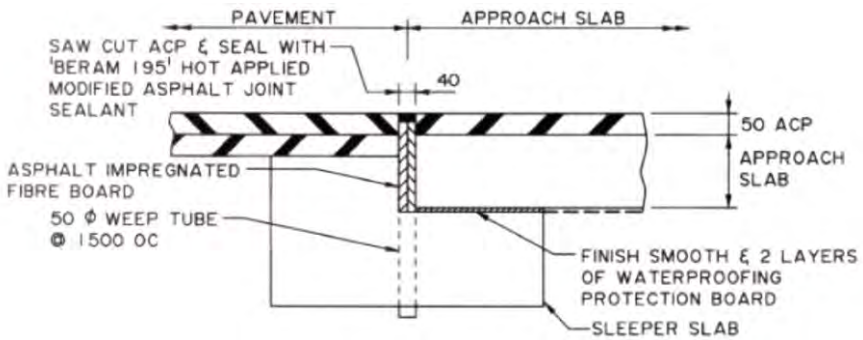

Figure 39: Cycle control joint type 2 – For Intermediate length bridges with light traffic - Short Integral Abutment Bridges, Alberta guidelines for design of integral abutments (2003)

The expected degradation is a somewhat long term progression of 5 to 10 years. The pavement failure will result in a localised "bump" in the pavement structure. The bump is generally of a minor problem to fix in comparison to the conventional deck joint maintenance. The ideal situation is to retrofit the joint with a neoprene compression seal after the head-slope and abutment backfill at the end of approach slab has settled down and stabilized according to the Alberta guidelines (2003).

Joint Type 3 -The joint shown in the figure 40 is also preferred for intermediate length bridges but on *main highways*. This type of joint is generally adopted where traffic interruptions must be avoided due to joint maintenance. The compression seal will prevent any deleterious material from entering the joint and may allow acceptable minor leakage. As an alternative to the above system, an asphaltic plug joint may be considered according to the Alberta guidelines (2003).

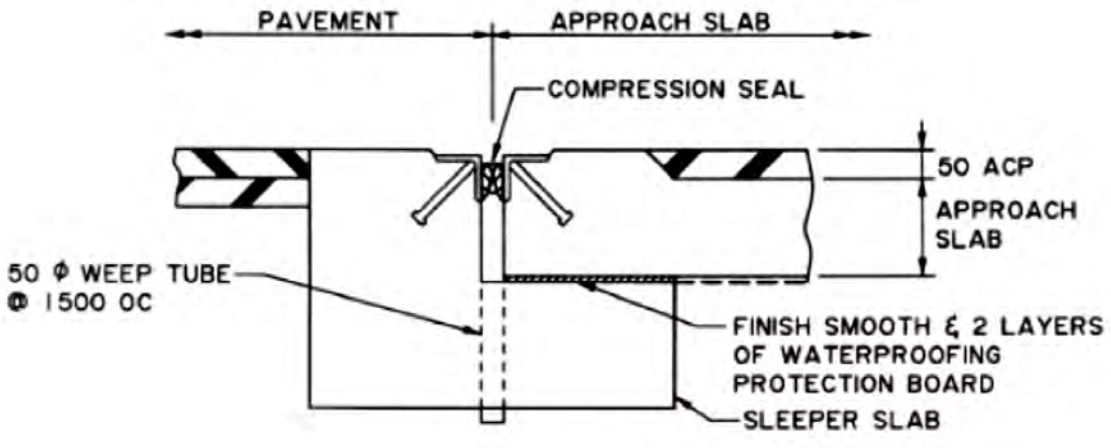

Figure 40: Cycle Control Joint Type 3- For Intermediate length bridges on main highways (Alberta guidelines, 2003)

Joint Type 4 – This joint as shown in Figure 41 is adopted for *long* span integral bridges, a large neoprene strip seal or finger joint may be used. This large joint requires proper support from a piled grade beam as they cannot tolerate any settlement. A roof slab connects the end of the bridge deck such that it can span from the girder end to the grade beam. An approach slab is then provided from the pile grade beam, beyond the roof slab. The above arrangement in Figure 41 may also be considered for intermediate length bridges with high traffic volumes (Alberta guidelines 2003).

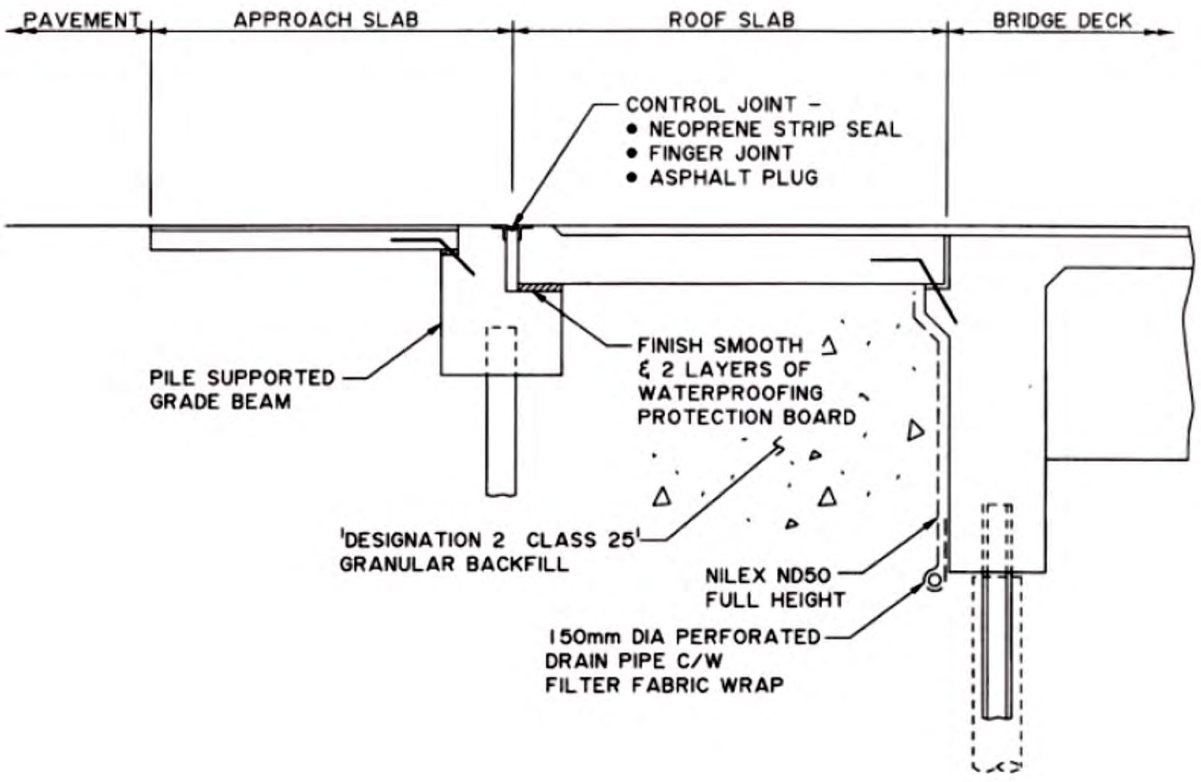

Figure 41: Cycle Control Joint Type 4- For long bridges (Alberta guidelines 2003)

The Alberta Transportation Board's (2003) guidelines on the design of integral abutments proposes joint types as summarised in the Table 10 below, provides general guidance for joint types based on varying integral bridge lengths.

Table 10: General guidance for joint type for various bridge lengths (Alberta guidelines 2003)

Steel girder bridges	Concrete girder bridges	Joint Type	Approx. movement range
< 40 m	< 50 m	1	< 16 mm
40 m to 75 m	50 m to 100m	2 or 3	16 < range < 32 mm
> 75 m	> 100 m	4	> 32 mm

Figure 42 is adapted from the Ministry of Transportation (Ontario) and was developed with the aim to improve the riding quality and also to reduce frequent repair work. The detail shown in Figure 42 is for integral bridges where the total length is more than 75m for steel structures and 100m for concrete bridges. One should note that this is somewhat different to the type 4 expansion joint discussed previously yet the limitations are the same (Husain & Bagnariol, 2000).

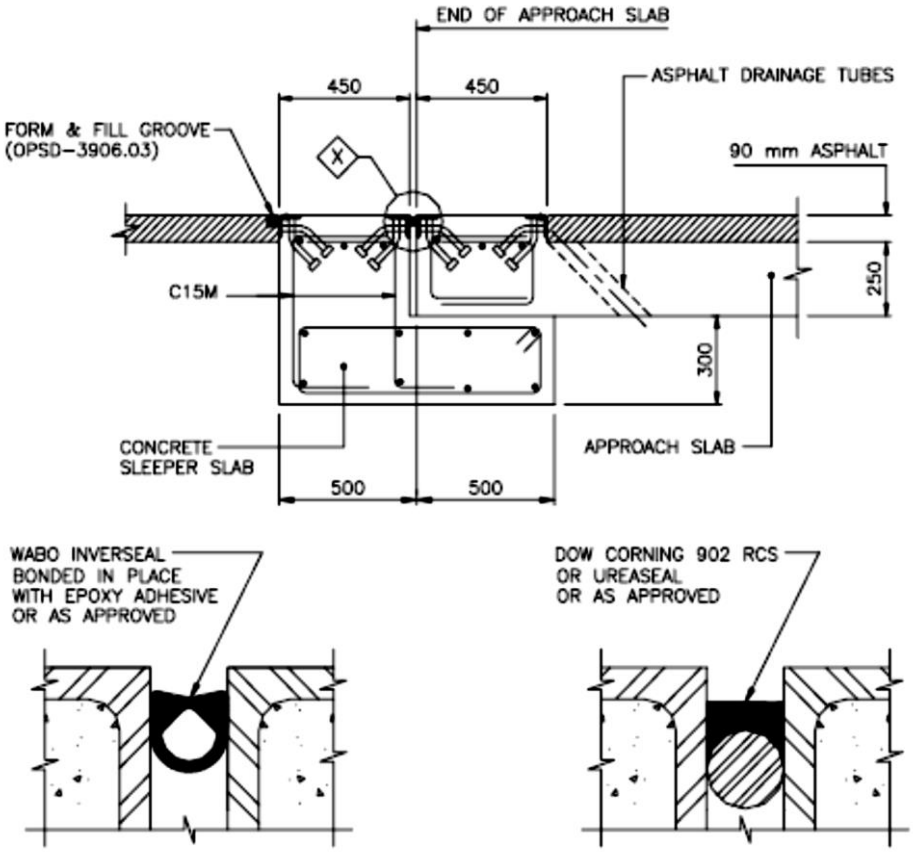

Figure 42: Expansion joint detail at the end of Integral Abutment approach slab (Husain & Bagnariol, 2000)

It could be argued that the integral abutment bridge concept moves the problem of an expansion joint from the bridge end to the approach slab end. However the North American opinion suggests that it is more economical and convenient to repair a damaged joint between the approach slab end and the highway itself rather than to do repairs to the expansion joint on the bridge deck itself. In places where de-icing salts are used, the leakage of expansion joints results in the spread of detrimental chloride-laden liquid. The chloride impregnation damage to the concrete elements and bearings (if used) is certainly more difficult and troublesome than repairing the premix layer at the end of approach slabs. The actual thermal movements that take place daily are much less than the theoretically calculated movements and it is the seasonal or extreme variations that lead to the rare limit state conditions (Lee, 1994). The de-icing salts and daily/ seasonal temperatures discussed by Lee (1994) is not applicable to most areas in South Africa.

It is important that the designer, before adopting an integral bridge design concept, considers all the constraints. Some additional matters over and above the normal structural evaluation are listed below by Lee (1994), as:

I. Climatic effects in the area
II. Soil-structure interaction evaluation
III. Traffic intensity, urban or rural
IV. Quality / budget of maintenance authority
V. Consequence of low performance
VI. Accessibility for repairs and the ease of lane closures etc.

During the construction of an integral bridge isolation joint, the quality control and the preparation of the sub-base greatly influences the long term durability and working functionality of the joint. A well-constructed expansion joint should be placed on a well compacted sub-base layer between sawn cut edges. The Figure 43 shown below illustrates an example of a well-constructed joint (Husain & Bagnariol, 2000).

Figure 43: Integral Bridge joint that is performing adequately (Husain & Bagnariol 2000)

An isolation joint that is carelessly made and where there is insufficient compaction of the subbase, results in the area around the joint being highly prone to early deterioration of the pavement, leading to more frequent maintenance. The Figure 44 depicts a joint which has had a poorly compacted sub-base (Husain & Bagnariol, 2000).

Figure 44: Low performance of integral abutment bridge joint due poorly compacted material under approach slab (Husain & Bagnariol 2000)

The Ontario Ministry of Transportation has gained considerable experience in the design, construction and performance of Integral Bridges. They have reported that;

> *"Bridges with less than 100m in length have performed well and appear to be ideally suited for this design . . ."*

3.5 Integral Abutment Bridge Transition Slabs

> *"Bridges of this type are widely spread in the United States but are also becoming popular in Europe, but the technical solutions are very different in different countries"*
>
> Frangi, Collin & Geier - 2011

The previous section discussed different types of isolation joints / expansion joints generally adopted at the end of integral abutment transition slabs. The transition slabs in the previous section were directly below the graded premix level. The statement above by Frangi et al (2011) refers to how various technical solutions are implemented by different organisations or countries. This section discusses the transition slab of integral abutment bridges, the concept differs from the previous section.

3.5.1 Summary of Research Work by Dreier, Burdet & Muttoni (2011)

One of the main issues with integral abutment bridges is the soil structure interaction, in particular between the compacted embankment and the transition slab or approach slab. For integral abutment bridges the transition slabs are directly connected to the end of the integral abutment deck. This chapter discusses an "alternative" where the transition slab end has no expansion but is rather buried under the premix layer into the actual layerworks. Dreier et al (2011) discuss the settlement of the pavement at the end of the transition slab and the cracking that forms in the premix pavement layer as shown in Figure 45 and thus requires in modifying details of the transition slab.

The use of conventional bridges with expansion joints can lead to costly and complicated maintenance issues as these mechanical elements must be replaced every 20 to 30 years as discussed in section 2.1.2. These degradations are significant for countries where de-icing salts are used such as Switzerland; also for bridges exposed to coastal areas and cold temperatures. The problem of de-icing salts is not relevant to South Africa as snow on the roads is not a major issue compared to countries such Switzerland. The replacement of bridge expansion joints in South Africa depends on a number of factors such as the type of joint, the regular maintenance and checking of the existing joint and also the initial installation of the joint. Joints and /or seals generally need to be replaced between 10 to 15 years in South Africa.

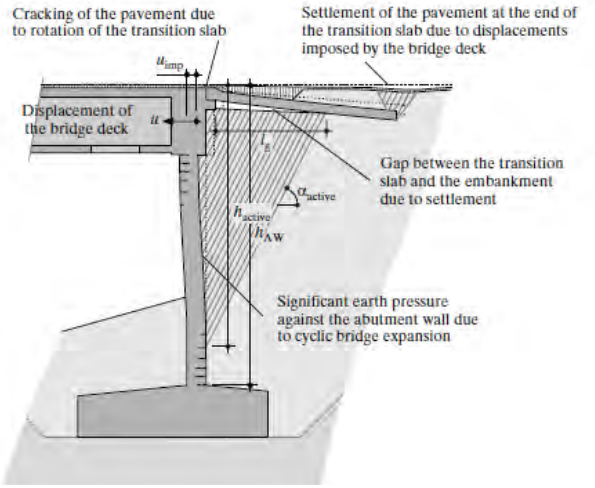

Figure 45: The effect of longitudinal movements on an integral bridge abutment (Dreier et al 2011)

The term u_{imp} is the imposed displacement from temperature, creep and shrinkage deformations of the bridge superstructure. Since the approach slab is connected, it also experiences the deformations. As the abutment wall moves, it inherently causes a change in the distribution and intensity of the earth pressure behind the abutment wall. The deformation of the abutment wall results in local settlement of the pavement at the end of the transition slab. This phenomenon is due to an induced active plastic mechanical development in the embankment. The settlement of the slab can become problematic at the serviceability limit state since the comfort of the road is reduced and alters the planarity of the road pavements (Dreier et al, 2011).

3.5.1.1 Numerical Model

The authors used finite element software to simulate the complex soil structure interaction between the end of the integral abutment approach slab and the soil. The model of a semi-integral abutment was adopted for the investigation as shown in Figure 46 below. For the study, the difference between an integral and semi-integral abutment model are negligible as the main difference is that semi-integral bridge has bearings. The assumption is also valid since the main concern is at the end of the approach slab which is similar for integral and semi-integral bridges.

The important variables used in the study of the transition slab were;

L_{TS} – length of transition slab

α_{TS} – slope

h_{TS} – thickness

$e_{TS,0}$ - buried depth of the transition slab at the point 0, where the bridge deck and transition slab connect

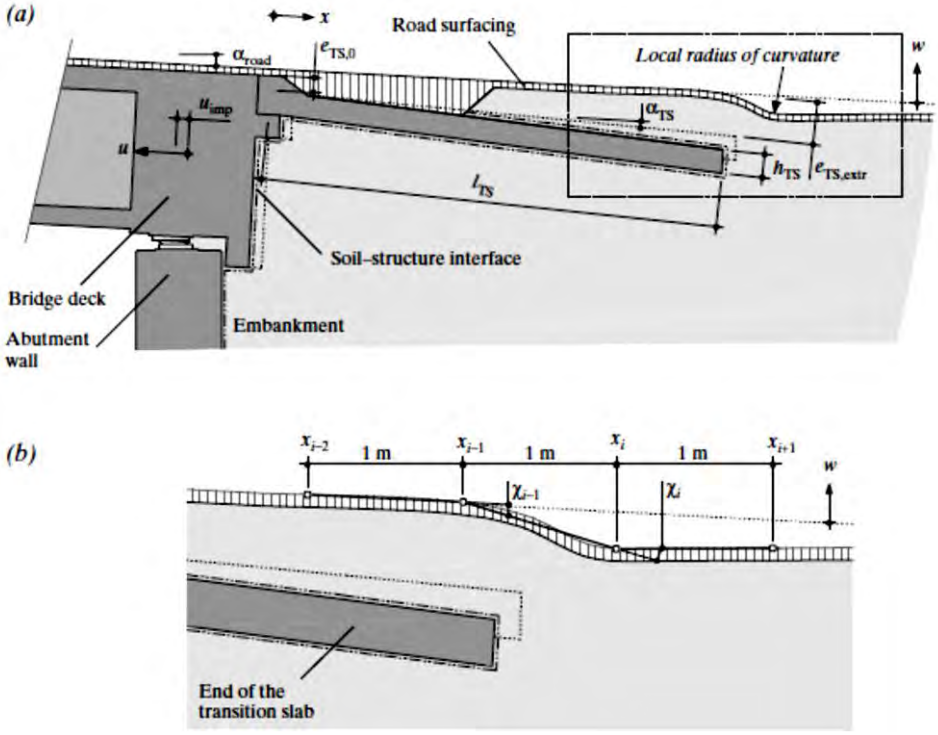

Figure 46: (a) Geometrical model adopted for the numerical analysis; (b) definition of slope variation criterion χ (Dreier et al, 2011)

According to Figure 46a, the assumed geometry of the transition slab is consistent with the Swiss recommendations for transition slabs of integral abutment bridges.

L_{TS} – length = 6m

α_{TS} – slope = 10%

h_{TS} – thickness = 0.3m

$e_{TS,0}$ - buried depth of the transition slab at the point 0, were the bridge deck and transition slab connect = 0.1m

The thickness of the premix in the model was 70mm. The slope of the road α_{road} is assumed to be zero and this variable does not influence the results. The imposed displacement (u_{imp}) for the study was chosen to equal 50mm.

The Swiss recommendations discussed above is generally similar to the approach slabs constructed in South Africa.

3.5.1.2 Road Pavement Planarity Limit State

A slope variation criterion χ according to the Swiss code was adopted to quantify the planarity of the road. It considers the depth and length of the settlement and yields an efficient evaluation of the local curvature, thus the comfort of the road. This slope variation χ must always be less than the limit value of χ_{adm} (admissible slope variation) and according to the Swiss codes χ_{adm} is equal to 28% for normal roads and 20% for highways.

To investigate if the imposed displacement is u_{imp} is acceptable for road users i.e. it must pass limiting value of χ_{adm}. The Figure 47 was generated by plotting the maximum and minimum values of χ in

the range of the transition slab displacement. The useful parameter from this graph is obtaining the maximum admissible displacement $u_{imp,adm}$ for a given χ_{adm}.

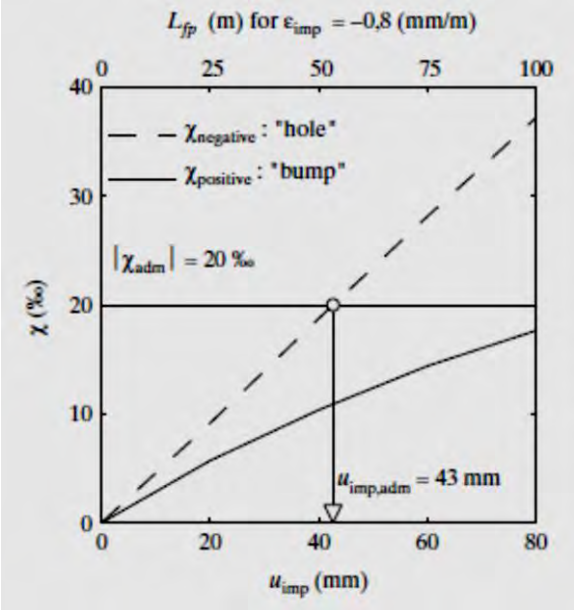

Figure 47: Graph showing admissible imposed displacement ($u_{imp,adm}$) for χ_{adm} of 20% based on the Swiss codes (Dreier et al, 2011)

The admissible imposed displacement $u_{imp,adm}$ for highways (χ=20%) for the standard geometry of a transition slab provides 43mm. According to the Swiss national codes if a total imposed deformation ε_{imp} = - 0.8mm/m for a concrete bridge deck (sum of ε_{cr}= - 0.2, $\varepsilon_{c,sh}$= - 0.35mm/m and $\varepsilon\Delta$T = -0.25mm/m due to ΔT= - 25 C°), this provides a maximum distance between the concerned abutment and the fixed point of the bridge deck of 54m.

Bridge ends that undergo major retrofitting to transform a conventional bridge into a bridge with integral or semi-integral abutments do not have to consider creep and shrinkage effects. It is assumed that the creep and shrinkage effects on a conventional bridge have already taken place. Thus for admissible imposed displacement $u_{imp,adm}$ of 43mm and assuming a residual deformation of ε_{imp} = - 0.4mm/m, the maximum possible length between the newly converted integral abutment and fixed point of the bridge is 108m. Thus, the longest possible length of a bridge with two retrofitted abutments and fixed point in the centre is 216m.

The situation that generally governs is for movement away from the abutment i.e. active soil conditions. Research has shown that in the passive direction, the settlements in this case are significantly less problematic because the displacement to activate the passive plastic mechanism is much higher than for active mechanism conditions. For concrete conditions the active mechanism also has creep and shrinkage in the active direction.

3.5.1.3 Cracking of the Road Pavement at the Bridge Deck and Transition Slab Interface

The displacement of the transition slab can lead to cracking of the road pavement at the connection between the transition slab and the bridge deck as shown in the Figure 48 below. These cracks

generally occur during the winter season when the road premix is brittle due to low temperatures. The low temperatures (i.e. below 0^{o}) is very localised, and occurs only in certain regions of South Africa. The cracks are a result of the following:

- Rotation of the transition slab around the connection due to settlement behind the abutment wall induced by the imposed displacement.
- Repeated deflections caused by flexure when trucks and heavy vehicles move over the transition slab.

Figure 48: Cracking of the road pavement at the transition slab and bridge deck interface for a 68m semi-integral bridge (Dreier et al, 2011)

3.5.1.4 Improved Connection Detail of the Transition Slab and Integral Abutment

Figure 49, below shows a connection detail with a dowel bar where the transition slab rotates around the steel stud. The rotation propagates to the surface thus this detail is prone to localised cracking. This detail is unfortunately not ideal for integral or semi-integral bridges because the stud/dowel connection is too weak to transfer the longitudinal forces generated from the displacements.

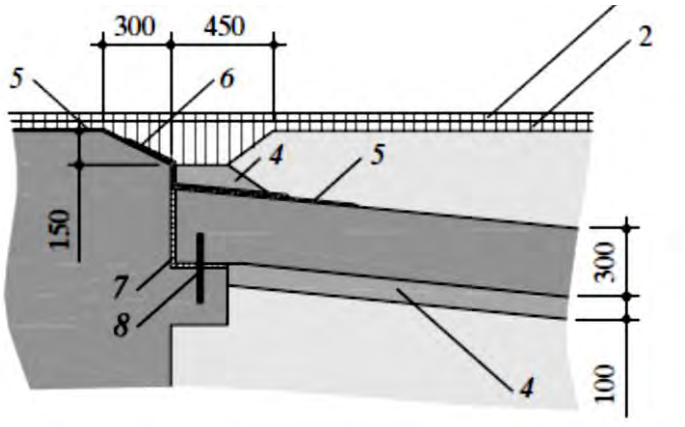

Figure 49: Standard abutment/transition slab joint with dowel bar (Dreier et al 2011)

Figure 50, below shows the detail currently recommended in Switzerland for integral abutment decks. This detail is favourable with respect to cracking as the centre of rotation of the transition slab is at the level of the connection reinforcement. This connection can carry the internal forces from imposed

displacements. This detail is slightly difficult to construct as it is monolithic with the abutment and the bitumen layer (no.11 as shown in Figure 50) must be placed before the connection reinforcement is fixed.

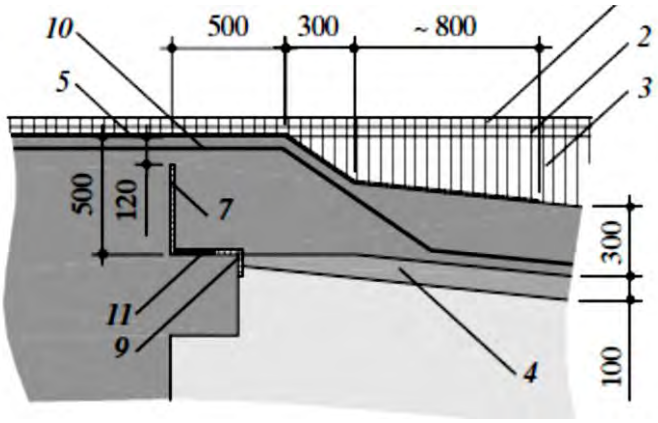

Figure 50: Detail of abutment/transition slab for integral abutment bridges according to Swiss recommendations (Dreier et al 2011)

Figure 51, below is an improved detail by Dreier et al (2011) and adopts the principle of a concrete hinge. The reinforcement is such that the shear failure is prevented by diagonal connection reinforcement. The construction is simpler and the distribution of the rotation of the transition slab over the entire length of the concrete hinge l_{ch}. The cracks from this detail showed small openings that cannot propagate to the road surfacing.

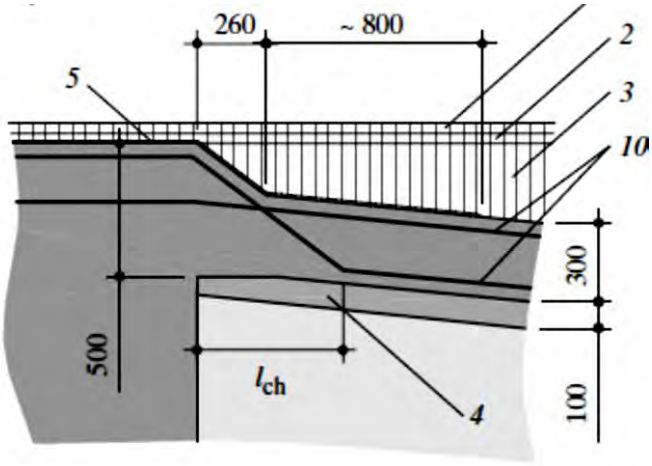

Figure 51: Improved detail for integral abutment bridges (Dreier et al 2011)

3.6 Behaviour of Piles Supporting Integral Abutment Bridges

SUMMARY OF RESEARCH WORK BY ARSOY, DUNCAN AND BARKER (2002)

The literature regarding the behaviour of piles supporting integral abutment bridges under cyclic loading is limited. Published papers on this subject used actual behaviour of the following bridges;

- Cass County Bridge
- Boone River Bridge
- Maple River Bridge
- And a bridge in Rochester, Minnesota.

These bridges were monitored for approximately 2 years. They were subjected to real-life temperature cyclic loading. A summary of the bridge details and behavioural performance is discussed in Table 11.

Table 11: Summary of Integral Bridge pile details and performance (Arsoy et al 2002)

Bridge Name	**Location**	**Overall Length (m)**	**Type of superstructure**	**Type of Piles & Orientation**	**Pile Behaviour and results from monitoring period (mm)**
Cass County Bridge	North of Fargo – North Dakota	137 m (6 Spans)	Concrete deck & Prestressed concrete girders	• HP 10x42 Piles orientated in weak-axis bending under abutments and strong-axis bending under piers. • 6.1m predrilled boreholes were used.	• During monitoring period, strain gauges failed. Stress was based on analytical methods and concluded that maximum pile stresses were around yield stress. • Piles were able to tolerate 50mm bridge contraction and about 75mm total displacement.
Boone River Bridge	Central Iowa	98.9m (4 spans) & skew of 45 degrees	Concrete deck & Prestressed concrete girders	• HP 10x42 Piles orientated in weak-axis bending and battered 4:1 in the movement direction of the bridge. • 2.74m predrilled boreholes were used.	• Maximum pile stress was about 60% of nominal yield stress of piles • Bridge experienced 30mm contraction and about 50mm total displacement without any damage to piles.
Maple River Bridge	Northwest Iowa	97.5m (3 spans) & skew of 30 degrees	Composite Concrete deck & steel girders.	• HP 10x42 Piles orientated in weak-axis bending and battered 3:1 in the movement direction of the bridge. • 3.66m predrilled boreholes were used.	• Maximum pile stress was about 75% of nominal yield stress of piles • Bridge experienced maximum 40mm contraction and total bridge displacement was around 76mm.
Bridge in Rochester	Minnesota	66m (3 spans)	Concrete deck & Prestressed concrete girders	• Integral abutments are 0.9m wide and 1.5m high. • Supported on HP 12x53 piles orientated in weak-axis bending.	• Piles were able to tolerate 20mm bridge contraction and 32mm total displacement • Maximum pile stresses slightly above nominal yield stress of piles

Laboratory testing was performed on different types of piles by simulating them to similar conditions as piles supporting integral abutment bridges and conclusions regarding their performance have been reported. The piles were subjected to 75 years of simulated bridge life by subjecting the piles to cyclic lateral load tests. Over 27,000 displacement cycles were applied. The piles investigated were an H-pile, a pipe pile and a prestressed reinforced concrete pile.

"*Bridge superstructures are so stiff in comparison with approach fills and piles supporting abutments that the magnitude of the temperature-induced displacements are almost unaffected by the stiffness of the abutment piles. The stiffest abutment piles and the most flexible abutment piles are subjected to the same displacements. The ability of the piles to accommodate lateral displacements without distress is a significant factor in determining the maximum possible length of integral bridges, because temperature-induced displacements are proportional to bridge length.*"

(Arsoy et al 2002)

The statement above by Arsoy et al (2002) argues that due to the high difference in stiffness between the superstructure and abutment piles, any thermal movements will cause the pile to deform accordingly irrespective of the pile stiffness. This is also an important key for determining the maximum possible lengths of integral bridges. The piles behave as an equivalent cantilever with a free head at the top of pile easily moving to accommodate the deck thermal movements. The concept is illustrated in the Figure 52 i.e. pile is fixed at one end and free headed at the other end.

Figure 52 shows the configuration that was used in the laboratory testing. For convenience the test pile cap and pile were inverted. It is important to note that the study does not include soil-structure interactions. The investigation studies the pile behaviour under realistic cyclic displacements induced due to thermal effects.

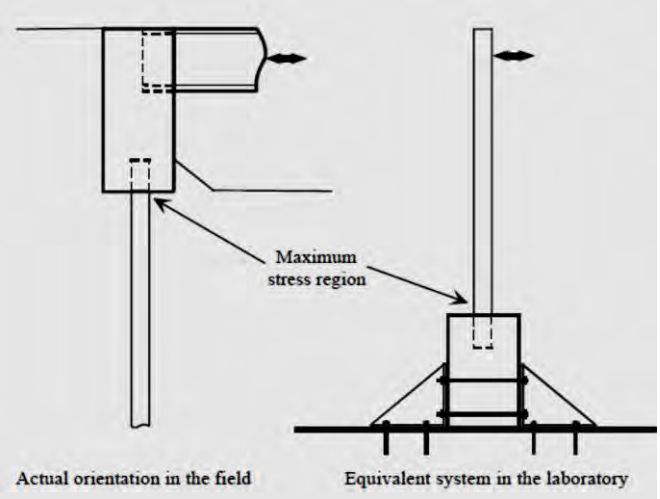

Figure 52: Pile and pile cap configuration adopted for laboratory testing (Arsoy et al 2002)

The three types and details of the piles used for the testing are listed below;

- The H-pile that was tested was an HP 10x42.
- The pipe pile had a 356mm outer diameter and 12.7mm wall thickness.
- The prestressed concrete pile that was adopted was a square pile (305mm x 305mm). Five 12,7mm, 1862 MPa low relaxation steel strands were used in the pile.

Table 12 provides more details of the piles used in the investigation.

Table 12: Properties of piles tested in the laboratory investigation (Arsoy et al 2002)

Pile Type	Strength * (MPa)	Area (cm^2)	Area Moment of Inertia (cm^4)
H-pile	372.3	80.0	463
Pipe pile	310.3	136.8	3,123
Concrete**	34.5	929.0	11,148

* Tensile yield strength of the H- and the pipe pile, and compressive strength of the concrete pile.
** Prestressed reinforced concrete pile.

The Figure 53 shown below is a schematic diagram showing the fixity of the pile cap at one end. Figure 53(a) is the plan view and Figure 53(b) is the cross-sectional view.

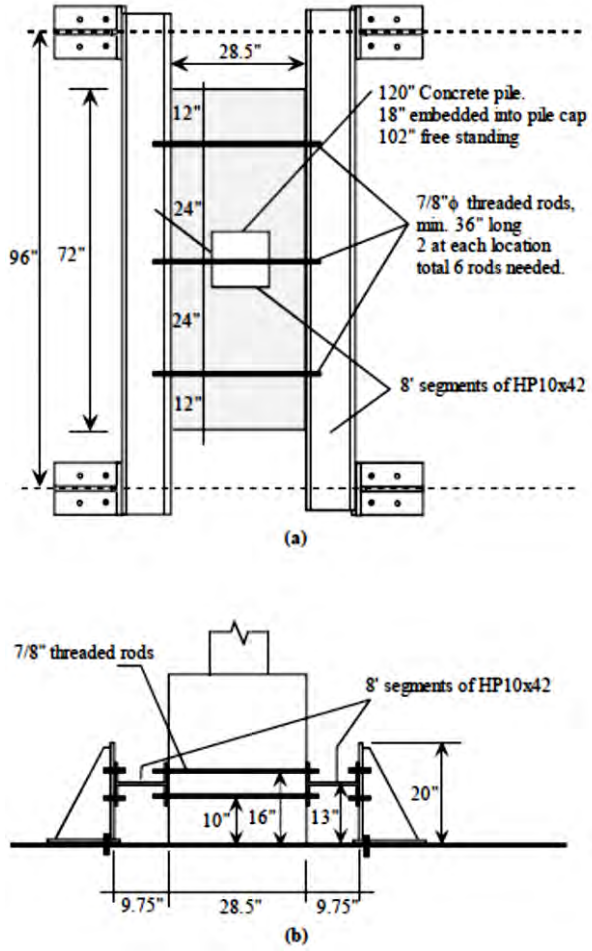

Figure 53: Method adopted for mounting pile caps for the laboratory investigation (Arsoy et al, 2002)

The Figure 54 is a photograph of the test that was conducted in the laboratory.

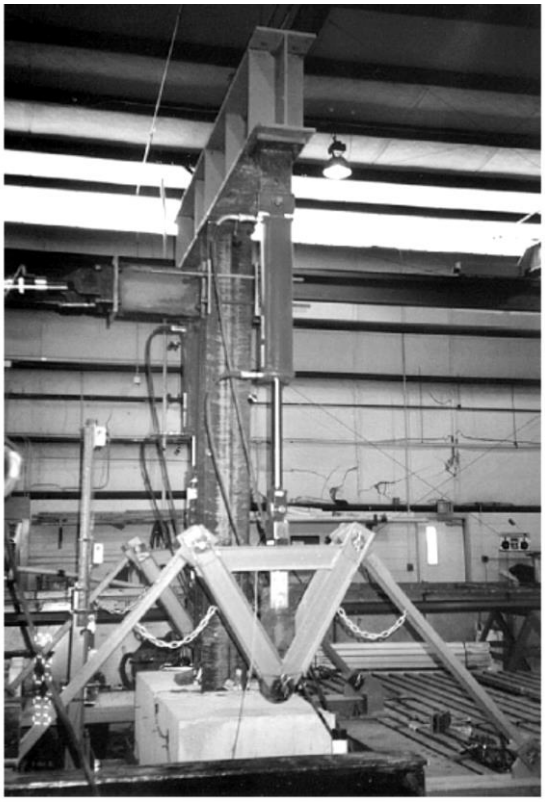

Figure 54: Photograph of experimental setup (Arsoy et al 2002)

Results and recommendations from investigation by Arsoy et al (2002)

H-pile Test

The investigation showed that for a given load, the maximum measured strain was about half of the strain calculated for a fixed-end column (pile was free at one end and fixed at the other end). The reason for this behaviour was because the pile cap was not fully fixed against rotation. Pile displacements were plotted along the pile for selected loads as shown in Figure 55. The graph shows that the slope at the bottom of the pile is not zero, which indicates there is some rotation of the pile cap thus the pile behaves as a "partially fixed column". The H-pile, when orientated about its weak axis displayed the best behaviour of the piles tested. The pile experienced cyclic loading stress in excess of 138 MPa and static loading stress of 241 MPa without any signs of distress and deformation.

> *"This superior level of performance under cyclic loading makes H-piles a good choice for support of integral bridges.*
>
> *(Arsoy et al 2002)*

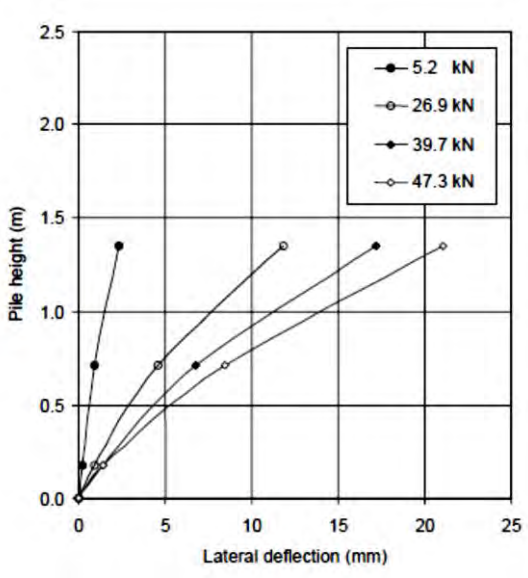

Figure 55: Graph showing displacements for H-pile based on selected lateral loads (Arsoy et al 2002)

Pipe Pile Test

The pipe pile was approximately twice as stiff as the pile cap thus the pile cap of the pipe pile rotated more than that of the H-pile. No damage was observed on this type of pile. The researchers anticipated that an abutment supported by this type of stiff pile would be subjected to higher stresses because the loads required to deflect the pile would be larger. The piles could support an integral abutment bridge but special attention should be given to the design details to prevent damage due to cyclic loading as advised by the authors.

Prestressed Concrete Pile Test

In the first trial, tension cracks developed at the bottom of the pile where it was connected to the pile cap. During the testing the tension cracks gradually increased in the pile from the bottom and progressed to the top. It was also noted that the five cracks gradually enlarged as the load cycles continued. Figure 56 shows a typical tension crack through one of the strain gauges. The concrete piles were tested with no vertical load and it was anticipated that more severe damage to the piles would have occurred with vertical loads. At the end of the test, it was observed that approximately 20% of the original pile cross-sectional area was still in contact. The vertical load would have induced a very high compressive stress due to the significantly reduced cross-sectional area. The research concluded that the use of concrete piles to support integral abutment bridges is not the best solution due to the formation of cracks with a gradual increase of cracks under cyclic loading, and more research work was required.

Figure 56: Formation of tension cracks on the precast concrete pile (Arsoy et al 2002)

3.7 Pile Pre-Drilling and Sleeving of Piles

Piled abutments are commonly used in North America for integral abutment bridges. As discussed in the previous section, the research by Arsoy et al (2002) found that, for integral abutment piles, it is advantageous that the piles can accommodate any lateral displacements induced from the deck. Designers have thus adopted techniques such as (Card & Carder):

I. Adopting slender piles such as steel H-piles or precast concrete piles
II. To improve the flexing behaviour, limit the number of piles to a single row
III. Orientate piles vertically to minimise resistance
IV. Orientate the weak axis of H-piles normal to the direction of movement
V. Where the insitu foundation materials are very stiff or rigid, oversized pre-bored holes are used. The primary purpose of pre-boring is to allow the upper zone of the pile to have sufficient flexibility to deflect without the rigid soil restraining the movement. The pre-bored holes are typically 2m to 5m deep. Prior to the installation of the piles they are filled with loose granular material (Girton 1991 cited in Card and Carder 1993)
VI. Piles are generally limited to steel H-piles as they have longer fatigue life
VII. Reduce depth of abutment embedment into embankments to reduce resistance
VIII. Control bridge skews

An alternative to pre-boring as discussed by the guidelines for design of integral abutments by Alberta Infrastructure and Transportation (2007) is to install the single row of steel H-piles in permanent steel casings, also orientated for weak-axis bending. However due to the probability of the loose granular fill being compacted over time thus restraining the pile, it is preferred to leave the casing voided unless some type of elastic fill material is adopted.

Some other relevant considerations that the guideline provides are listed below;

I. Steel casing around piles should be designed to last the same life span of the bridge
II. A sacrificial corrosion thickness should be allowed for in the pile section
III. The H-piles should be embedded at least two pile sizes into the abutment beam

The Figure 57 shows a schematic diagram of a steel H-pile that is isolated by using a corrugated steel pipe (CSP) and filled with loose sand.

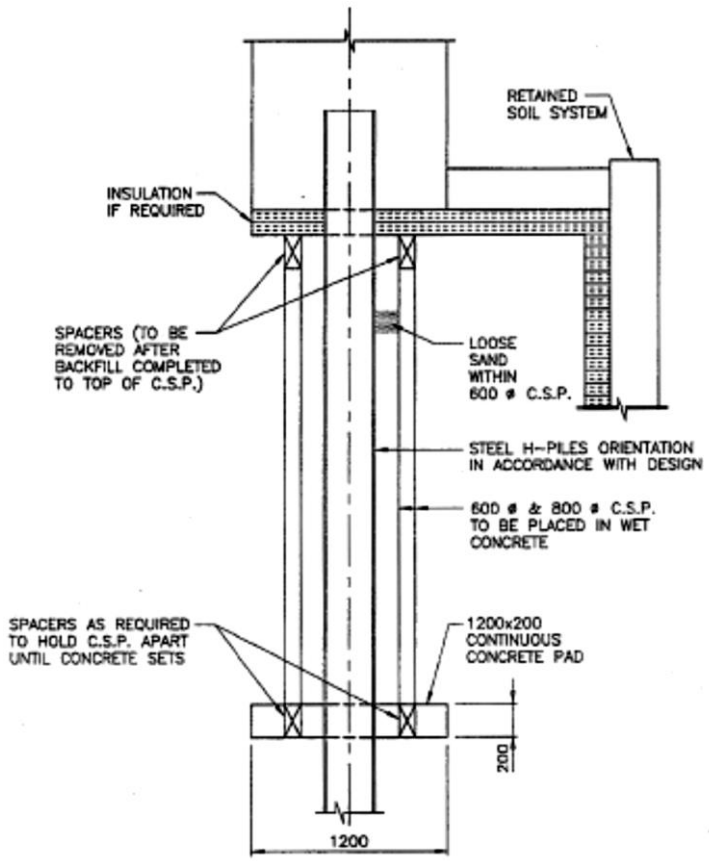

Figure 57: Integral abutment bridge piles with sleeve detail as per Ontario Ministry of Transportation (Husain & Bagnariol, 1996)

The Figure 58 shown below is a photograph of a single row of steel H-piles being isolated by using pipes around the pile.

Figure 58: Corrugated plastic pipe sleeving around steel H-piles used in UK (White 2007)

A European Survey conducted revealed that some countries such as England and Sweden adopt sleeves around the piles to easily allow for the free bending of the piles due to superstructure translations. The longitudinal translation is distributed along a greater length of the freestanding pile thus the moment induced in the pile is reduced. Since there is no soil around the pile shaft to prevent buckling, the pile inherently behaves similar to a freestanding column thus requires durable piles to accommodate the unsupported length. One of the disadvantages is that once backfill is around the sleeves, inspections of piles is virtually impossible (White 2007).

3.8 Front Elevation of Integral Bridge Abutments

The front elevation of integral abutment bridges predominantly depends on what the bridge primarily spans over and the purpose for the bridge. Most integral bridge abutments generally act as a typical pier to simply achieve sufficient flexibility whilst the soil mass behind the abutment is retained by separate retaining mechanisms. A commonly adopted mechanism used with integral abutments is the use of mechanically stabilised earth retaining walls. Figure 59 shows the different concepts for integral abutments generally constructed (Concrete Bridge Development Group 2014).

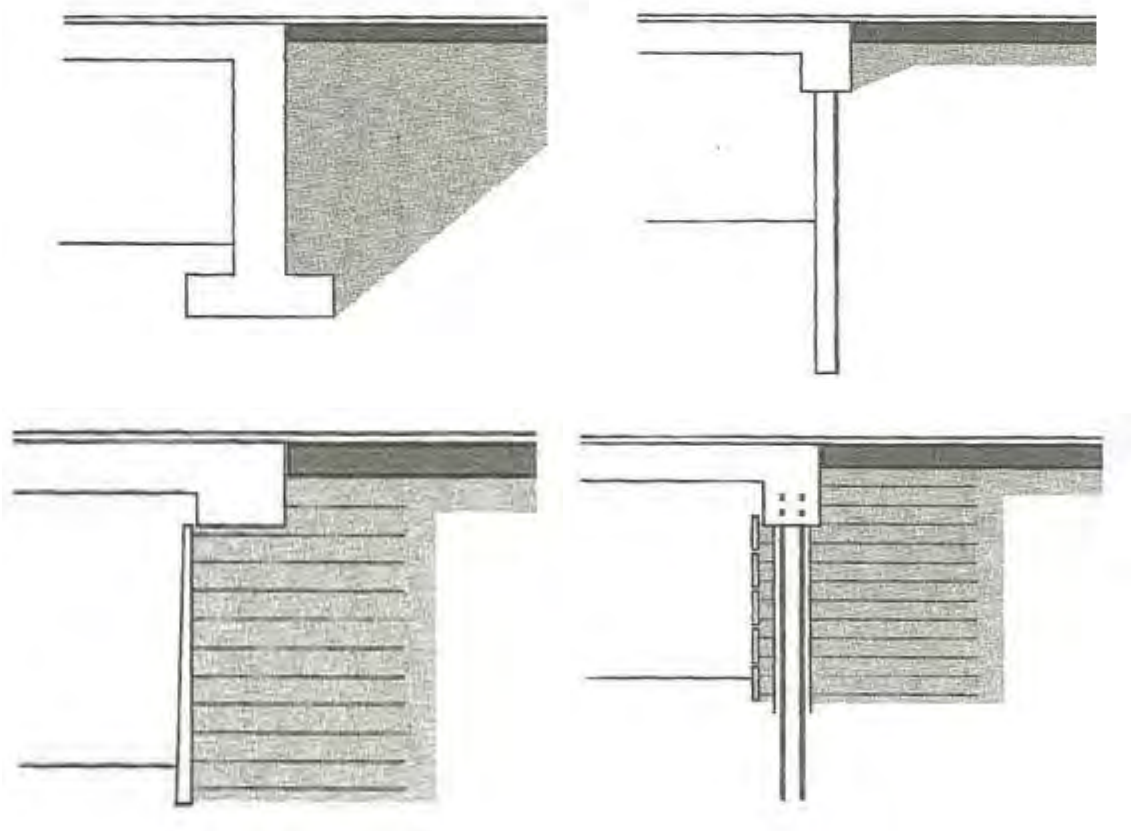

Figure 59: Different concepts for Integral abutment bridges (Concrete Bridge Development Group, 2014)

Figure 60 shown below is the front elevation of an integral bridge abutment with the fill being retained by mechanically stabilised earth retaining walls. The superstructure consists of prestressed beams with a top slab.

Figure 60: Integral abutment with retained soil system (Ontario Ministry of Transportation 2008)

Figure 61 is a cross-section of an integral abutment bridge showing the soil retaining system and the isolation of the piles in the top few meters.

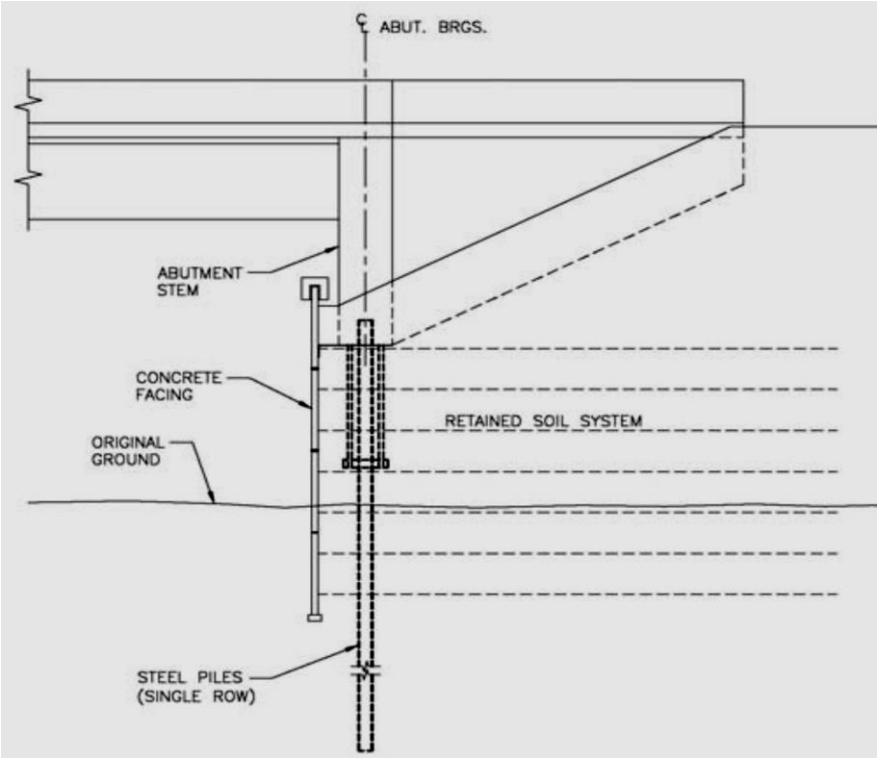

Figure 61: Section of integral abutment showing sleeves around piles and retained soil system in place (Ontario Ministry of Transportation 2008)

3.9 Nature of Backfill behind Integral Abutment Bridges

The backfill material behind integral abutments should be a designed material with specified properties that are validated during the construction phase. The specification should cover two important aspects; stiffness and flexibility. Well-rounded compacted granular material of uniform grading can provide a peak angle of internal friction (Φ) of about 35°. This may accommodate the thermal expansion without inducing high earth pressures but may undergo settlement. On the other hand, well graded and compacted, hard angular particles may produce a peak angle of internal friction as high as 55°. This will have very high resistance to thermal movements and less vulnerability to settlement. According to the BA 42/96 Highways Agency guidelines (2003), for integral bridges exceeding 40m, the granular backfill should have a peak angle of friction of not greater than 45° when tested in accordance with the Specification for Highway Works. The zone of granular backfill should be an angle of at least 45° from the bottom of the wall extending to the top (BA 42/96 Highways Agency guidelines 2003).

3.10 Chapter Summary

Based on the calculated movement of the superstructure the bridge designer should appropriately select the expansion joint as proposed in Section 3.4 of the literature review. The most suitable type of expansion joint to be chosen for the end of the approach slab is suggested in Table 10, adapted from the Alberta Guidelines (2003) which are widely used. The designer also has the option of not using any expansion joint at the end of the approach slab. This concept is discussed by the research done by Dreier, Burdett and Muttoni (2011). This concept has no form of joints as the approach slab is embedded within the road layerworks fill, however it is anticipated that a “bump” in the roadway may result. This issue of the undulation in the road surface is not considered a major serviceability concern provided it is within tolerable limits as proposed by Dreier et al (2011). The second concept of no joint is assumed to be most appropriate, however the integral bridge length is limited to a maximum of 108m as discussed in the research work.

Integral bridges have numerous advantages but also has their own unique challenges. The main aim of this chapter was an extension of Chapter 2 addressing issues and solutions proposed concerning integral bridge abutments. This chapter introduced the soil-structure interaction and discussed a few design concepts such the equivalent cantilever method. The equivalent cantilever method is widely used by many bridge design offices to design the piles for integral abutment bridges. The fundamentals of laterally loaded piles were briefly described. Other solutions to isolate the soil and structure were introduced such as adopting a stress-absorbing layer behind the abutment structure. An important aspect regarding the ratcheting effect and failure was discussed and concepts using stress-absorbing layers where introduced. Under the latter subject, the approach slab and sleeving of piles was introduced and is an important practice to try and increase flexibility of the abutment system. The approach slab for integral abutments is slightly different to convention bridge abutments. The concepts presented showed that the approach slabs are generally fixed for integral bridge abutments and not pinned as per the conventional. This chapter also presented interesting findings on the behaviour of different pile types under cyclic loading. As per the literature from various authors, the investigation showed that the steel H-pile is very superior for this type of application. There are a number of issues and challenges with integral abutment bridges, however there are just as many concepts and theories at present to resolve these problems.

4 PROCEDURE OF INVESTIGATION

4.1 Introduction

The aim of the investigation was to identify some of the suitable pile types that a bridge designer should consider for an integral abutment bridge and to understand their behavioural performance. Various pile types that are commonly used for conventional bridges in South Africa were adopted in the study such as PC piles and auger piles. Steel H-piles and pipe piles are not common in South Africa but were considered in the investigation for comparative purposes as they are usually adopted in integral bridges in other countries, as shown by the research in Section 2.4 from the literature review. Other piles are also used for integral bridges but there are certain concerns as highlighted in Section 3.6, the research work done by Arsoy et al (2002).

The theoretical desktop study simplifies the analysis of piles by disregarding the soil spring interaction which was discussed in section 3.1.2.1, thus considering the pile to act as an equivalent cantilever column. Some authorities design integral abutment piles by modelling in the soil spring stiffness while many other bridge authorities have mastered the equivalent cantilever pile concept method. Many integral abutment bridges have been designed successfully by adopting the equivalent cantilever pile concept such as the M50 Freeway Bridge in Ireland (Figure 18). Ontario also adopts pile design using the equivalent cantilever method and the results are reported as being reasonable. Another reason this method is favourable is because the top portion of piles for integral abutment bridges is generally free as it is sleeved to allow sufficient flexibility to accommodate the deck movements as discussed in Section 3.7 and examples provided in Table 11. The bottom of pile is almost fixed into the ground, free along the sleeve and able to accommodate the deck movements at the top of pile, thus the idealisation as a cantilever is reasonable.

The approach taken in this investigation aims to provide the designer with a rudimentary understanding of the behavioural performance of the pile type that should be adopted. To obtain more accurate results, the designer should perform further analysis with soil spring stiffness and appropriate software, if required. The spring constants often remain a challenge and some guidance is provide in Section 3.1 and 3.2.

4.2 Formulas and Methods Adopted

Different types of piles were chosen for the study to determine the behaviour of piles for integral abutment bridges. The length of the effective cantilever of the pile was also varied and a number of cantilever lengths were used in the study to investigate the relevant parameters. The guidance for choosing suitable effective cantilever lengths was discussed in Section 3.7 and typical examples provided in Table 11. The lengths used (also referred to as effective pile height) were 2m, 3m, 3.5m and 4m.

It is important to note that the study was based on the pile being fixed at the bottom and free at the top i.e. free pile head. This assumption is supported by the work done by Arsoy et al (2002) as discussed in Section 3.6. The statement at the top of page 60 describes how irrespective of the stiffness of the piles, the superstructure is considerably more stiffer and any displacements from the superstructure (e.g. thermal movements) will directly result in the piles absorbing and moving accordingly to the magnitude of this movement. The work done by Arsoy et al (2002) implies that the top of pile is essentially free to move although it is fixed to the deck. This theory is backed up by Figure 52 which shows the actual orientation on a construction site, and the equivalent system in the laboratory. The model also shows no springs as in most cases the top zone of the pile is within a sleeve.

The discussion above assumes that the soil behind the abutment is not involved in restraining the movements from the deck. As highlighted in Chapter 3.3, common practice in many countries is to isolate the structure from the soil thus preventing the ratcheting effect discussed in Section 3.3.2. This is often done by adopting a mechanically stabilised earth retaining wall to hold the fill material and using a stress-absorbing layer (e.g. expanded polystyrene) directly behind the abutment as emphasised in Section 3.3.3 and illustrated in Figure 30. Coupled with this detail is a joint used at the end of the approach slab as discussed in Section 3.4.

There are two scenarios to consider regarding the deflection of vertical piles carrying lateral loads as discussed by Tomlinson (1994);

I. Free pile head – top of pile is unrestrained and tends to rotate and undergo a degree of translation.
II. Fixed pile head – top of pile is restrained (fixed) to the pile cap or braced but has the freedom to translate.

Figures 62 and 63 shown below illustrate this concept. Based on the findings in the literature review the free headed pile was adopted, but fixed headed pile is shown for comparative purposes.

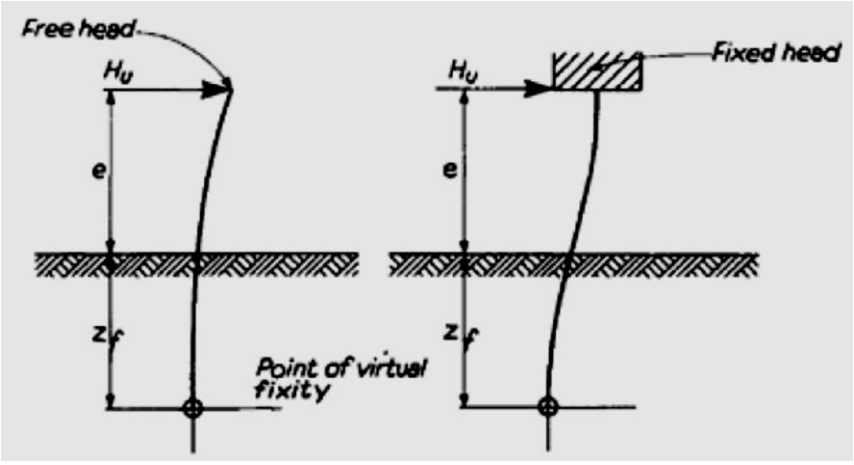

Figure 62: The cantilever concept of free pile head and fixed pile head (Tomlinson 2004)

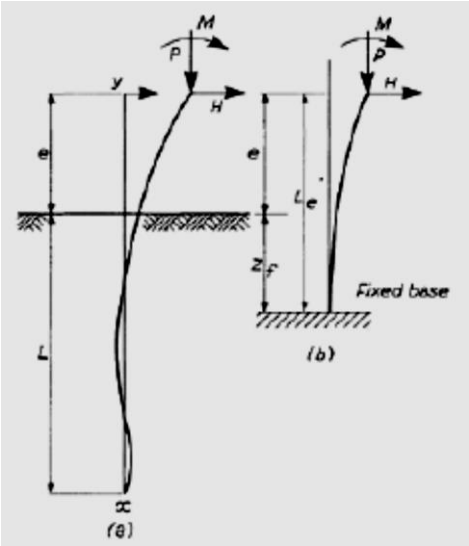

Figure 63: Bending of pile under vertical and horizontal loads (a) Partially embedded pile; (b) Equivalent cantilever pile (Tomlinson 2004)

The analysis made use of the following equations which were derived from structural theory as the piles under horizontal load are considered as simple cantilevers (Tomlinson 2004). The derivations are shown in Appendix F.

1) Horizontal deflection at head of fixed-headed pile: $y = \frac{H(e+ z_f)^3}{12EI}$

2) Horizontal deflection at head of free-headed pile: $y = \frac{H(e+ z_f)^3}{3EI}$

Where:

y = Horizontal deflection at the head of pile investigated about each axis

H = Horizontal force at the head of pile

E = Elastic modulus of material forming the pile shaft

I = Moment of inertia of the cross-section of the pile shaft

z_f = Assumed arbitrary depth to point of virtual fixity

e = Free length of pile shaft

The analysis was done by calculating the typical range of movements of integral abutment bridge decks (according to the formula discussed above). The same amount of translation was assumed to be transferred to the top of pile heads. The effective pile height refers to the length of the pile that is sleeved i.e. *Length of pile sleeve* = $z_f + e$.

The important results obtained from this study were pile bending moments and pile shear forces. The most important aspect that these parameters are associated with is the translation or deflection at the head of the pile as these are the typical translations of the actual bridge deck at the abutments due to thermal effects, creep and shrinkage as discussed in Sections 2.3.1 and 2.3.2 respectively. The relationship between slenderness ratios and stiffness of the piles was also investigated.

Table 13 shown below contains details of the piles chosen for this study. The concept was adapted from the work done by Arsoy et al (2002) discussed in the literature review. The study done by Arsoy made use of steel H-piles (both axes investigated), a pipe pile and a square precast concrete pile. The authors recommended that more research on the different types of pile for integral abutment bridges should be carried out.

Table 13 lists the typical piles used in South Africa such as the square precast pile and the 600mm diameter auger pile. The H-pile is not generally used in South Africa due to the high costs (Section 2.4.1.1) but had to be investigated to check if other more common feasible piles can be substituted for steel H-piles. Pipe piles are also not commonly used in South Africa but were considered to understand the behaviour of a stiff pile. The material strengths shown in Table 13 are commonly used and available in South Africa.

Table 13: Properties of Piles used in the study

Pile Type	**Pile Details**	**Strength** (MPa)**	**Area (m^2) (x 10^{-2})**	**Moment of Inertia (m^4) (x 10^{-4})**	**Elastic Modulus (GPa)**
Square Precast Concrete pile #	350 x 350	30	12.30	12.51	28
Square Precast Concrete pile #	250 x 250	30	6.25	3.255	28
Circular Augered Pile	600 Diameter	30	28.30	63.620	28
H-Pile SA (strong axis)	254 x 254 x 89	350	1.14	1.430	206
H-Pile WA (weak axis)	254 x 254 x 89	350	1.14	0.483	206
Pipe Pile	356 Outer Diameter (10mm wall thickness)	350	1.09	1.628	206

*** Compressive strength of concrete piles at 28 days and tensile yield strength of steel H-pile and steel pipe pile*

 # Reinforced concrete precast concrete pile

NOTE: ***ALL graphs/figures shown in the forthcoming chapter are based on values at serviceability limit state i.e. they are un-factored.***

4.3 Assumptions

For this study some reasonable assumptions have been made and are listed below. These assumptions are based on the findings from the literature review and are referenced accordingly in brackets.

a) It was assumed that the point of "virtual fixity" of the fixed end of the pile cantilever is indeed fully fixed (Section 3.1.2.1 and 3.6).
b) The top of the pile was assumed to be a free headed-pile moving as the deck experiences varying translation movements, the reason for this was described at the beginning of this chapter (Section 3.6 and 3.7).
c) It was assumed that the free end pile conditions could result if some sort of elastic material such as geofoam is placed between the integral abutment wall face and backfill soil to reduce the earth pressures on the back wall, as discussed in Section 3.3 of the literature review.
d) It was assumed that if geofoam or some sort of elastic membrane was used then any horizontal loads on the bridge deck should ideally be absorbed by a structural member such as an intermediate stiff column or fixing one end of the deck rigidly to an abutment such that this abutment experiences minimal or no displacements (Section 3.3). If the elastic membrane concept was not adopted for this research, it can be assumed that any horizontal forces are absorbed by the soil fill behind abutments thus activating the passive conditions of soil.
e) The formulas adopted calculate deflections of the top of piles within tolerable limits.
f) It is assumed that the equivalent cantilever of the pile is actually the free length of the pile that is within a sleeve. As discussed in the literature this concept of sleeving is commonly adopted for integral abutment bridge piles to allow for increased flexibility to accommodate deck movements. Pre-boring serves a similar purpose as sleeving (Section 3.7).
g) Pile bending moment and shear force will be calculated at the fixed end of the cantilever which is the base (bottom end) of the pile.

The assumption of the lower fixity at the bottom of the pile is perhaps debatable and in reality it is most probably not fully fixed and actually *partially fixed* to some extent. This also depends on the material and method of construction of the pile. In the analysis done fully fixed conditions has been assumed.

In practice another important aspect that needs to be considered is ensuring that no backfill material enters into the sleeve as this will reduce the designed flexibility. This problem can be overcome by the engineer providing good construction details and stringent site supervision.

The Figure 64 shown below illustrates the concept of an integral bridge pile within a pre-bored hole (similar to sleeving). The bottom and top of the idealised *equivalent cantilever pile* has fixed conditions.

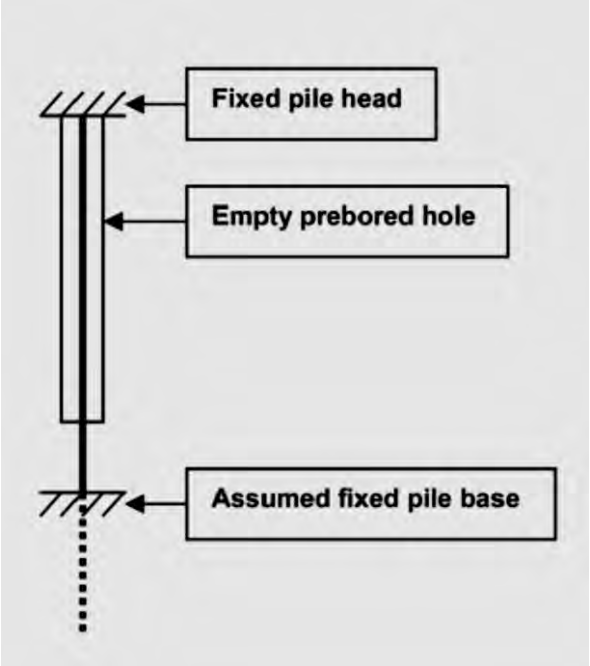

Figure 64: Equivalent cantilever concept of a pre-bored integral bridge pile with both ends fixed (Dunker and Abu-Hawash 2005, cited in Holloway 2012)

Example:

Assume the sectional elevation of the integral bridge shown in Figure 65 is located in East London. The calculation of the overall movement of the bridge deck is given in Appendix H and the overall calculated movement is 13mm. Note that the bridge super-structure and sub-structure is rigidly fixed in the centre thus the end portion of deck at the abutments can move inwards and outwards from the fixed point which implies that 26m in length is used to calculate the permissible movement. The fixity in the centre is advantageous as the pier was designed to absorb any;

I. Longitudinal force resulting from traction or braking of vehicles (NA/ NB or NC loading).
II. Any accidental force caused by skidding.

The Figure 65 shows an elastic type of material used behind the abutment wall, thus if the centre fixity was not present the passive resistance from the soil to balance any horizontal forces will be minimal and certainly not desired as this could result in high deflections in the abutment piles. The pile sleeves (i.e. the effective pile height) chosen was 3.5m. The results for the piles are presented in the next chapter.

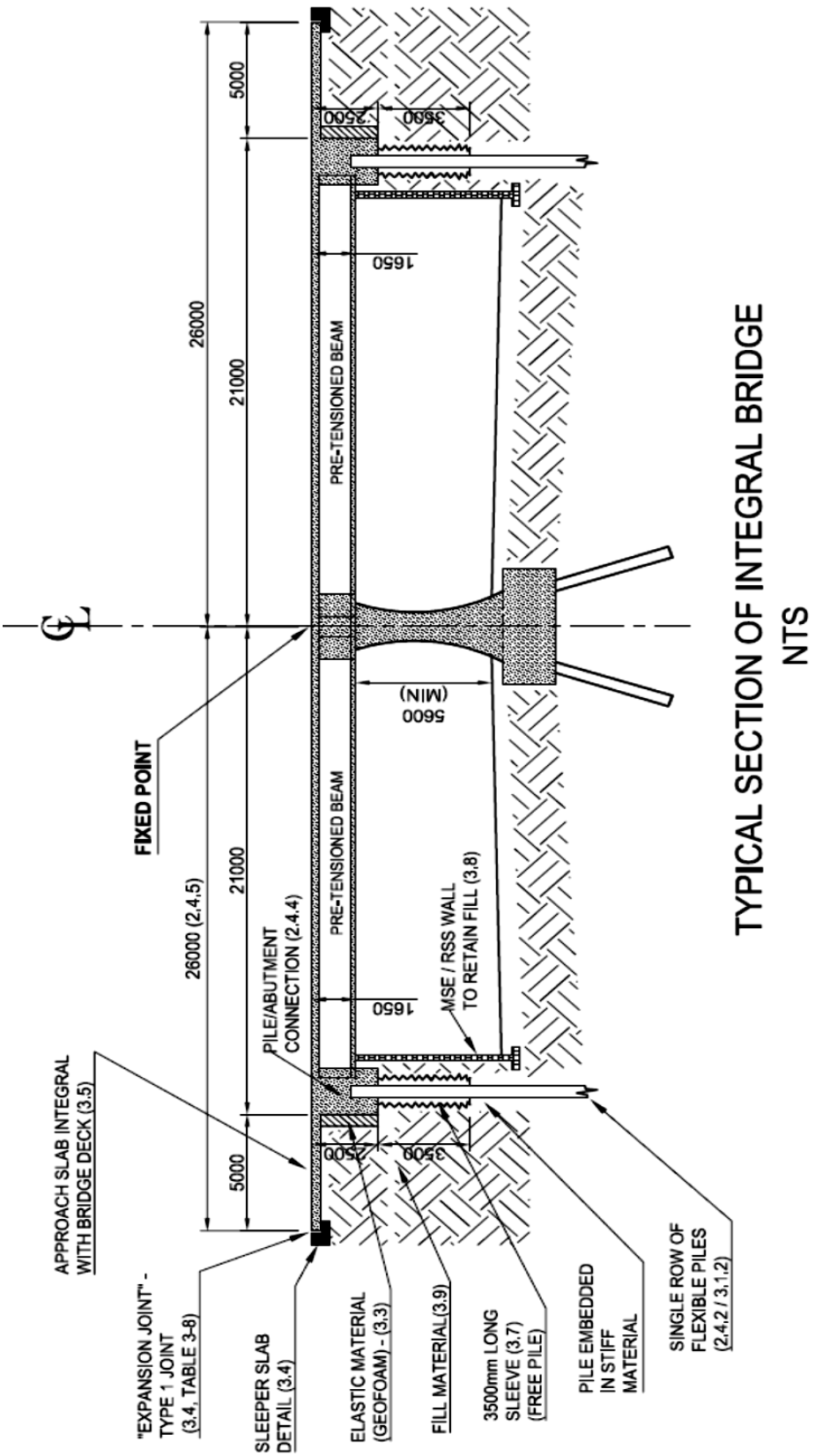

Figure 65: Example of an integral bridge

5 RESULTS AND DISCUSSION

The investigation varied the pile type that could be adopted for integral bridge structures with different effective pile lengths. The effective pile length is the proposed equivalent pile length based on the *equivalent pile cantilever* concept. The equivalent pile length (effective pile height) is that portion of the pile that is within the pre-bored hole or pile sleeve.

The results aim to assist the bridge designer in determining:

I. The most appropriate pile type for the integral bridge structure subject to other factors that must be considered such as ground conditions, environment, cost and pile availability etc.
II. The influence of the effective pile "cantilever" length on pile moments and the maximum moment that the pile section can carry.
III. The corresponding pile moments at the virtually fixed position is related to the bridge deck translation expected (movement at top of pile).
IV. The relationship between slenderness ratio and pile stiffness is compared.

The results below will also assist the designer in ensuring that based on the effective pile length, type of pile chosen and calculated deck movement, the number of piles is appropriate i.e. each pile must be able to withstand the moment and shear forces. In addition as discussed by many bridge designers and researchers presented in the literature review, the top part of the pile is essentially designed as a column. Typical working loads are generally provided by the pile fraternity however the designer should check if the amount of prestress or reinforcement in a concrete pile is sufficient to withstand the anticipated loads provided from the corresponding moments and shear forces as well as the vertically induced load and any other additional moments.

The study conducted shows that longer effective pile cantilever length results in a lower magnitude of moments and shear forces but it is important to ensure that the pile section is capable of carrying the corresponding moments and shears. If there was no accommodation of movement of the piles (i.e. effective pile cantilever length of zero), it is anticipated that there is the high probability that the pile will experience high stresses and could shear-off at the pile and deck interface as it cannot allow the deck to move.

The results show a distinct difference between using a 2m effective pile cantilever length compared to using other effective pile cantilever lengths such as 3m, 3.5m and 4m etc. It shows that pile moments and shears are significantly higher if a 2m (or lower) effective cantilever length is used rather than a 3m. There is a big difference in moments and shears from 2m to 3m effective cantilever length compared to a 3m to 4m effective length. This also proves that using a sleeve or pre-bored hole for an integral bridge pile of 3m or more is very beneficial compared to smaller effective pile cantilever lengths. The literature also considers 2m of free effective pile cantilever length of pile as the minimum length and suggests the effective pile cantilever be between 2m and 5m (Girton 1991 cited in Card and Carder 1993). Table 11 from the literature review describes a few of the integral bridges constructed and it is also noted that typically the sleeve length or pre-bored depth is more than 3m.

Figure 66 shown below is the bending moments induced for typical integral bridge movements (i.e. max 25mm) for a 350 square PC concrete pile. The Figure 66 shows a distinct red, dashed line which represents the maximum moment the pile can carry at serviceability limit state (calculations provided in Appendix D). Four practical effective pile heights were considered. The intersection with the red/ dashed line is the maximum anticipated lateral deflection this pile can carry. As an example, for the 2m effective pile height, the maximum lateral deflection is 4mm whilst for a 4m effective pile height, the maximum lateral deflection is 13mm. This was also discussed in the literature review; the longer pile is more flexible and can accommodate for movement easily, but it must be able to carry the induced moments and axial loads as well. An example of the different effective pile height calculations are provided in Appendix A).

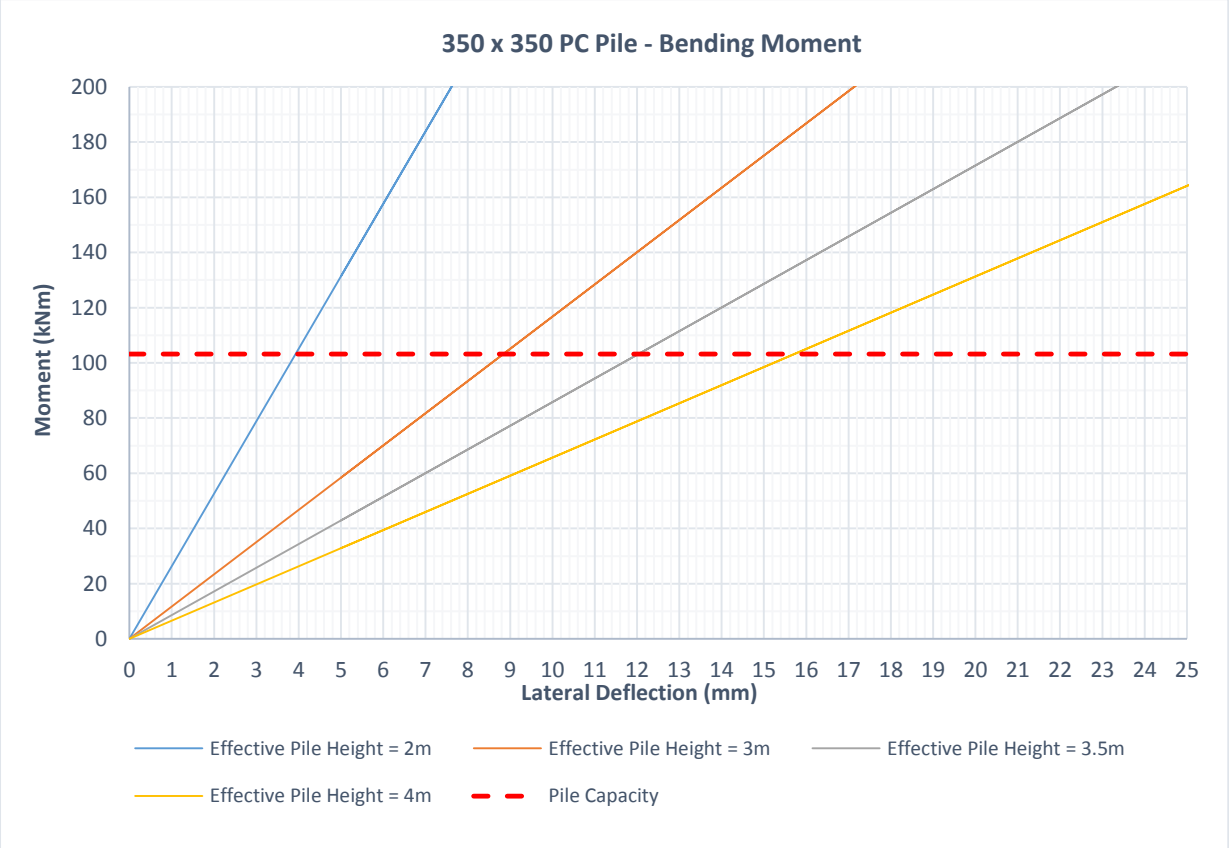

Figure 66: Pile bending moment based on lateral deflection of a 350 x 350 PC pile

Figure 67 shows the corresponding horizontal forces that are required at the top of the pile cantilever to induce the anticipated movements. In reality this force will be provided by the superstructure as it moves. The horizontal force is actually the shear force at the base or point of fixity of the pile. Note the very high forces required to allow for displacements when the 2m effective pile height is considered yet it reduces sharply when a 3m effective pile height adopted. This relates to the literature review as the examples presented used pile sleeves greater than 3m. Effective pile heights such as 6m, 8m and 10m are shown as extreme scenarios but are not practical and will be too slender to carry moments and axial loads. The calculations used to obtain these curves are presented in Appendix A and B.

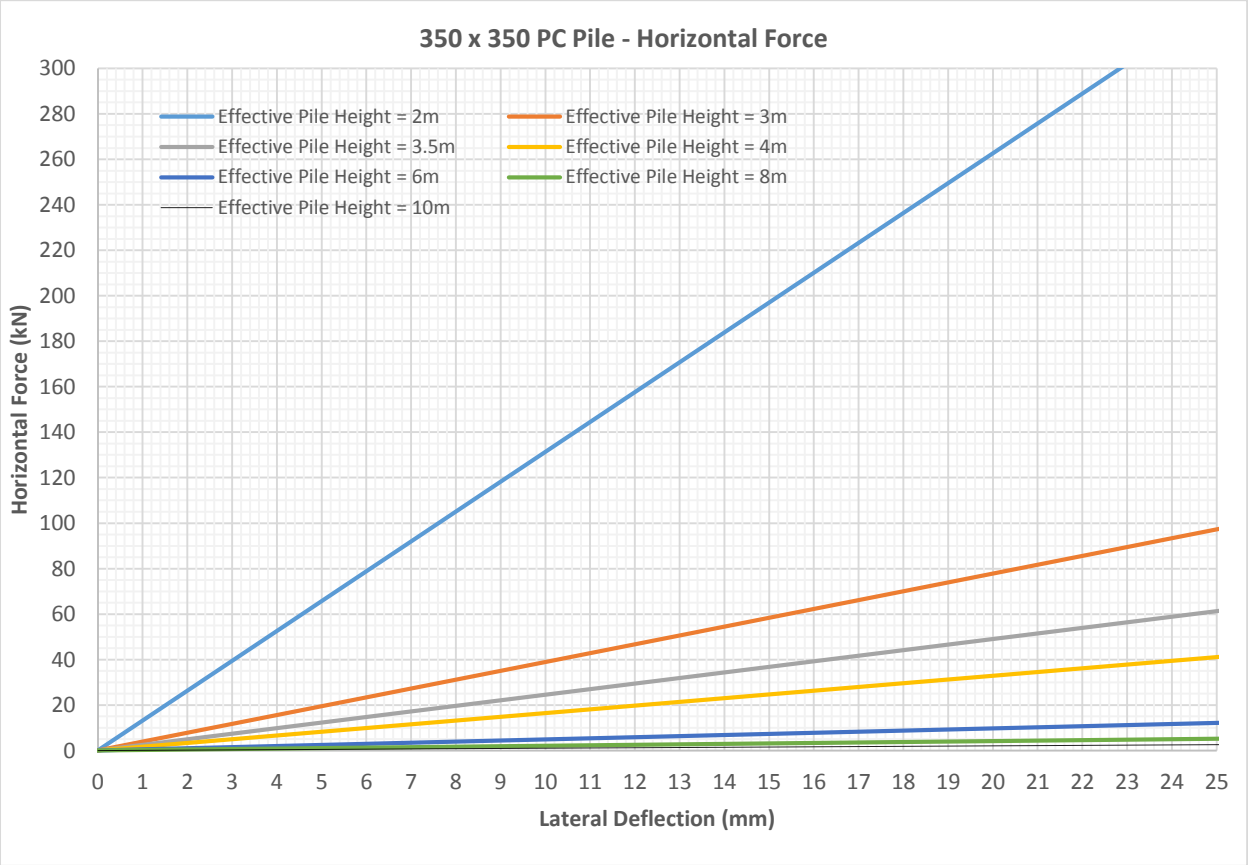

Figure 67: Pile horizontal force (shear force) based on lateral deflection of a 350 x 350 PC pile

The slope (gradients) of the line graphs shown in Figure 67 actually represent the stiffness as discussed in the literature review, Section 3.1.2.2. The stiffness corresponds to each effective pile height. Figure 68 shown below, illustrates a graph of stiffness (gradient from line graphs in Figure 67) and the slenderness ratio (calculations provided in Appendix B). The relationship between the stiffness and slenderness, certainly shows an inverse relationship, as expected. Note that below a slenderness ratio of 11, the stiffness grows extremely high.

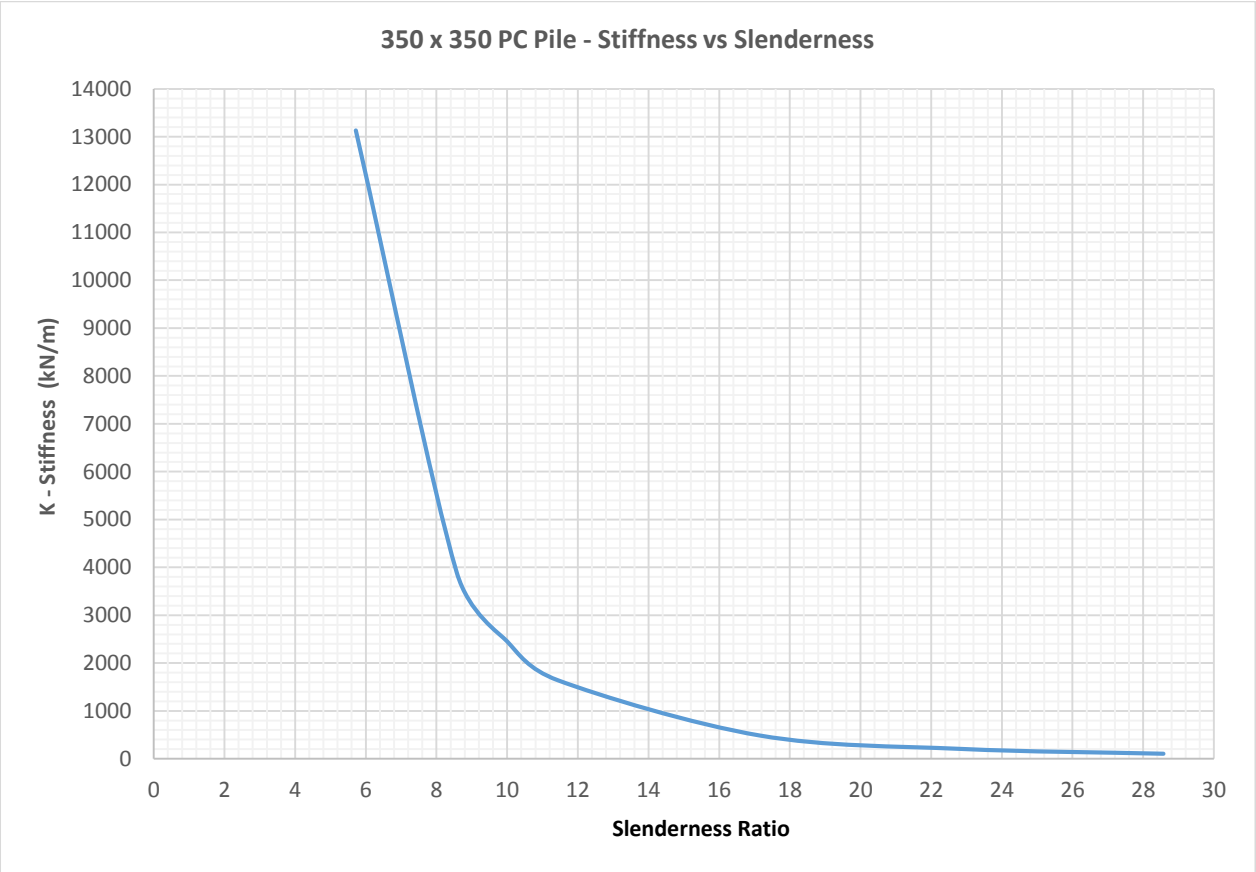

Figure 68: Stiffness and slenderness relationship of a 350 x 350 PC pile

Figure 69 below shows the bending moments for different effective pile heights for a 250 square PC Pile. The same concepts as described for the 350 square pile applies. Due to the 250 x 250 pile being more slender the overall lateral deflections the pile can tolerate are slightly higher than the 350 x 350. The 4m effective pile height allows for a maximum lateral deflection of 19.8mm whereas the maximum deflection for the 350 x 350 was 15.8mm.

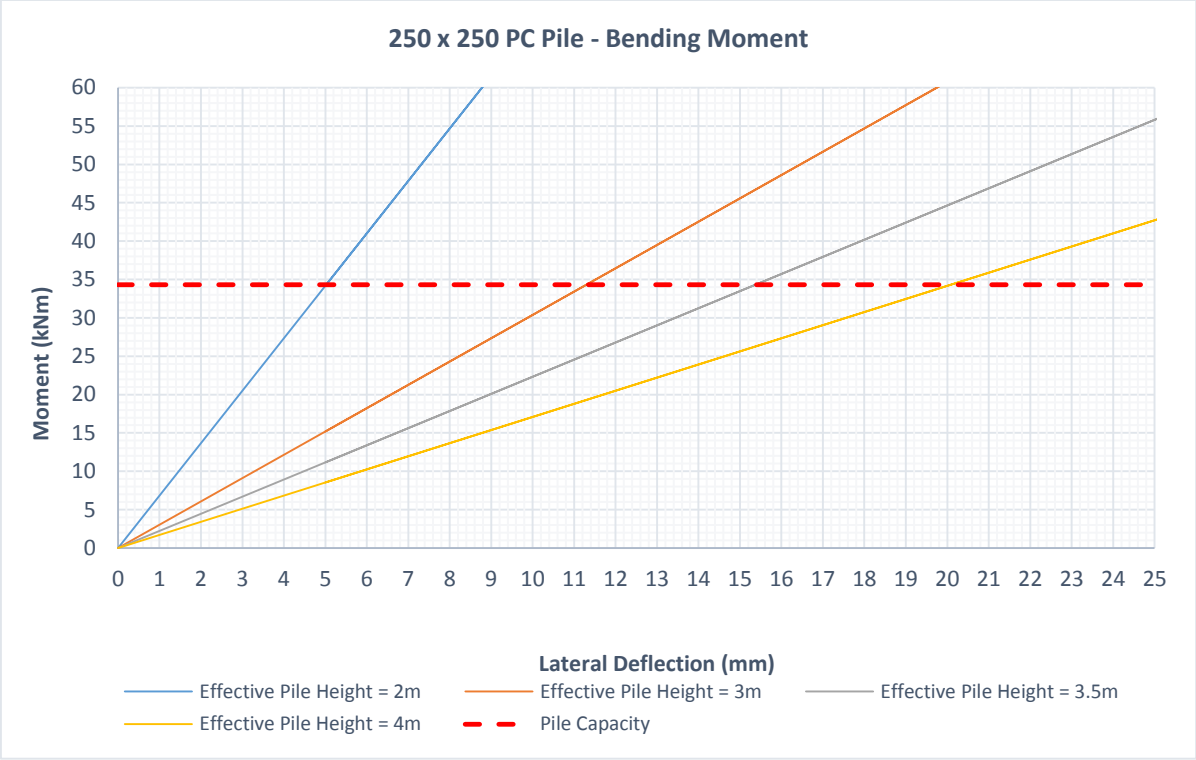

Figure 69: Pile bending moment based on lateral deflection of a 250 x 250 PC pile

Figure 70 shown below illustrates the inverse relationship between stiffness and slenderness for a 250 square pile. Note the reduced stiffness values compared to the 350 square pile.

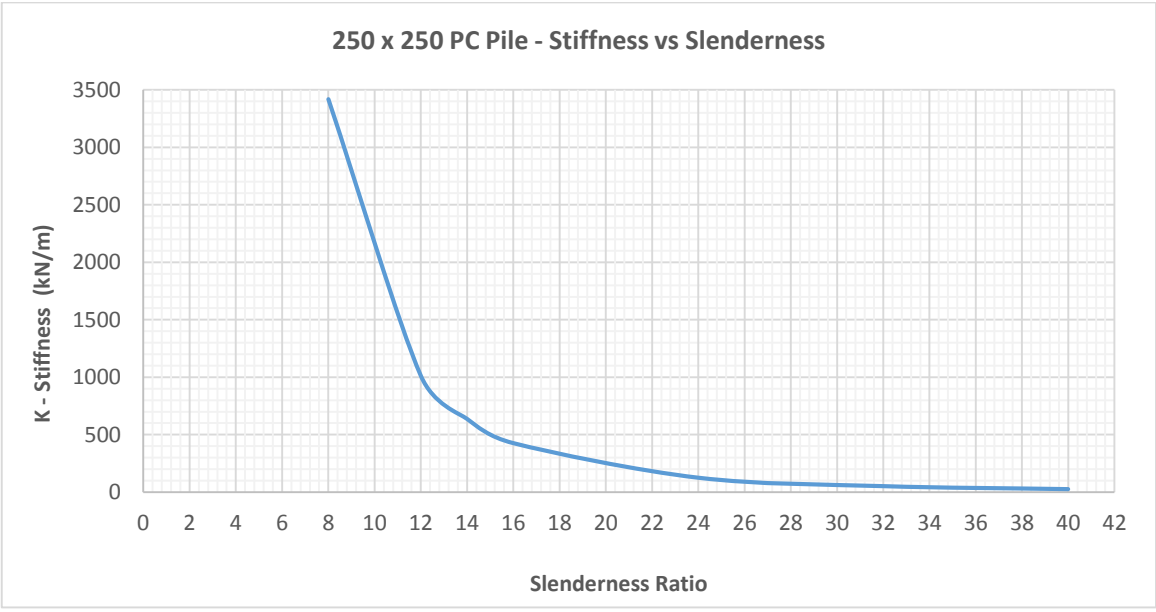

Figure 70: Stiffness and slenderness relationship of 250 x 250 PC pile

Figure 71 shows moments for a 600mm diameter pile against lateral deflections. The moment capacity is comparably high and accommodates reasonable amount of movement i.e. below 22mm.

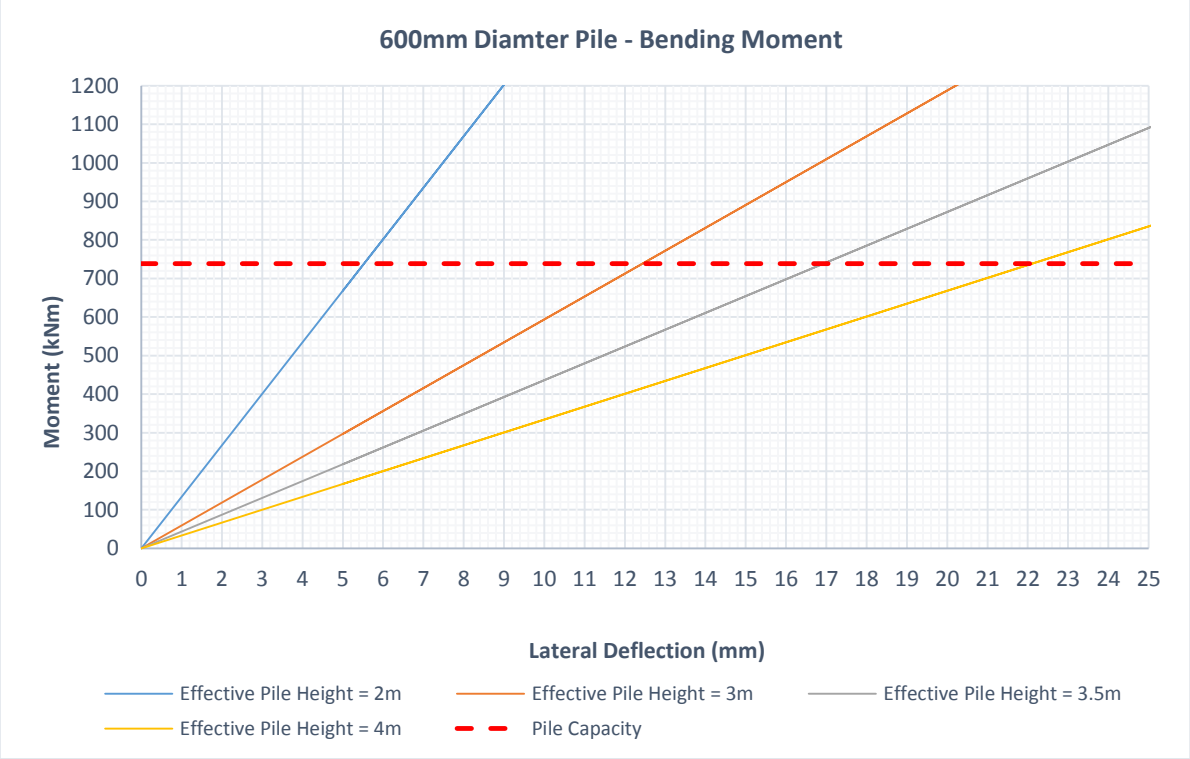

Figure 71: Pile bending moment based on lateral deflection of a 600mm diameter concrete pile

Figure 72 shows the relationship between stiffness and slenderness for a circular section concrete pile. Note that due to properties of the pile such as high moment of inertia, the stiffness is very high compared to the square piles.

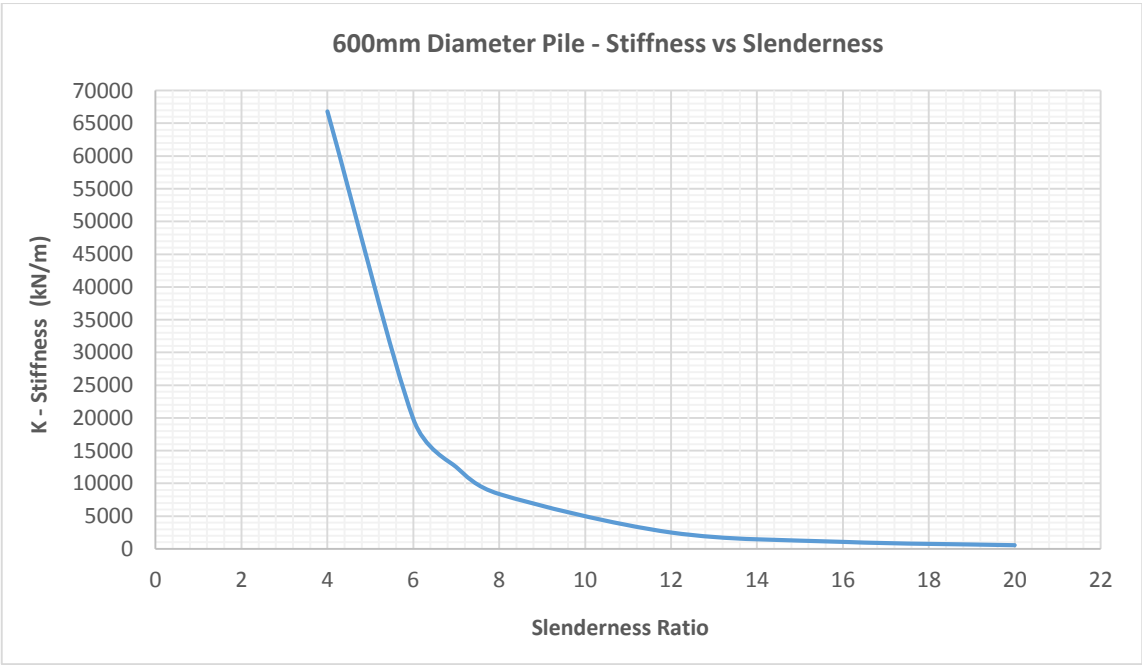

Figure 72: Stiffness and slenderness relationship of a 600mm diameter concrete pile

Figure 73 shows bending moments for a 254 x 254 x 89 steel H-pile, bending about its strong axis. Note the high moment capacity and how this value does not intersect the 3m, 3.5m and 4m effective length moment curves therefore it easily allows for movement.

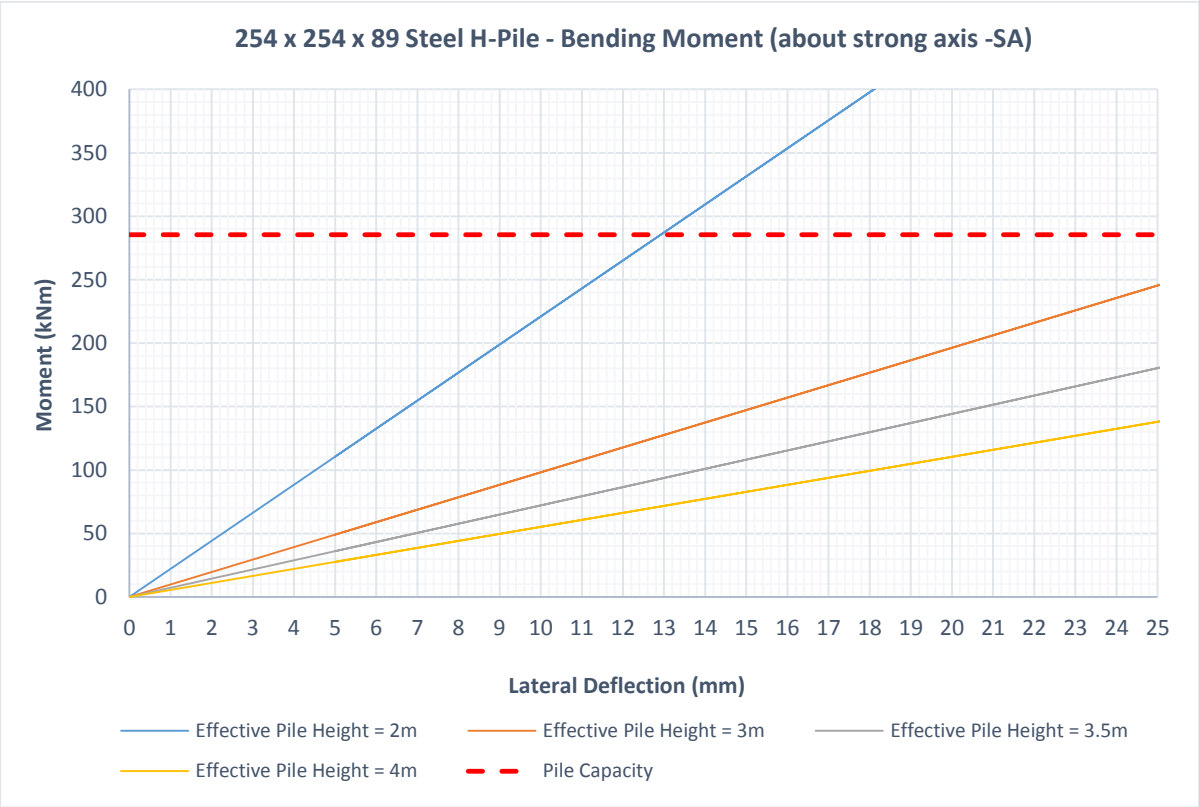

Figure 73: Pile bending moment based on lateral deflection of a 254 x 254 x 89 H-pile about strong axis

Figure 74 shows the relationship between stiffness and slenderness (calculations in Appendix B).

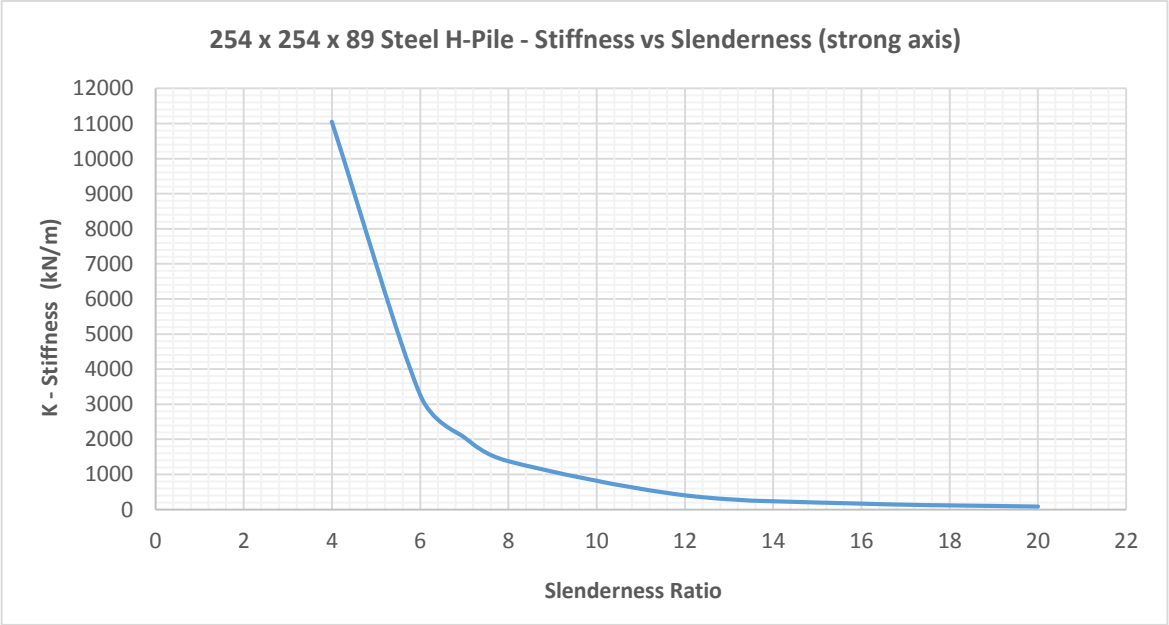

Figure 74: Stiffness and slenderness relationship of a 254 x 254 x 89 H-pile about strong axis

Figure 75 shows bending moments with deflection for a 254 x 254 x 89 steel H-pile, bending about the weak axis. Note the high moment capacity line is much higher than the moment-deflection curves for the effective lengths of 3m, 3.5m and 4m, thus implying this pile will tolerate the horizontal loads easily with low stress. This shows that the steel H-pile is favourable when bending is about the weak axis as extensively discussed in the literature review.

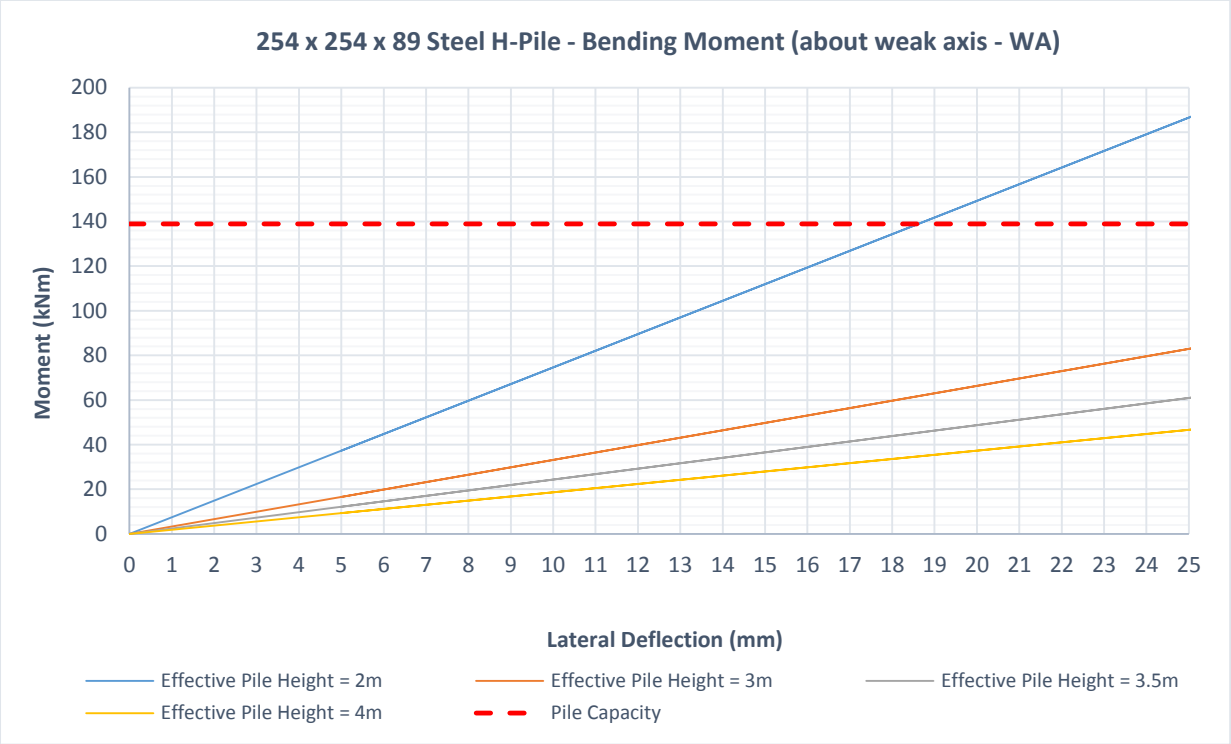

Figure 75: Pile bending moment based on lateral deflection of a 254 x 254 x 89 H-pile about weak axis

Figure 76 shows the relationship between stiffness and slenderness. Note the low stiffness values are in the same range as the 250 square pile.

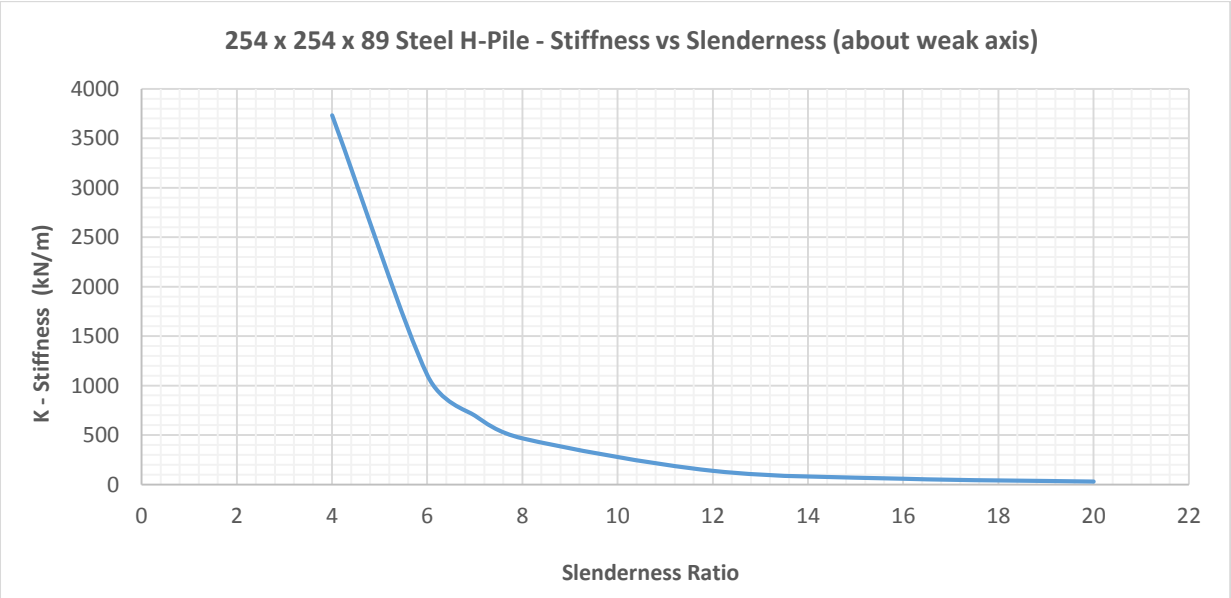

Figure 76: Stiffness and slenderness relationship of a 254 x 254 x 89 H-pile about weak axis

Figure 77 shows moments for a pipe pile against lateral deflections.

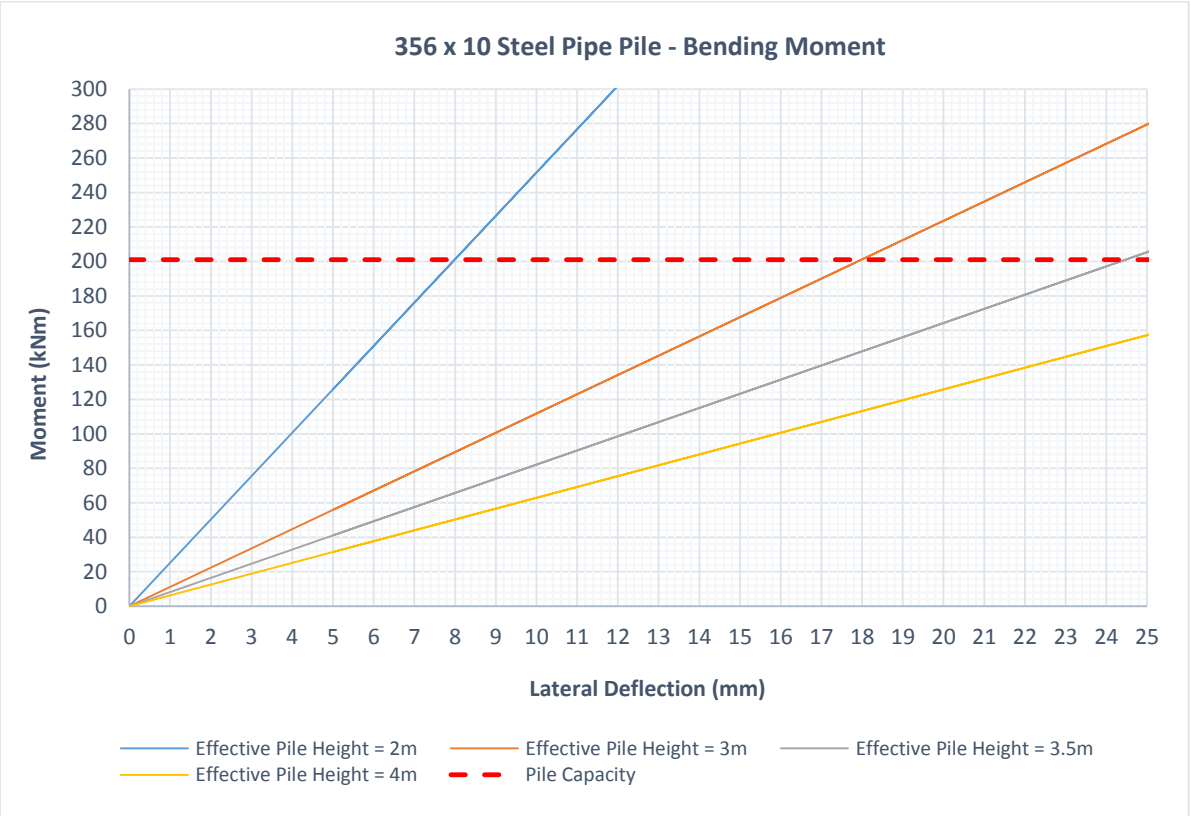

Figure 77: Pile bending moment based on lateral deflection of 356 x 10 pipe pile

Figure 78 shows the relationship between stiffness and slenderness for a pipe pile.

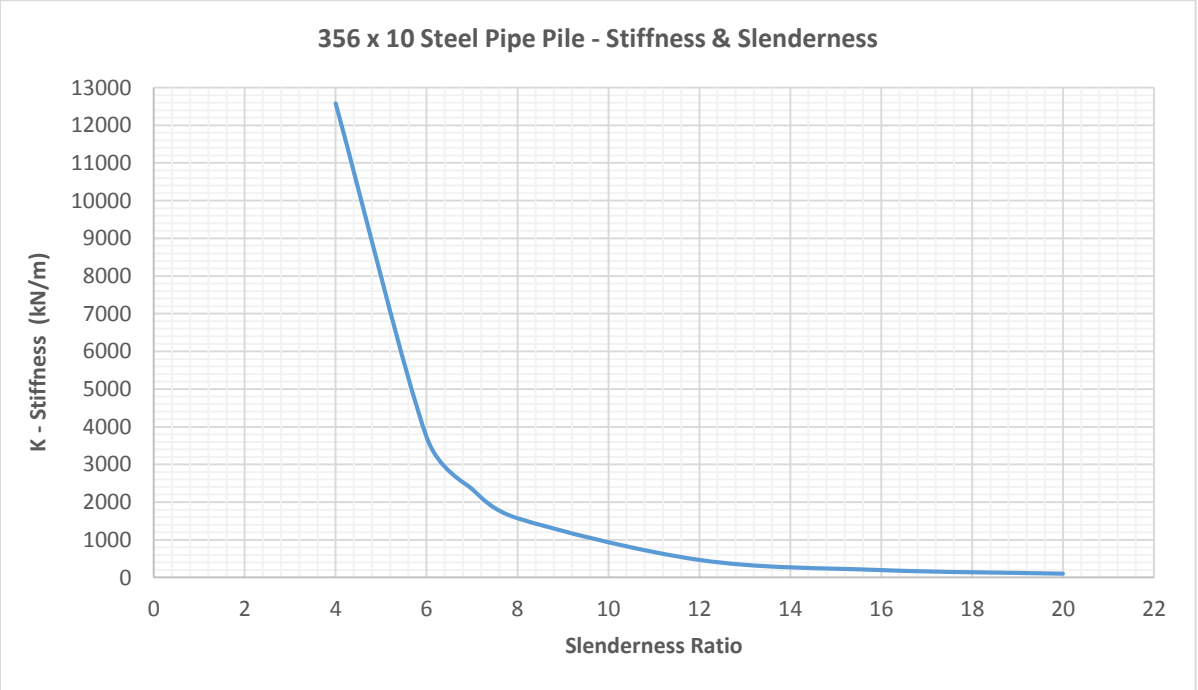

Figure 78: Stiffness and slenderness relationship of a 356 x 10 pipe pile

Figure 79 and Figure 80 show the primary difference between the free headed-pile and fixed headed-pile (two types of piles are used to illustrate an example). The stiffness values based on these two boundaries have a large variation. These graphs are based on the formulae discussed in Chapter 4. Realistically the values will be best calculated by setting up and monitoring a laboratory model as carried out by Arsoy et al (2002). The partially fixed pile is merely the average of the two extremities (calculations and assumptions are provided in Appendix G). The calculations for the curves below are presented in Appendix B.

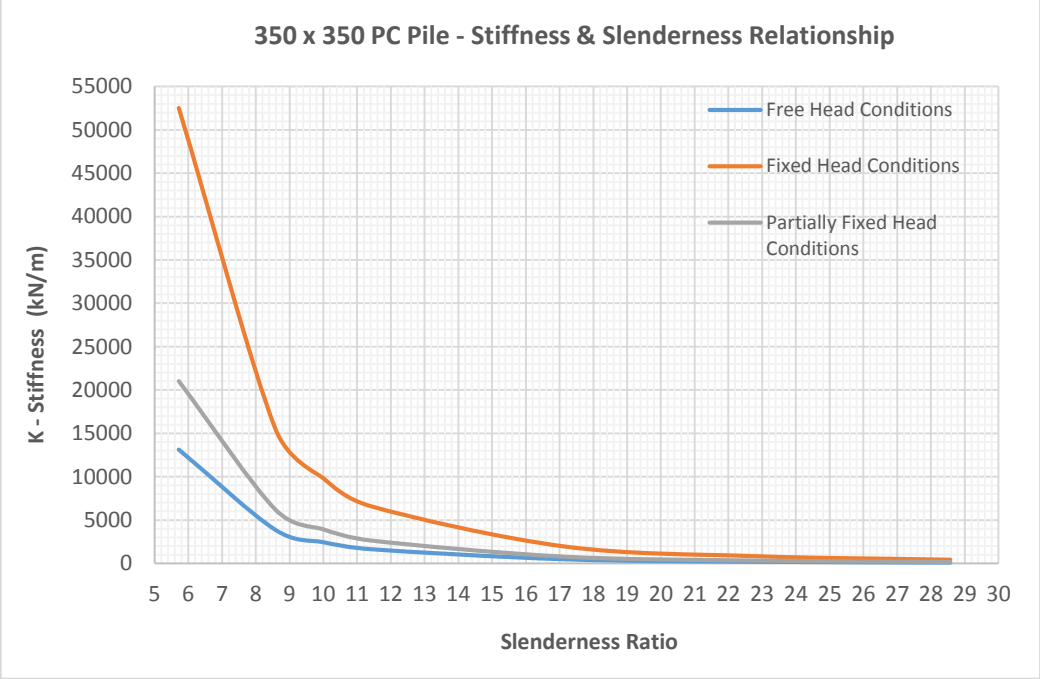

Figure 79: Stiffness and slenderness relationship for a 350 x 350 PC concrete pile showing free, fixed and partially fixed pile heads

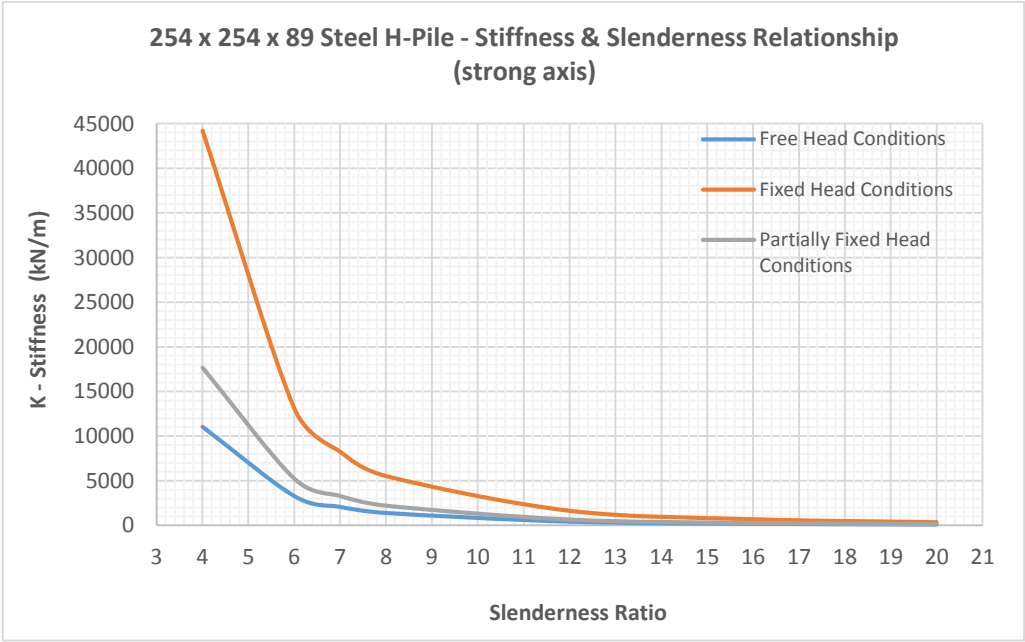

Figure 80: Stiffness and slenderness relationship for a 254 x 254 89 steel H-pile showing free, fixed and partially fixed pile heads

Figure 81 shown below now collate the different pile types for the same effective length (3.5m), the aim is to assist the designer by illustrating the influence of moment for varying pile types with the same pile effective length and same translation (pile deflection). The following are the results of the example provided in the methodology section (Chapter 4).

- For the purposes of illustrating the behavioural characteristics of piles, an effective pile cantilever length is chosen as 3.5m only.

- For the purposes of clarity and reading off the graphs, the data for the 600mm diameter concrete pile has been excluded due to the high stiffness it shall not be considered as appropriate for an integral bridge. The results however are shown in Appendix C.

Figure 81 shown below plots moment-deflection curves for 5 different types of piles and includes the maximum moment (horizontal dashed lines) each pile can carry and thus suggests the corresponding amount of lateral movement the pile can take. The vertical solid thick purple line is the calculated movement of 13mm from the example provided in Chapter 4 and calculations are provided in Appendix H. Note the high moment capacity of the H-pile orientated about the strong axis as well as the capacity of H-pile orientated about the weak axis. Note the 350 x 350 pile would not be able to tolerate the 13mm movement as it is limited to 11.6mm. The 250 x 250 pile also has a limit to the deflection i.e. 15.5mm. *Note: SA (strong axis) and WA (weak axis).*

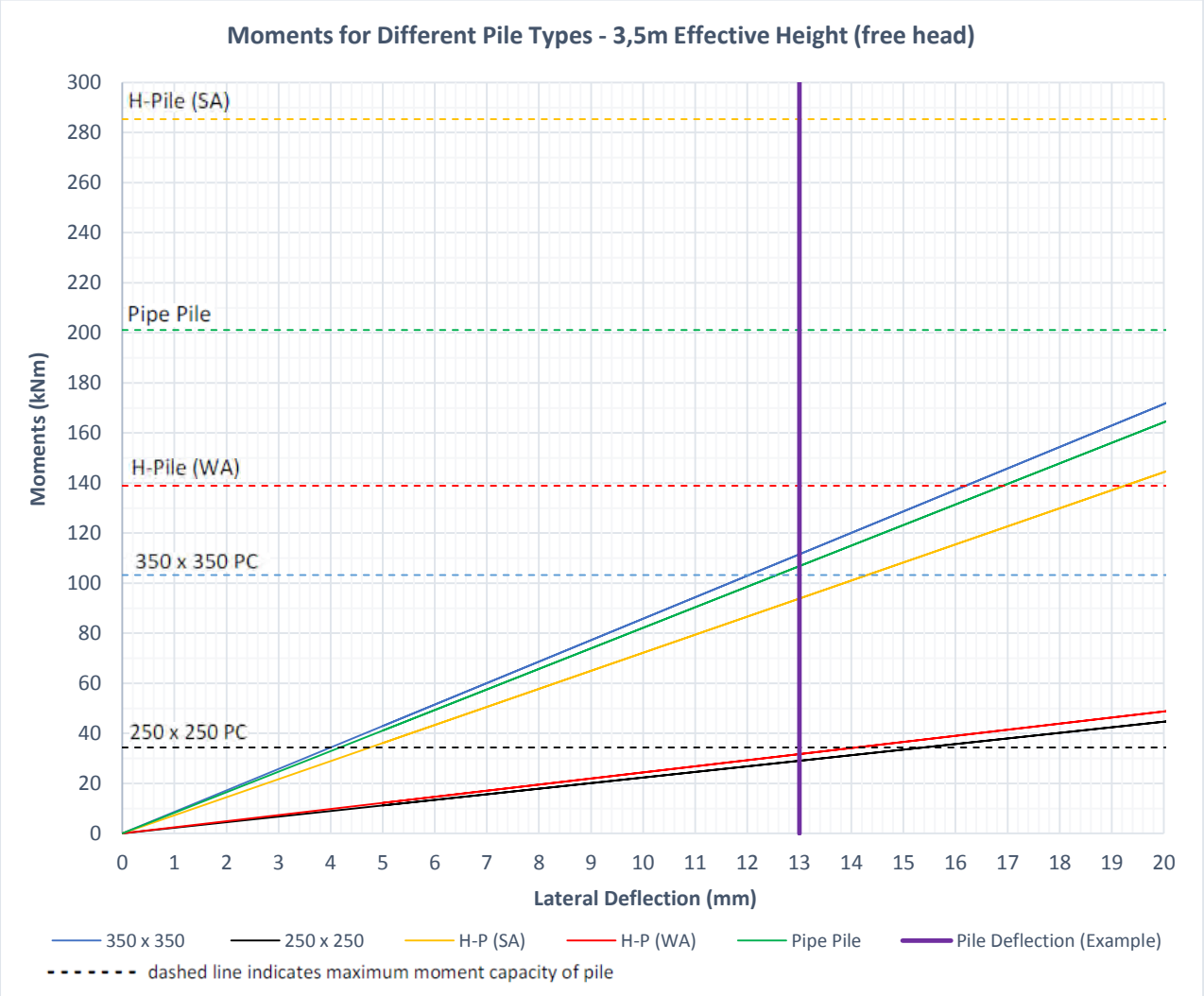

Figure 81: Moments for different pile types for 3.5m equivalent free length

Figure 81 shown above indicate the order of the stiffness of the piles i.e. (as listed in decreasing stiffness based on the linear curve);

1. 600mm diameter concrete pile (not shown in graph above but in Appendix C)
2. 350 x 350 PC concrete pile
3. Steel Pipe pile
4. H-pile, bending about strong axis
5. H-pile, bending about weak axis
6. 250 x 250 PC concrete pile

One should note that the H-pile along its weak axis and the 250 x 250 PC pile are very comparable in terms of flexibility, moments and shear. From this behavioural characteristic this could imply that if steel H-piles in South Africa are expensive to manufacture, the 250 x 250 PC pile could be used as an alternative. For approximate cost comparison, consider a 350 x 350 PC pile to be supplied and installed would cost about R 850.00/m, a 600mm diameter auger pile about R790.00/m whilst a steel H-pile to be supplied and installed would cost in the range of R 1500.00/m to R 3000.00/m (all establishment and de-establishment cost have been ignored). From Figure 81, although the 250 x 250 PC and H-pile (weak axis bending) are comparable, the deflection limit on the 250 x 250 PC pile is much smaller than that of the H-pile.

It is also important to acknowledge the results from Arsoy et al (2002), where the research concluded that PC concrete piles when subjected to cyclic loading are prone to forming tension cracks. The most appropriate pile based on the Figure 81 above and considering the work done by Arsoy et al (2002) is thus an H-pile positioned along its weak axis. The graphs above explain why the extensive literature of integral abutment bridges strongly recommend the steel H-pile to be adopted along its weak axis.

This certainly does not imply that other piles are not applicable. In Germany for example, concrete foundation piles and sub-structure are used for integral bridges but to attain the required flexibility different types of aggregate are carefully blended to essentially reduce its stiffness (Young's Modulus). If the PC piles are prone to tension cracking, perhaps additional reinforcement and /or pre-tension wires need to be included to make them more ductile. The final decision is based on which pile the designer chooses and which pile passes all the checks, requirements, costs and availability.

Table 14 shown below is the pile results for the example illustrated in Chapter 4. Table 14 below shows a summary of moments of the pile at the point of virtual fixity (bottom of the pile). The designer should check if the proposed pile section can accommodate these inherent parameters as well as all other additional loading as per TMH7 (parts 1 and 2) as discussed in Section 2.2 of the literature review. The number of piles adopted is very important as the forces applied must be within the working load of the pile and the reinforcement (or prestress) should be able to accommodate for such vertical loads. One should note that since the pile now behaves as a column within the sleeve, the pile section has the probability of actually having a working load less than what the pile manufacturer or piling guidelines propose, thus performing this check is important. Second order effects should also be considered. The cost factor plays an important role but the long term performance of the pile must also be thoroughly investigated. Calculations for the example scenario are provided in Appendix C and Appendix E).

Table 14: Summary of results obtained from the 3,5m effective cantilever pile length data for varying pile types (values are all un-factored i.e. at SLS)

Proposed Piles		3.5m effective cantilever graph (free-headed pile)		
Pile Type	Pile Details	Movement of deck due to temp, creep & shrinkage (mm)	Moment at point of fixity (kNm) – **From Figure 81**	Stress Calculation (N/mm^2) **(Appendix E)**
Square Precast Concrete pile	350 x 350	13	112	N/A (limit exceeded)
Square Precast Concrete pile	250 x 250	13	29	11.14
Circular Augered Pile	600 Diameter	13	-	-
H-Pile (strong axis)	254 x 254 x 89	13	94	83.48
H-Pile (weak axis)	254 x 254 x 89	13	31	81.51
Pipe Pile	356 Outer Diameter (10mm wall thickness)	13	104	113.71

The required movement in the example scenario was calculated to be 13mm thus according to Table 10 from the literature review, a Type 1 joint would suffice at the end of the approach slab. The alternative of embedding the approach slab in the layer works material is also appropriate, however special connection details must be adopted as discussed in Section 3.5.

6 CONCLUSIONS AND RECOMMENDATIONS

6.1 Conclusions

Integral abutment bridges of the form and concept discussed in this dissertation are relatively new to South Africa. Many countries have strongly favoured this type of bridge especially when bridge lengths are within a small to medium range. There are numerous benefits associated with integral abutment bridges by just considering the maintenance aspects, but a poor design or lack of understanding of the concept could prove to be problematic for the bridge authority as it will require regular maintenance thus leading to high unanticipated costs.

One of the most challenging issues with integral abutment bridges is the soil-structure interaction. The concept of modelling the soil as a spring is often used but modelling the piles as an equivalent cantilever is also very widespread and popular. This research demonstrates that it is possible as the reasoning behind adopting the equivalent cantilever method is appropriate when pile sleeves or similar are used. The tops of piles should be given allowance to be free and flexible to accommodate any movements from the deck. The abutment back face should be lined with an appropriate geofoam and of the correct thickness to avoid compression set when loads are released. The approach slab for integral abutment bridges is very important and the details of integral abutment bridge transition slabs are different when compared to conventional bridges.

The research work shows that if the pile is flexible and/or the appropriate equivalent pile cantilever length (i.e. free pile within a sleeve) is adopted then the corresponding bending moments and shear force at the point of virtual fixity are minimal. A steel H-pile positioned along its weak axis proves to be superior compared to other types of pile, also considering the ductility and durability for the long term cyclic movements the pile needs to accommodate. The influence of pile sleeves or pre-boring is significant and this research work has shown that the minimum sleeve length should be 3m. Steel H-piles in South Africa are not commonly used. One of the reasons for this is the high associated costs. This needs to be carefully weighed-off against costly and maintenance-prone bearings, expansion joints and with other pile types. Alternative piles types are possible but the designer must be aware of the limitations such as tension cracks on concrete piles under cyclic loading. Certainly more research is required on alternative pile types and their behaviour in integral abutment bridges.

Integral bridges have proven to be superior in certain countries as many authorities have mastered the design of these structures. If these structures are to be adopted in South Africa, and certainly they should, the first few should be instrumented and behaviours studied in detail and also the performance analysed after a few years. Caution should be exercised as constructing too many in haste could result in poor performance only at a much later time due to soil ratcheting effects which may not be seen in the first few years. One of the most important aspects of integral abutment bridges is the length. Many countries and authorities have different limiting lengths which are based on their experience. Similarly, if these type of bridges are used in South Africa they should only be considered for small to medium spans (overall bridge length of about 60m) and after monitoring the performance, then only longer lengths should be constructed or allowed. The research work from the literature

review concludes that even integral bridges may require some sort of a joint at the end of the approach slab. One may now argue, that by having the joint, it is essentially moving the problem from the deck to the end of the approach slab and once again similar to the conventional bridge type where maintenance is required. If the length is limited then specially detailed approach slabs can be buried in the roadwork's fill material and no joint is required as discussed in the literature review.

Integral bridges are not common in South Africa and this is perhaps due to the uncertainty of the soil-structure interaction, thus bridge designers often choose to adopt bearings and expansion joints. Overseas the norm is that, if the bridge length is considerably small (< 60m), it is considered standard practice to adopt an integral bridge arrangement whereas in South Africa it is common to find bearings and expansion joints on considerably short spans (< 20m). Integral bridge concepts for shorter lengths need to be adopted in South Africa to reduce the maintenance and replacement costs of bearings and expansion joints. The issue of de-icing salts is not applicable in South Africa but the issue of bearings corroding and seizing is not uncommon. The thermal effects in South Africa are somewhat similar to those covered in the references, as the literature for integral bridges constructed in various countries with varying temperature ranges indicates that these structures seem to be performing well. The biggest difference is the piling system specified with the use of steel H-piles not common in South Africa. However this is certainly possible and does not pose major construction challenges.

The conventional approach in South Africa is that the majority of bridges are designed such that the bridge abutment (open or closed) are very rigid or stable, with the superstructure seated on bearings which in turn rests on the rigid abutments. However with integral bridge abutments, the aim is to design the abutment such that they have a certain degree of flexibility. Perhaps moving away from the conventional approach may create uncertainties for the bridge designer, initially resulting in some resistance to the use of integral bridges, however this is easily overcome. Integral bridges are certainly applicable in South Africa and bridge designers should consider them as appropriate for short to medium span structures, providing a feasible technical solution as well as reducing maintenance costs.

6.2 Future Work

- The piles investigated in the desktop study need to be investigated in the laboratory by simulating an equivalent model. This will establish the actual moments and shear forces experienced and provide information regarding these values between the fully fixed and fully free conditions. From this same experiment, it is possible to confirm the work done by Arsoy et al (2002) and check how the different piles behave under cyclic loading. In South Africa steel piles are not often used and if precast piles could be adopted then this type of bridge will certainly become more popular. The research should also include pretension precast piles.

- If these bridges of the concept described in this dissertation are to be adopted in South Africa, the first few should be well instrumented to determine their actual performance.

- The concept of the geofoam and elastic material behind the abutment to reduce high passive pressures will also be better understood if they are somewhat instrumented and performance monitored while they are actually being used.

- Pile sections should also be investigated, that is, designing the top few meters (say 6m) of a pile of a different section (stiffness) to the rest of the shaft to ensure that pile deflections are as per the optimal requirements or to accommodate the most appropriate joint.

- Option of semi-integral bridges and applicability.

REFERENCES

Abendroth, R. E., Greimann, L. F. & LaViolette, M. D., 2007. An integral abutment bridge with precast concrete piles. Report No. IHRB (Iowa Highway Research Board Project TR-438.

Alberta Transportation Board Bridge structure design criteria (2003). Appendix C – guidelines for integral bridge abutments.

Arsoy, S., Barker, R.M. & Duncan, J.M., 1999. The behaviour of integral abutment bridges. Report No. FHWA/VTRC 00-CR3, Virginia Transportation Research Council.

Arsoy, S., Duncan, J.M. & Barker, R.M., 2002. Performance of piles supporting integral bridges. *Transportation Research Record: Journal of the Transportation Research Board*, (1808), 162-167.

BA 42/06 Highways Agency, 2003. *The Design of Integral Bridges. Design Manual for Roads and Bridges*. The Stationery Office, London, Vol. 1.2.12.

Benaim, R., 2008. The design of prestressed concrete bridges, concepts and principles. Abingdon, UK: Taylor & Francis.

Bezgin, O., 2010. An insight into the theoretical background of: Soil structure interaction analysis of deep foundation. Lecture notes/website, Istanbul, January 2010.

Bowles, J. E., (1996). Foundation analysis and design. 5th ed. New York: McGraw-Hill Companies

Broms, B. B., 1965. Design of laterally loaded piles. *Journal of Soil Mechanics & Foundations Division*, Proceedings of the American Society of Civil Engineers, Volume 91, p 79-99.

Burke Jr, M. P., 2009. Integral and semi-integral bridges. United Kingdom: John Wiley & Sons.

Byrne, G., Everett, J.P. & Schwartz, K., 1995. A guide to practical geotechnical engineering in South Africa. South Africa: Frankipile

Card, G. B., & Carder, D. R., 1993. A literature review of the geotechnical aspects of the design of integral bridge abutments. Transport Research Laboratory, Project Report 52.

Carder, D. R., & Card, G. B., 1997. Innovative structural backfills to integral bridge abutments. *TRL REPORT 290*. Crowthorne: TRL Limited.

Carder, D.R., Barker, K.J. & Darley, P., 2002. Suitability testing of materials to absorb lateral stresses behind integral bridge abutments. *TRL REPORT 552*.

CBDG (Concrete Bridge Development Group), 2014. Concrete bridge design and construction series – No.2 Concrete bridge layouts. *The Structural Engineer*, February *2014*, 28-32.

Committee of State Road Authorities. *Code of Practice for the Design of Highway Bridges and Culverts in South Africa (TMH7).* Department of Transport, Pretoria, 1981. Revised 1988.

Chandra, S., 2013. Advanced Soil Mechanics. Lecture notes – PowerPoint slideshow – 2013

Concrete Bridge Development Group, 2013. *Current practice Sheet no.3: Integral Bridges.* Camberley, UK: CBDG.

David, T. K. & Forth, J. P., 2011. Modelling of soil structure interaction of integral abutment bridges. *World Academy of Science, Engineering and Technology*, 78, p 769-774.

Design Manual of Roads and Bridges, BA 42/96 (Highways Agency) 2003 – The Design of Integral Bridges.

Dreier, D., Burdet, O., & Muttoni, A., 2011. Transition slabs of integral abutment bridges. *Structural Engineering International*, *21*(2), 144-150.

Dunker, K. F. & Liu, D., 2007. Foundations for integral abutments. *Practice Periodical on Structural Design and Construction*, *12*(1), 22-30.

Elson, W.K., 1984. Design of laterally-loaded piles. London: Construction Industry Research & Information Association.

FitzGerald, P. & Steyn, K., 1998. The status of bridge loading in South Africa. South African National conference on loading, 1998, South Africa, Midrand.

Frangi, A., Collin, P., & Geier, R. (2011). Bridges with Integral Abutments: Introduction. *Structural Engineering International*, *21*(2), 144-150.

Guidelines for Design of Integral Abutments, 2007. Alberta Infrastructure and Transportation

Hambly, E.C., 1991. Bridge deck behaviour. 2nd ed. London: Chapman and Hall.

Holloway, P.K., 2012. Illinois integral abutment bridges: Behaviour under extreme thermal loading and design recommendations. M.Sc. University of Illinois at Urbana-Champaign.

Horvath, J. S., 2005. Integral-abutment bridges: geotechnical problems and solutions using geosynthetics and ground improvement. In *Integral Abutment and Jointless Bridges (IAJB 2005)*.

Husain, I. & Bagnariol, D., 1996. Ontario Ministry of Transportation – Integral abutment bridges, Report SO-96-01. Ontario: The Queen's Printer.

Husain, I. & Bagnariol, D., 2000. *Performance of integral abutment bridges*. Queen's Printer for Ontario.

Jaradat, Y.M.M., 2005. Soil-structure interaction of FRP piles in integral abutment bridges. PhD, University of Maryland

Lee, D. J., 1994. *Bridge bearings and expansion joints*. CRC Press.

National Institute for Transport and Road Research, Code of practice for the design of highway bridges and culverts in South Africa. Technical Methods for Highways, TMH 7 – Parts 1 and 2. CSIR, Pretoria, 1981.

O'Brien, E.J. & Keogh, D.L., 1999. Bridge deck analysis. London: E & FN Spon.

Ohio Department of Transportation, Office of Structural Engineering, 2003. Bridge Design Manual. Ohio 43223, Columbus.

Ontario Ministry of Transportation (MTO), 2008. RSS (Retained soil systems) Design Guidelines

Poulos, H. G. & Davis, E. H., 1980. Pile foundation analysis and design. Toronto: John Wiley and Sons Inc.

Radolli, M., & Green, R., 1976. Thermal stress analysis of concrete bridge superstructures. Transportation Research Record 607.

Rajapakse, R., 2008. Pile Design for structural and geotechnical engineers. New York: Butterworth-Heinemann.

Reid, I.L.K., Thayre, P.A., Jenkins, D.E. & Broom, R.A., 2008. Bridge accessories. In G. Parke & N. Hewson, eds. *ICE manual of bridge engineering*. UK, ICE. P. 553-565.

Roebuck, C.S., 2005. Department of *Civil Engineering: style guide*. KwaZulu-Natal: University of KwaZulu-Natal.

Rombach, G. A., 2011. Finite-element design of concrete structures: Practical problems and their solutions. 2nd ed. London: Thomas Telford.

Skempton, A.W., 1951. The bearing capacity of clays. *Building Research Congress, London 1951.*

Sisk, G. & Terzaghi, S., 2009. Integral bridge design: derivation of the spring constant for modelling the soil-structure interaction. 7th Austroads bridge conference, May 2009, Auckland, New Zealand.

Thevaneyan, K. D. & Forth, J. P., 2013. Soil structure interaction of integral abutment bridges.

Tlustochowicz, G., 2005. Optimized design of integral abutments for a three span composite bridge. M.Sc. Lulea University of Technology.

Tomlinson, M.J., 1994. Pile design and construction practice. 4th ed. London: E & FN Spon.

Vesic, A.B., 1961. Beams on elastic subgrade and the Winkler's hypothesis. In *Proceedings, 5th International Conference on Soil Mechanics and Foundation Engineering* (Vol. 1, pp. 845-850).

VTrans, Integral Abutment Committee, 2009. Integral Abutment Bridge design guidelines. 2nd ed. Vermont: Agency of Transportation.

VTrans, Performance Monitoring of Jointless Bridges, Phase 1 Report - Synthesis of Technical Information for Jointless Bridge Construction, 2002 Vermont: Agency of Transportation.

Wagle, G. N. & Watt, D., 2011. Design of integral bridges on M50, Ireland. *Structural Engineering International*, *21*(2), 202-205.

White. H., 2007. *Integral abutment bridges: Comparison of current practice between European countries and the United States of America*. Transportation Research and Development Bureau, New York State Department of Transportation.

Zakrzewski, M.S., 1962. Foundations for the ocean terminal in Durban. *Transactions of the South African Institution of civil engineers*, Trans.S.Afr.Instn.Civ.Engrs. 4, Sept., 1962, p175-188.

APPENDIX A – Pile Head Calculations

This Appendix contains the raw data and calculations for the free pile head for the 350 x 350 PC pile and 254 x 254 x 89 H-pile. The raw data shown in the Table A-1 below was used to generate the graphs and curves presented in the Chapter 5. Since for all different piles the calculation method is the same, the Table A-1 and Table A-2 below uses two types of pile to illustrate an example. All other pile types are based on the same concept.

Table A-1: Data for free pile head for 350 x 350 PC pile

δ =	$\frac{PL^3}{3EI}$			Formular for free headed pile					
Type of pile : 350 x 350 concrete pile					b (m)=	0,35	d (m)=	0,35	
L (m)=	(varies)	(effective length based on virtual fixity) - effective cantilever concept for piles							
P=	(varies)	(determined from the movement applicable to integral bridges)							
δ =	(varies)	(based on typical movements for integral bridges in 2.5mm increments - see literature)							
I =	0,00125052	(second moment of inertia of pile)							
E =	2,80E+07	(pile Young's Modulus)							
L (m)=	2,00	3,00	3,50	4,00	6,00	8,00	10,00		
δ (mm)	P (kN)	P (kN)	P (kN)	P (kN)	P (kN)	P (kN)	P (kN)	(mm)	(m)
0,0	0,000	0,000	0,000	0,000	0,000	0,000	0,000	0,0	0
2,5	32,826	9,726	6,125	4,103	1,216	0,513	0,263	2,5	0,0025
5,0	65,652	19,453	12,250	8,207	2,432	1,026	0,525	5,0	0,005
7,5	98,479	29,179	18,375	12,310	3,647	1,539	0,788	7,5	0,0075
10,0	131,305	38,905	24,500	16,413	4,863	2,052	1,050	10,0	0,01
12,5	164,131	48,631	30,625	20,516	6,079	2,565	1,313	12,5	0,0125
15,0	196,957	58,358	36,750	24,620	7,295	3,077	1,576	15,0	0,015
17,5	229,783	68,084	42,875	28,723	8,510	3,590	1,838	17,5	0,0175
20,0	262,609	77,810	49,000	32,826	9,726	4,103	2,101	20,0	0,02
22,5	295,436	87,536	55,125	36,929	10,942	4,616	2,363	22,5	0,0225
25,0	328,262	97,263	61,250	41,033	12,158	5,129	2,626	25,0	0,025
27,5	361,088	106,989	67,375	45,136	13,374	5,642	2,889	27,5	0,0275
30,0	393,914	116,715	73,500	49,239	14,589	6,155	3,151	30,0	0,03
32,5	426,740	126,442	79,625	53,343	15,805	6,668	3,414	32,5	0,0325
35,0	459,566	136,168	85,750	57,446	17,021	7,181	3,677	35,0	0,035
37,5	492,393	145,894	91,875	61,549	18,237	7,694	3,939	37,5	0,0375
40,0	525,219	155,620	98,000	65,652	19,453	8,207	4,202	40,0	0,04
42,5	558,045	165,347	104,125	69,756	20,668	8,719	4,464	42,5	0,0425
45,0	590,871	175,073	110,250	73,859	21,884	9,232	4,727	45,0	0,045
47,5	623,697	184,799	116,375	77,962	23,100	9,745	4,990	47,5	0,0475
50,0	656,523	194,525	122,500	82,065	24,316	10,258	5,252	50,0	0,05

L(m)	Moment (5mm)	Moment (10mm)	Moment (15mm)	Moment (20mm)	Moment (25mm)	Moment (30mm)	Moment (35mm)	Moment (40mm)	Moment (45mm)	Moment (50mm)
2,00	131,30	262,61	393,91	525,22	656,52	787,83	919,13	1050,44	1181,74	1313,05
3,00	58,36	116,72	175,07	233,43	291,79	350,15	408,50	466,86	525,22	583,58
3,50	42,88	85,75	128,63	171,50	214,38	257,25	300,13	343,00	385,88	428,75
4,00	32,83	65,65	98,48	131,30	164,13	196,96	229,78	262,61	295,44	328,26
6,00	14,59	29,18	43,77	58,36	72,95	87,54	102,13	116,72	131,30	145,89
8,00	8,21	16,41	24,62	32,83	41,03	49,24	57,45	65,65	73,86	82,07
10,00	5,25	10,50	15,76	21,01	26,26	31,51	36,77	42,02	47,27	52,52
DEFLECTIONS mm	**5**	**10**	**15**	**20**	**25**	**30**	**35**	**40**	**45**	**50**
L(m)	Shear(5mm)	Shear (10mm)	Shear (15mm)	Shear (20mm)	Shear (25mm)	Shear (30mm)	Shear (35mm)	Shear (40mm)	Shear (45mm)	Shear (50mm)
2,00	65,652	131,305	196,957	262,609	328,262	393,914	459,566	525,219	590,871	656,523
3,00	19,453	38,905	58,358	77,810	97,263	116,715	136,168	155,620	175,073	194,525
3,50	12,250	24,500	36,750	49,000	61,250	73,500	85,750	98,000	110,250	122,500
4,00	8,207	16,413	24,620	32,826	41,033	49,239	57,446	65,652	73,859	82,065
6,00	2,432	4,863	7,295	9,726	12,158	14,589	17,021	19,453	21,884	24,316
8,00	1,026	2,052	3,077	4,103	5,129	6,155	7,181	8,207	9,232	10,258
10,00	0,525	1,050	1,576	2,101	2,626	3,151	3,677	4,202	4,727	5,252
DEFLECTIONS mm	**5**	**50**	**15**	**20**	**25**	**30**	**35**	**40**	**45**	**50**

Table A-2: Data for free pile head for 254 x 254 x 89 H-Pile about strong axis

δ	=	$\frac{PL^3}{3EI}$		Formular for free headed pile					
	254x254x89	11.40E-3			143.0E-6	48.30E-6		Steel:350W	
Type of pile :									
L (m)=	(varies)	(effective length based on virtual fixity) - effective cantilever concept for piles							
P=	(varies)	(determined from the movement applicable to integral bridges)							
δ =	(varies)	(based on typical movements for integral bridges in 2.5mm increments - see literature)							
I =	0,000143	(second moment of inertia of pile)							
E =	2,06E+08	(pile Young's Modulus)							

L (m)=	2,00	3,00	3,50	4,00	6,00	8,00	10,00
δ (mm)	P (kN)	P (kN)	P (kN)	P (kN)	P (kN)	P (kN)	P (kN)
0,0	0,000	0,000	0,000	0,000	0,000	0,000	0,000
2,5	27,617	8,183	5,153	3,452	1,023	0,432	0,221
5,0	55,234	16,366	10,306	6,904	2,046	0,863	0,442
7,5	82,851	24,548	15,459	10,356	3,069	1,295	0,663
10,0	110,468	32,731	20,612	13,808	4,091	1,726	0,884
12,5	138,084	40,914	25,765	17,261	5,114	2,158	1,105
15,0	165,701	49,097	30,918	20,713	6,137	2,589	1,326
17,5	193,318	57,279	36,071	24,165	7,160	3,021	1,547
20,0	220,935	65,462	41,224	27,617	8,183	3,452	1,767
22,5	248,552	73,645	46,377	31,069	9,206	3,884	1,988
25,0	276,169	81,828	51,530	34,521	10,228	4,315	2,209
27,5	303,786	90,011	56,683	37,973	11,251	4,747	2,430
30,0	331,403	98,193	61,836	41,425	12,274	5,178	2,651
32,5	359,019	106,376	66,989	44,877	13,297	5,610	2,872
35,0	386,636	114,559	72,142	48,330	14,320	6,041	3,093
37,5	414,253	122,742	77,295	51,782	15,343	6,473	3,314
40,0	441,870	130,924	82,448	55,234	16,366	6,904	3,535
42,5	469,487	139,107	87,601	58,686	17,388	7,336	3,756
45,0	497,104	147,290	92,754	62,138	18,411	7,767	3,977
47,5	524,721	155,473	97,907	65,590	19,434	8,199	4,198
50,0	552,338	163,656	103,060	69,042	20,457	8,630	4,419

L(m)	Moment (5mm)	Moment (10mm)	Moment (15mm)	Moment (20mm)	Moment (25mm)	Moment (30mm)	Moment (35mm)	Moment (40mm)	Moment (45mm)	Moment (50mm)
2,00	110,47	220,94	331,40	441,87	552,34	662,81	773,27	883,74	994,21	1104,68
3,00	49,10	98,19	147,29	196,39	245,48	294,58	343,68	392,77	441,87	490,97
3,50	36,07	72,14	108,21	144,28	180,36	216,43	252,50	288,57	324,64	360,71
4,00	27,62	55,23	82,85	110,47	138,08	165,70	193,32	220,94	248,55	276,17
6,00	12,27	24,55	36,82	49,10	61,37	73,65	85,92	98,19	110,47	122,74
8,00	6,90	13,81	20,71	27,62	34,52	41,43	48,33	55,23	62,14	69,04
10,00	4,42	8,84	13,26	17,67	22,09	26,51	30,93	35,35	39,77	44,19
EFLECTIONS m	**5**	**10**	**15**	**20**	**25**	**30**	**35**	**40**	**45**	**50**

L(m)	Shear(5mm)	Shear (10mm)	Shear (15mm)	Shear (20mm)	Shear (25mm)	Shear (30mm)	Shear (35mm)	Shear (40mm)	Shear (45mm)	Shear (50mm)
2,00	55,234	110,468	165,701	220,935	276,169	331,403	386,636	441,870	497,104	552,338
3,00	16,366	32,731	49,097	65,462	81,828	98,193	114,559	130,924	147,290	163,656
3,50	10,306	20,612	30,918	41,224	51,530	61,836	72,142	82,448	92,754	103,060
4,00	6,904	13,808	20,713	27,617	34,521	41,425	48,330	55,234	62,138	69,042
6,00	2,046	4,091	6,137	8,183	10,228	12,274	14,320	16,366	18,411	20,457
8,00	0,863	1,726	2,589	3,452	4,315	5,178	6,041	6,904	7,767	8,630
10,00	0,442	0,884	1,326	1,767	2,209	2,651	3,093	3,535	3,977	4,419
EFLECTIONS m	**5**	**10**	**15**	**20**	**25**	**30**	**35**	**40**	**45**	**50**

APPENDIX B – Variation in Pile Head Conditions

This Appendix contains the raw data and calculations for the different pile head conditions for the 350 x 350 PC pile and 254 x 254 x 89 H-pile. The data presented below in Table B-1 and Table B-2 are based on a fixed pile head. Only two pile type examples are provided below.

Table B-1: Data for fixed pile head for 350 x 350 PC pile

δ	=	$\frac{PL^3}{12EI}$		Formular for fixed headed pile						
Type of pile : 350 x 350 concrete pile					b (m)=	0,35	d (m)=	0,35		
L (m)=	(varies)	(effective length based on virtual fixity) - effective cantilever concept for piles								
P=	(varies)	(determined from the movement applicable to integral bridges)								
δ =	(varies)	(based on typical movements for integral bridges in 2.5mm increments - see literature)								
I =	0,00125052	(second moment of inertia of pile)								
E =	2,80E+07	(pile Young's Modulus)								

L (m)=	2,00	3,00	3,50	4,00	6,00	8,00	10,00
δ (mm)	P (kN)	P (kN)	P (kN)	P (kN)	P (kN)	P (kN)	P (kN)
0,0	0,000	0,000	0,000	0,000	0,000	0,000	0,000
2,5	131,305	38,905	24,500	16,413	4,863	2,052	1,050
5,0	262,609	77,810	49,000	32,826	9,726	4,103	2,101
7,5	393,914	116,715	73,500	49,239	14,589	6,155	3,151
10,0	525,219	155,620	98,000	65,652	19,453	8,207	4,202
12,5	656,523	194,525	122,500	82,065	24,316	10,258	5,252
15,0	787,828	233,431	147,000	98,479	29,179	12,310	6,303
17,5	919,133	272,336	171,500	114,892	34,042	14,361	7,353
20,0	1050,438	311,241	196,000	131,305	38,905	16,413	8,404
22,5	1181,742	350,146	220,500	147,718	43,768	18,465	9,454
25,0	1313,047	389,051	245,000	164,131	48,631	20,516	10,504
27,5	1444,352	427,956	269,500	180,544	53,495	22,568	11,555
30,0	1575,656	466,861	294,000	196,957	58,358	24,620	12,605
32,5	1706,961	505,766	318,500	213,370	63,221	26,671	13,656
35,0	1838,266	544,671	343,000	229,783	68,084	28,723	14,706
37,5	1969,570	583,576	367,500	246,196	72,947	30,775	15,757
40,0	2100,875	622,481	392,000	262,609	77,810	32,826	16,807
42,5	2232,180	661,387	416,500	279,022	82,673	34,878	17,857
45,0	2363,484	700,292	441,000	295,436	87,536	36,929	18,908
47,5	2494,789	739,197	465,500	311,849	92,400	38,981	19,958
50,0	2626,094	778,102	490,000	328,262	97,263	41,033	21,009

L(m)	Moment (5mm)	Moment (10mm)	Moment (15mm)	Moment (20mm)	Moment (25mm)	Moment (30mm)	Moment (35mm)	Moment (40mm)	Moment (45mm)	Moment (50mm)
2,00	525,22	1050,44	1575,66	2100,88	2626,09	3151,31	3676,53	4201,75	4726,97	5252,19
3,00	233,43	466,86	700,29	933,72	1167,15	1400,58	1634,01	1867,44	2100,88	2334,31
3,50	171,50	343,00	514,50	686,00	857,50	1029,00	1200,50	1372,00	1543,50	1715,00
4,00	131,30	262,61	393,91	525,22	656,52	787,83	919,13	1050,44	1181,74	1313,05
6,00	58,36	116,72	175,07	233,43	291,79	350,15	408,50	466,86	525,22	583,58
8,00	32,83	65,65	98,48	131,30	164,13	196,96	229,78	262,61	295,44	328,26
10,00	21,01	42,02	63,03	84,04	105,04	126,05	147,06	168,07	189,08	210,09
FLECTIONS	5	10	15	20	25	30	35	40	45	50
L(m)	Shear(5mm)	Shear (10mm)	Shear (15mm)	Shear (20mm)	Shear (25mm)	Shear (30mm)	Shear (35mm)	Shear (40mm)	Shear (45mm)	Shear (50mm)
2,00	65,652	131,305	196,957	262,609	328,262	393,914	459,566	525,219	590,871	656,523
3,00	19,453	38,905	58,358	77,810	97,263	116,715	136,168	155,620	175,073	194,525
3,50	12,250	24,500	36,750	49,000	61,250	73,500	85,750	98,000	110,250	122,500
4,00	8,207	16,413	24,620	32,826	41,033	49,239	57,446	65,652	73,859	82,065
6,00	2,432	4,863	7,295	9,726	12,158	14,589	17,021	19,453	21,884	24,316
8,00	1,026	2,052	3,077	4,103	5,129	6,155	7,181	8,207	9,232	10,258
10,00	0,525	1,050	1,576	2,101	2,626	3,151	3,677	4,202	4,727	5,252
EFLECTIONS m	5	10	15	20	25	30	35	40	45	50

Table B-2: Data for free pile head for 254 x 254 x 89 H-Pile about strong axis

δ	=	$\frac{PL^3}{12EI}$		Formular for fixed headed pile					
	254x254x89	11.40E-3			143.0E-6	48.30E-6		Steel:350W	
Type of pile :									
L (m)=	(varies)	(effective length based on virtual fixity) - effective cantilever concept for piles							
P=	(varies)	(determined from the movement applicable to integral bridges)							
δ =	(varies)	(based on typical movements for integral bridges in 2.5mm increments - see literature)							
I =	0,000143	(second moment of inertia of pile)							
E =	2,06E+08	(pile Young's Modulus)							

L (m)=	2,00	3,00	3,50	4,00	6,00	8,00	10,00
δ (mm)	P (kN)	P (kN)	P (kN)	P (kN)	P (kN)	P (kN)	P (kN)
0,0	0,000	0,000	0,000	0,000	0,000	0,000	0,000
2,5	110,468	32,731	20,612	13,808	4,091	1,726	0,884
5,0	220,935	65,462	41,224	27,617	8,183	3,452	1,767
7,5	331,403	98,193	61,836	41,425	12,274	5,178	2,651
10,0	441,870	130,924	82,448	55,234	16,366	6,904	3,535
12,5	552,338	163,656	103,060	69,042	20,457	8,630	4,419
15,0	662,805	196,387	123,672	82,851	24,548	10,356	5,302
17,5	773,273	229,118	144,284	96,659	28,640	12,082	6,186
20,0	883,740	261,849	164,896	110,468	32,731	13,808	7,070
22,5	994,208	294,580	185,508	124,276	36,823	15,534	7,954
25,0	1104,675	327,311	206,120	138,084	40,914	17,261	8,837
27,5	1215,143	360,042	226,732	151,893	45,005	18,987	9,721
30,0	1325,610	392,773	247,344	165,701	49,097	20,713	10,605
32,5	1436,078	425,504	267,956	179,510	53,188	22,439	11,489
35,0	1546,545	458,236	288,568	193,318	57,279	24,165	12,372
37,5	1657,013	490,967	309,180	207,127	61,371	25,891	13,256
40,0	1767,480	523,698	329,792	220,935	65,462	27,617	14,140
42,5	1877,948	556,429	350,404	234,743	69,554	29,343	15,024
45,0	1988,415	589,160	371,016	248,552	73,645	31,069	15,907
47,5	2098,883	621,891	391,628	262,360	77,736	32,795	16,791
50,0	2209,350	654,622	412,240	276,169	81,828	34,521	17,675

L(m)	Moment (5mm)	Moment (10mm)	Moment (15mm)	Moment (20mm)	Moment (25mm)	Moment (30mm)	Moment (35mm)	Moment (40mm)	Moment (45mm)	Moment (50mm)
2,00	441,87	883,74	1325,61	1767,48	2209,35	2651,22	3093,09	3534,96	3976,83	4418,70
3,00	196,39	392,77	589,16	785,55	981,93	1178,32	1374,71	1571,09	1767,48	1963,87
3,50	144,28	288,57	432,85	577,14	721,42	865,70	1009,99	1154,27	1298,56	1442,84
4,00	110,47	220,94	331,40	441,87	552,34	662,81	773,27	883,74	994,21	1104,68
6,00	49,10	98,19	147,29	196,39	245,48	294,58	343,68	392,77	441,87	490,97
8,00	27,62	55,23	82,85	110,47	138,08	165,70	193,32	220,94	248,55	276,17
10,00	17,67	35,35	53,02	70,70	88,37	106,05	123,72	141,40	159,07	176,75
EFLECTIONS m	**5**	**10**	**15**	**20**	**25**	**30**	**35**	**40**	**45**	**50**

L(m)	Shear(5mm)	Shear (10mm)	Shear (15mm)	Shear (20mm)	Shear (25mm)	Shear (30mm)	Shear (35mm)	Shear (40mm)	Shear (45mm)	Shear (50mm)
2,00	55,234	110,468	165,701	220,935	276,169	331,403	386,636	441,870	497,104	552,338
3,00	16,366	32,731	49,097	65,462	81,828	98,193	114,559	130,924	147,290	163,656
3,50	10,306	20,612	30,918	41,224	51,530	61,836	72,142	82,448	92,754	103,060
4,00	6,904	13,808	20,713	27,617	34,521	41,425	48,330	55,234	62,138	69,042
6,00	2,046	4,091	6,137	8,183	10,228	12,274	14,320	16,366	18,411	20,457
8,00	0,863	1,726	2,589	3,452	4,315	5,178	6,041	6,904	7,767	8,630
10,00	0,442	0,884	1,326	1,767	2,209	2,651	3,093	3,535	3,977	4,419
EFLECTIONS m	**5**	**10**	**15**	**20**	**25**	**30**	**35**	**40**	**45**	**50**

The data presented below in Table B-3 and Table B-4 are based on a partially fixed pile head. Note the partially fixed pile head condition is assumed to be an average of the free pile head condition and fixed pile head conditions. The derivation of this equation is shown in Appendix G.

Table B-3: Data for partially-fixed pile head for 350 x 350 PC pile

δ	=	$\frac{5PL^3}{24EI}$		Formular for partially fixed headed pile					
Type of pile : 350 x 350 concrete pile					b (m)=	0,35	d (m)=	0,35	
L (m)=	(varies)	(effective length based on virtual fixity) - effective cantilever concept for piles							
P=	(varies)	(determined from the movement applicable to integral bridges)							
δ =	(varies)	(based on typical movements for integral bridges in 2.5mm increments - see literature)							
I =	0,00125052	(second moment of inertia of pile)							
E =	2,80E+07	(pile Young's Modulus)							

L (m)=	2,00	3,00	3,50	4,00	6,00	8,00	10,00
δ (mm)	P (kN)	P (kN)	P (kN)	P (kN)	P (kN)	P (kN)	P (kN)
0,0	0,000	0,000	0,000	0,000	0,000	0,000	0,000
2,5	52,522	15,562	9,800	6,565	1,945	0,821	0,420
5,0	105,044	31,124	19,600	13,130	3,891	1,641	0,840
7,5	157,566	46,686	29,400	19,696	5,836	2,462	1,261
10,0	210,088	62,248	39,200	26,261	7,781	3,283	1,681
12,5	262,609	77,810	49,000	32,826	9,726	4,103	2,101
15,0	315,131	93,372	58,800	39,391	11,672	4,924	2,521
17,5	367,653	108,934	68,600	45,957	13,617	5,745	2,941
20,0	420,175	124,496	78,400	52,522	15,562	6,565	3,361
22,5	472,697	140,058	88,200	59,087	17,507	7,386	3,782
25,0	525,219	155,620	98,000	65,652	19,453	8,207	4,202
27,5	577,741	171,182	107,800	72,218	21,398	9,027	4,622
30,0	630,263	186,744	117,600	78,783	23,343	9,848	5,042
32,5	682,784	202,306	127,400	85,348	25,288	10,669	5,462
35,0	735,306	217,869	137,200	91,913	27,234	11,489	5,882
37,5	787,828	233,431	147,000	98,479	29,179	12,310	6,303
40,0	840,350	248,993	156,800	105,044	31,124	13,130	6,723
42,5	892,872	264,555	166,600	111,609	33,069	13,951	7,143
45,0	945,394	280,117	176,400	118,174	35,015	14,772	7,563
47,5	997,916	295,679	186,200	124,739	36,960	15,592	7,983
50,0	1050,438	311,241	196,000	131,305	38,905	16,413	8,404

L(m)	Moment (5mm)	Moment (10mm)	Moment (15mm)	Moment (20mm)	Moment (25mm)	Moment (30mm)	Moment (35mm)	Moment (40mm)	Moment (45mm)	Moment (50mm)
2,00	210,09	420,18	630,26	840,35	1050,44	1260,53	1470,61	1680,70	1890,79	2100,88
3,00	93,37	186,74	280,12	373,49	466,86	560,23	653,61	746,98	840,35	933,72
3,50	68,60	137,20	205,80	274,40	343,00	411,60	480,20	548,80	617,40	686,00
4,00	52,52	105,04	157,57	210,09	262,61	315,13	367,65	420,18	472,70	525,22
6,00	23,34	46,69	70,03	93,37	116,72	140,06	163,40	186,74	210,09	233,43
8,00	13,13	26,26	39,39	52,52	65,65	78,78	91,91	105,04	118,17	131,30
10,00	8,40	16,81	25,21	33,61	42,02	50,42	58,82	67,23	75,63	84,04
EFLECTIONS m	**5**	**10**	**15**	**20**	**25**	**30**	**35**	**40**	**45**	**50**
L(m)	Shear(5mm)	Shear (10mm)	Shear (15mm)	Shear (20mm)	Shear (25mm)	Shear (30mm)	Shear (35mm)	Shear (40mm)	Shear (45mm)	Shear (50mm)
2,00	65,652	131,305	196,957	262,609	328,262	393,914	459,566	525,219	590,871	656,523
3,00	19,453	38,905	58,358	77,810	97,263	116,715	136,168	155,620	175,073	194,525
3,50	12,250	24,500	36,750	49,000	61,250	73,500	85,750	98,000	110,250	122,500
4,00	8,207	16,413	24,620	32,826	41,033	49,239	57,446	65,652	73,859	82,065
6,00	2,432	4,863	7,295	9,726	12,158	14,589	17,021	19,453	21,884	24,316
8,00	1,026	2,052	3,077	4,103	5,129	6,155	7,181	8,207	9,232	10,258
10,00	0,525	1,050	1,576	2,101	2,626	3,151	3,677	4,202	4,727	5,252
EFLECTIONS m	**5**	**10**	**15**	**20**	**25**	**30**	**35**	**40**	**45**	**50**

Table B-4: Data for free pile head for 254 x 254 x 89 H-Pile about strong axis

δ	=	$\frac{5PL^3}{24EI}$		Formular for partially fixed headed pile					
	254x254x89	11.40E-3			143.0E-6	48.30E-6		Steel:350W	
Type of pile :									
L (m)=	(varies)	(effective length based on virtual fixity) - effective cantilever concept for piles							
P=	(varies)	(determined from the movement applicable to integral bridges)							
δ =	(varies)	(based on typical movements for integral bridges in 2.5mm increments - see literature)							
I =	0,000143	(second moment of inertia of pile)							
E =	2,06E+08	(pile Young's Modulus)							

L (m)=	2,00	3,00	3,50	4,00	6,00	8,00	10,00
δ (mm)	P (kN)	P (kN)	P (kN)	P (kN)	P (kN)	P (kN)	P (kN)
0,0	0,000	0,000	0,000	0,000	0,000	0,000	0,000
2,5	44,187	13,092	8,245	5,523	1,637	0,690	0,353
5,0	88,374	26,185	16,490	11,047	3,273	1,381	0,707
7,5	132,561	39,277	24,734	16,570	4,910	2,071	1,060
10,0	176,748	52,370	32,979	22,094	6,546	2,762	1,414
12,5	220,935	65,462	41,224	27,617	8,183	3,452	1,767
15,0	265,122	78,555	49,469	33,140	9,819	4,143	2,121
17,5	309,309	91,647	57,714	38,664	11,456	4,833	2,474
20,0	353,496	104,740	65,958	44,187	13,092	5,523	2,828
22,5	397,683	117,832	74,203	49,710	14,729	6,214	3,181
25,0	441,870	130,924	82,448	55,234	16,366	6,904	3,535
27,5	486,057	144,017	90,693	60,757	18,002	7,595	3,888
30,0	530,244	157,109	98,938	66,281	19,639	8,285	4,242
32,5	574,431	170,202	107,182	71,804	21,275	8,975	4,595
35,0	618,618	183,294	115,427	77,327	22,912	9,666	4,949
37,5	662,805	196,387	123,672	82,851	24,548	10,356	5,302
40,0	706,992	209,479	131,917	88,374	26,185	11,047	5,656
42,5	751,179	222,572	140,162	93,897	27,821	11,737	6,009
45,0	795,366	235,664	148,406	99,421	29,458	12,428	6,363
47,5	839,553	248,756	156,651	104,944	31,095	13,118	6,716
50,0	883,740	261,849	164,896	110,468	32,731	13,808	7,070

L(m)	Moment (5mm)	Moment (10mm)	Moment (15mm)	Moment (20mm)	Moment (25mm)	Moment (30mm)	Moment (35mm)	Moment (40mm)	Moment (45mm)	Moment (50mm)
2,00	176,75	353,50	530,24	706,99	883,74	1060,49	1237,24	1413,98	1590,73	1767,48
3,00	78,55	157,11	235,66	314,22	392,77	471,33	549,88	628,44	706,99	785,55
3,50	57,71	115,43	173,14	230,85	288,57	346,28	404,00	461,71	519,42	577,14
4,00	44,19	88,37	132,56	176,75	220,94	265,12	309,31	353,50	397,68	441,87
6,00	19,64	39,28	58,92	78,55	98,19	117,83	137,47	157,11	176,75	196,39
8,00	11,05	22,09	33,14	44,19	55,23	66,28	77,33	88,37	99,42	110,47
10,00	7,07	14,14	21,21	28,28	35,35	42,42	49,49	56,56	63,63	70,70
EFLECTIONS m	**5**	**10**	**15**	**20**	**25**	**30**	**35**	**40**	**45**	**50**
L(m)	Shear(5mm)	Shear (10mm)	Shear (15mm)	Shear (20mm)	Shear (25mm)	Shear (30mm)	Shear (35mm)	Shear (40mm)	Shear (45mm)	Shear (50mm)
2,00	55,234	110,468	165,701	220,935	276,169	331,403	386,636	441,870	497,104	552,338
3,00	16,366	32,731	49,097	65,462	81,828	98,193	114,559	130,924	147,290	163,656
3,50	10,306	20,612	30,918	41,224	51,530	61,836	72,142	82,448	92,754	103,060
4,00	6,904	13,808	20,713	27,617	34,521	41,425	48,330	55,234	62,138	69,042
6,00	2,046	4,091	6,137	8,183	10,228	12,274	14,320	16,366	18,411	20,457
8,00	0,863	1,726	2,589	3,452	4,315	5,178	6,041	6,904	7,767	8,630
10,00	0,442	0,884	1,326	1,767	2,209	2,651	3,093	3,535	3,977	4,419
EFLECTIONS m	**5**	**10**	**15**	**20**	**25**	**30**	**35**	**40**	**45**	**50**

The Table B-5 and Table B-6 shown below is a summary of the data for the different pile head conditions for the two pile types used as an example i.e. the 350 x 350 PC Pile and the Steel H-pile. The Data shown in Table B-5 and Table B-6 were used to draw the graphs showing the variations in Chapter 5.

Table B-5: Data for 350 x 350 PC pile showing different pile conditions

PILE STIFFNESS VERSUS EFF PILE LENGTH					
FREE					
	P (kN)	Deflect (m)	K=P (kN/m)	b (m)	Slenderness ratio
L (m)=			y		x
2,00	656,523	0,05	13130,469	0,35	5,714
3,00	194,525	0,05	3890,5093	0,35	8,571
3,50	122,500	0,05	2450	0,35	10,000
4,00	82,065	0,05	1641,3086	0,35	11,429
6,00	24,316	0,05	486,31366	0,35	17,143
8,00	10,258	0,05	205,16357	0,35	22,857
10,00	5,252	0,05	105,04375	0,35	28,571
FIXED					
	P (kN)	Deflect (m)	K=P (kN/m)	b (m)	Slenderness ratio
L (m)=	(Copy&paste)		y		x
2,00	2626,094	0,05	52521,875	0,35	5,714
3,00	778,102	0,05	15562,037	0,35	8,571
3,50	490,000	0,05	9800	0,35	10,000
4,00	328,262	0,05	6565,2344	0,35	11,429
6,00	97,263	0,05	1945,2546	0,35	17,143
8,00	41,033	0,05	820,6543	0,35	22,857
10,00	21,009	0,05	420,175	0,35	28,571
PARTIALLY FIXED					
	P (kN)	Deflect (m)	K=P (kN/m)	b (m)	Slenderness ratio
L (m)=	(Copy&paste)		y		x
2,00	1050,438	0,05	21008,75	0,35	5,714
3,00	311,241	0,05	6224,8148	0,35	8,571
3,50	196,000	0,05	3920	0,35	10,000
4,00	131,305	0,05	2626,0938	0,35	11,429
6,00	38,905	0,05	778,10185	0,35	17,143
8,00	16,413	0,05	328,26172	0,35	22,857
10,00	8,404	0,05	168,07	0,35	28,571

Table B-6: Data for 254 x 254 x 89 H-Pile showing different pile conditions

PILE STIFFNESS VERSUS EFF PILE LENGTH				FREE CONDITIONS		
	P (kN)	Deflect (m	K=P (kN/m)	b (m)	Slenderness ratio	
L (m)=			y		x	
2	552,338	0,05	11046,75	0,5	4	
3	163,656	0,05	3273,1111	0,5	6	
3,5	103,060	0,05	2061,2012	0,5	7	
4	69,042	0,05	1380,8438	0,5	8	
6	20,457	0,05	409,13889	0,5	12	
8	8,630	0,05	172,60547	0,5	16	
10	4,419	0,05	88,374	0,5	20	
PILE STIFFNESS VERSUS EFF PILE LENGTH				**FIXED CONDITIONS**		
	P (kN)	Deflect (m	K=P (kN/m)	b (m)	Slenderness ratio	
L (m)=	COPY&PASTE		y		x	
2	2209,350	0,05	44187	0,5	4	
3	654,622	0,05	13092,444	0,5	6	
3,5	412,240	0,05	8244,8047	0,5	7	
4	276,169	0,05	5523,375	0,5	8	
6	81,828	0,05	1636,5556	0,5	12	
8	34,521	0,05	690,42188	0,5	16	
10	17,675	0,05	353,496	0,5	20	
PILE STIFFNESS VERSUS EFF PILE LENGTH				**PARTIALLY FIXED CONDITIONS**		
	P (kN)	Deflect (m	K=P (kN/m)	b (m)	Slenderness ratio	
L (m)=	COPY&PASTE		y		x	
2	883,740	0,05	17674,8	0,5	4	
3	261,849	0,05	5236,9778	0,5	6	
3,5	164,896	0,05	3297,9219	0,5	7	
4	110,468	0,05	2209,35	0,5	8	
6	32,731	0,05	654,62222	0,5	12	
8	13,808	0,05	276,16875	0,5	16	
10	7,070	0,05	141,3984	0,5	20	

APPENDIX C – Calculation of Pile Parameters for Varying Pile Types with a 3.5m Long Pile Sleeve

This Appendix contains the data that was used to generate the different pile behaviour data for the same pile sleeve length of 3.5m. The 3.5m sleeve length was chosen as it was common length as discussed in the Literature Review. The Table C-1 shown below provides the data for free pile head. The data was calculated/obtained from the same formulas as presented above.

Table C-1: Moments and shear forces for the same pile head deflection for varying pile types (Free Pile Head Condition)

FREE HEAD

	Moments									
	5	**10**	**15**	**20**	**25**	**30**	**35**	**40**	**45**	**50**
350 x 350	43	86	129	171,50	214,38	257,25	300,13	343,00	385,88	428,75
250 x 250	11	22,32	33,48	44,64	55,80	66,96	78,13	89,29	100,45	111,61
600 diam	218,12	436,23	654,35	872,47	1090,58	1308,70	1526,81	1744,93	1963,05	2181,16
H-P (SA)	36,07	72,14	108,21	144,28	180,36	216,43	252,50	288,57	324,64	360,71
H-P (WA)	12,18	24,37	36,55	48,73	60,92	73,10	85,28	97,47	109,65	121,83
Pipe Pile	41,06	82,13	123,19	164,26	205,32	246,39	287,45	328,52	369,58	410,65

Shear - Horizontal Force	**Deflection**	**350 x 350**	**250 x 250**	**600 diam**	**H-P (SA)**	**H-P (WA)**	**Pipe Pile**
	0,00	0,00	0,00	0,00	0,00	0,00	0,00
	2,50	6,13	1,59	31,16	5,15	1,74	5,87
	5,00	12,25	3,19	62,32	10,31	3,48	11,73
	7,50	18,38	4,78	93,48	15,46	5,22	17,60
	10,00	24,50	6,38	124,64	20,61	6,96	23,47
	12,50	30,63	7,97	155,80	25,77	8,70	29,33
	15,00	36,75	9,57	186,96	30,92	10,44	35,20
	17,50	42,88	11,16	218,12	36,07	12,18	41,06
	20,00	49,00	12,76	249,28	41,22	13,92	46,93
	22,50	55,13	14,35	280,44	46,38	15,66	52,80
	25,00	61,25	15,94	311,59	51,53	17,40	58,66
	27,50	67,38	17,54	342,75	56,68	19,15	64,53
	30,00	73,50	19,13	373,91	61,84	20,89	70,40
	32,50	79,63	20,73	405,07	66,99	22,63	76,26
	35,00	85,75	22,32	436,23	72,14	24,37	82,13
	37,50	91,87	23,92	467,39	77,30	26,11	88,00
	40,00	98,00	25,51	498,55	82,45	27,85	93,86
	42,50	104,13	27,10	529,71	87,60	29,59	99,73
	45,00	110,25	28,70	560,87	92,75	31,33	105,60
	47,50	116,38	30,29	592,03	97,91	33,07	111,46
	50,00	122,50	31,89	623,19	103,06	34,81	117,33

The Figure C-1 shown below is for the 600mm diameter pile, this was omitted from the combination of graphs from the results as the moment capacity was significantly higher.

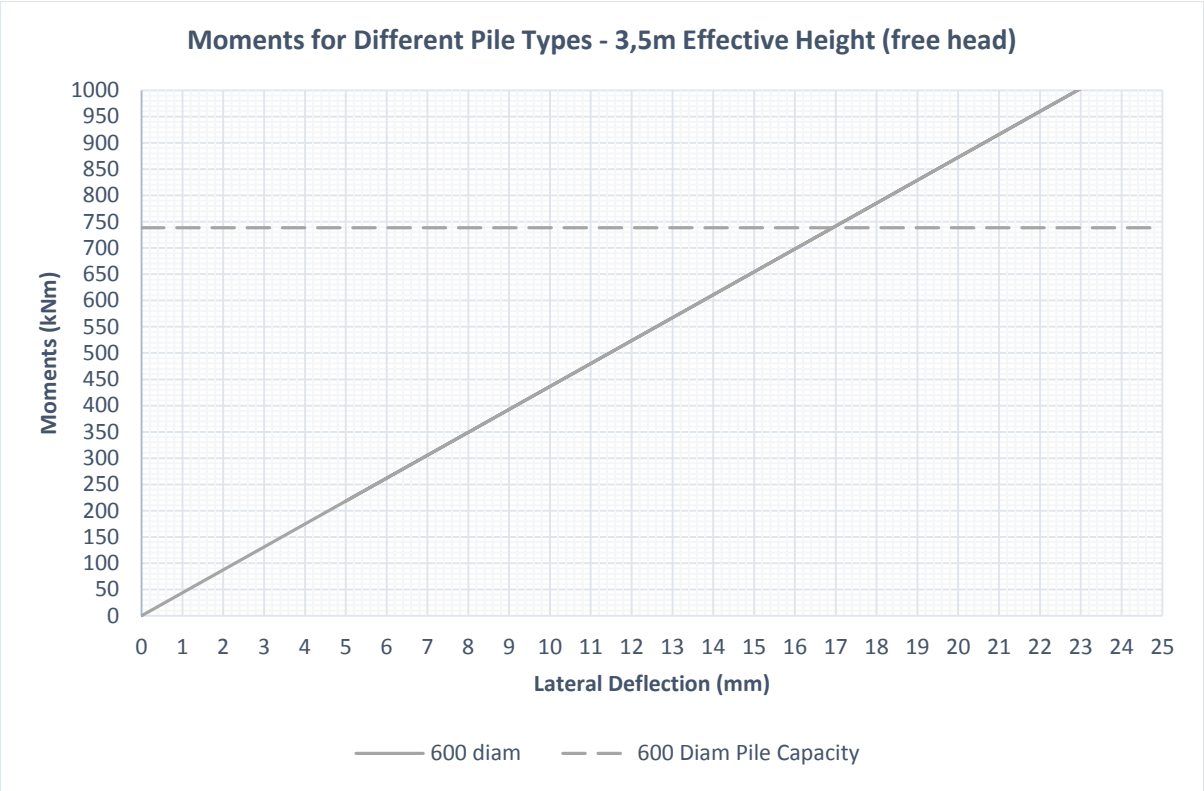

Figure C-1: 600mm diameter pile maximum moment capacity and lateral deflection

The Table C-2 shown below is the data shown for a fixed pile head. This was NOT represented in Chapter 5. The table is merely shown for comparative purposes.

Table C-2: Moments and shear forces for the same pile head deflection for varying pile types (Free Pile Head Condition)

FIXED HEAD

Moments										
	5	10	15	20	25	30	35	40	45	50
350 x 350	172	343	515	686,00	857,50	1029,00	1200,50	1372,00	1543,50	1715,00
250 x 250	45	89,29	133,93	178,57	223,21	267,86	312,50	357,14	401,79	446,43
600 diam	872,47	1744,93	2617,40	3489,86	4362,33	5234,79	6107,26	6979,72	7852,19	8724,65
H-P (SA)	144,28	288,57	432,85	577,14	721,42	865,70	1009,99	1154,27	1298,56	1442,84
H-P (WA)	48,73	97,47	146,20	194,93	243,67	292,40	341,14	389,87	438,60	487,34
Pipe Pile	164,26	328,52	492,78	657,04	821,30	985,56	1149,82	1314,08	1478,34	1642,60

Shear - Horizontal Force	Deflection	350 x 350	250 x 250	600 diam	H-P (SA)	H-P (WA)	Pipe Pile
	0,00	0,00	0,00	0,00	0,00	0,00	0,00
	2,50	24,50	6,38	124,64	20,61	6,96	23,47
	5,00	49,00	12,76	249,28	41,22	13,92	46,93
	7,50	73,50	19,13	373,91	61,84	20,89	70,40
	10,00	98,00	25,51	498,55	82,45	27,85	93,86
	12,50	122,50	31,89	623,19	103,06	34,81	117,33
	15,00	147,00	38,27	747,83	123,67	41,77	140,79
	17,50	171,50	44,64	872,47	144,28	48,73	164,26
	20,00	196,00	51,02	997,10	164,90	55,70	187,73
	22,50	220,50	57,40	1121,74	185,51	62,66	211,19
	25,00	245,00	63,78	1246,38	206,12	69,62	234,66
	27,50	269,50	70,15	1371,02	226,73	76,58	258,12
	30,00	294,00	76,53	1495,65	247,34	83,54	281,59
	32,50	318,50	82,91	1620,29	267,96	90,51	305,05
	35,00	343,00	89,29	1744,93	288,57	97,47	328,52
	37,50	367,50	95,66	1869,57	309,18	104,43	351,99
	40,00	392,00	102,04	1994,21	329,79	111,39	375,45
	42,50	416,50	108,42	2118,84	350,40	118,35	398,92
	45,00	441,00	114,80	2243,48	371,02	125,32	422,38
	47,50	465,50	121,17	2368,12	391,63	132,28	445,85
	50,00	490,00	127,55	2492,76	412,24	139,24	469,31

APPENDIX D – Calculation of Maximum Moment Capacity for Piles

This Appendix provides the assumptions and calculations for the maximum moment for the different piles investigated in this study.

CALCULATION FOR THE MAXIMUM MOMENT CAPACITY FOR 350 x 350 PC PILE:

NOTES & ASSUMPTIONS:

1) THE MOMENT CALCULATED IS THE MAX. MOMENT THE PILE CAN CARRY.

2) ACCORDING TO BS 5400 - PART 4, THE FREE PORTION OF PILE IS DESIGNED AS A COLUMN.

3) SINCE CALCULATING MAX. MOMENT, USE MAX A_s.

4) ACCORDING TO SANS 4.11.5.2 & BS 5400 - PART 4 (5.8.5), MAX A_s (AREA OF REINFORCEMENT) OF LONGITUDINAL A_s SHOULD NOT EXCEED 6%.

5) MAX. MOMENT BASED ON WORKING LOADS FROM "A GUIDE TO PRACTICAL GEOTECHNICAL ENGINEERING IN SOUTHERN AFRICA" (1995)

6) THESE NOTES & ASSUMPTIONS ALSO APPLY TO 250 X 250 PC PILE & 600 mm ∅ AUGER PILE

MOMENT CAPACITY OF 350 x 350 PC PILE

TYPICAL WORKING LOAD (350 mm SQUARE) = 2000 kN @ SLS
(FROM "FRANKI GUIDE" - 3RD ED)

MAX % A_s = 6 % (BS5400 - 5.8.5 & SANS 4.11.5.2)

$$\% A_s = \frac{100 A_s}{bh} = 6\% \qquad b = h = 350mm$$

$$A_s = \frac{6 \times 350 \times 350}{100} = 7350\ mm^2$$

EQUIVALENT TO < 8Y32 (6432)

VERY HIGH % A_s BUT FOR MAX MOMENT

ADOPT MAX A_s.

FROM INFO ABOVE & STD. COLUMN DESIGN CHARTS WE OBTAIN MAX. MOMENT.

- BASED ON RESEARCH WORK BY P.G. FENTON & C.v. HEERDAN ON EUROCODE VS. TMH7 BRIDGE LOADING CODE IN 2013 IT WAS FOUND THAT 2/3 BRIDGE LOADING IS FROM DEAD LOADS & 1/3 BRIDGE LOADING IS FROM LIVE LOADS.
- THIS IS BASE ON FULL CONCRETE BRIDGES ONLY.
- THE 2/3 DEAD LOAD (DL) & 1/3 LIVE LOAD (LL) IS ALSO BASED ON EXPERIENCE.
- AN EXAMPLE OF THE 2/3 DL & 1/3 LL FOR THE BELLAIR ROAD BRIDGE IS PROVIDED.

Table D-1: The percentage of live load and dead load off the total load for a pier from the Bellair Road Bridge

REACTIONS	AT	SLS		live load cases	TRAFFIC LOADING ONLY (KN)	% traffic load of total load	% Dead load of total load
Node 12	Load Case	Y-force (KN)					
Central Pier	D	5674,63		D	0	0	100
NC LOADINGS	D+NC-1	9799,63		NC-1	4124,63	42	58
	D+NC-2	7737,13		NC-2	2062,13	27	73
	D+NC-3	7737,13		NC-3	2062,13	27	73
NB LOADINGS	D+NB-1	6422,25		NB-1	747,25	12	88
	D+NB-2	6422,25		NB-2	747,25	12	88
	D+NB-3	6449,19		NB-3	774,19	12	88
NA LOADINGS	D+NA1	7079,8		NA1	1404,8	20	80
	D+NA2	7079,8		NA2	1404,8	20	80
	D+NA3	7833,3		NA3	2158,3	28	72
	D+NA4	7833,3		NA4	2158,3	28	72
	D+NA5	7833,3		NA5	2158,3	28	72
	D+NA6	7833,3		NA6	2158,3	28	72
	D+NA7	7833,3		NA7	2158,3	28	72
	D+NA8	7833,3		NA8	2158,3	28	72
	D+NA9	7848,42		NA9	2173,42	28	72
	D+NA10	7848,42		NA10	2173,42	28	72
	D+NA11	7848,42		NA11	2173,42	28	72
	D+NA12	7848,42		NA12	2173,42	28	72
	D+NA13	7848,42		NA13	2173,42	28	72
	D+NA14	7848,42		NA14	2173,42	28	72
	D+NA15	7230,4		NA15	1555,4	22	78
	D+NA16	6924,91		NA16	1249,91	18	82
	D+NA17	7983,9		NA17	2308,9	29	71
	D+NA18	7983,9		NA18	2308,9	29	71
	D+NA19	7983,9		NA19	2308,9	29	71
	D+NA20	7983,9		NA20	2308,9	29	71
	D+NA21	7678,41		NA21	2003,41	26	74
	D+NA22	7678,41		NA22	2003,41	26	74
	D+NA23	7999,02		NA23	2324,02	29	71
	D+NA24	7693,53		NA24	2018,53	26	74
	D+NA25	7999,02		NA25	2324,02	29	71
	D+NA26	7999,02		NA26	2324,02	29	71
NB LOADINGS	D+NB4	7043,9		NB4	1368,9	19	81
	D+NB5	5772,33		NB5	97,33	2	98
	D+NB6	6228,42		NB6	553,42	9	91

FROM THE DESIGN CHARTS FOR COLUMNS, FOR A GIVEN % A_s, THE HIGHER THE AXIAL LOAD THEN THE LOWER THE MOMENT CAPACITY.

THUS MOST CONSERVATIVE MOMENT WILL BE BASED ON LOW AXIAL LOAD.

2000 kN – WORKING LOAD

DL – 2/3	LL – 1/3	
1333 kN	667 kN	SLS
1333 x 1,2 x 1.1 = 1760 kN	667 x 1,5 x 1.1 = 1101 kN	ULS

NOTES:

DL
1,2 → γ_2
1,1 → γ_3
FROM TMH7 – PART 2

LL
1,5 → γ_2
1,1 → γ_3
FROM TMH7 – PART 2

ΣN (ULS) = 1760 + 1101 = 2861 kN

$d' = 30 + 16 + 8 = 54$ mm

$\frac{d'}{h} = \frac{54}{350} = 0,15$

(USE DESIGN CHART (SEE ATTACHED) FOR:

$f_y = 450$ N/mm²

$f_{cu} = 30$ MPa

$\frac{d'}{h} = 0,15$

NOW $\frac{N}{bh} = \frac{N}{b^2} = \frac{2861 \times 10^3 \text{ (N)}}{350 \text{ mm} \times 350 \text{ mm}} = 23,4$

FROM DESIGN CHART $\frac{M}{bh^2} = 3,4$

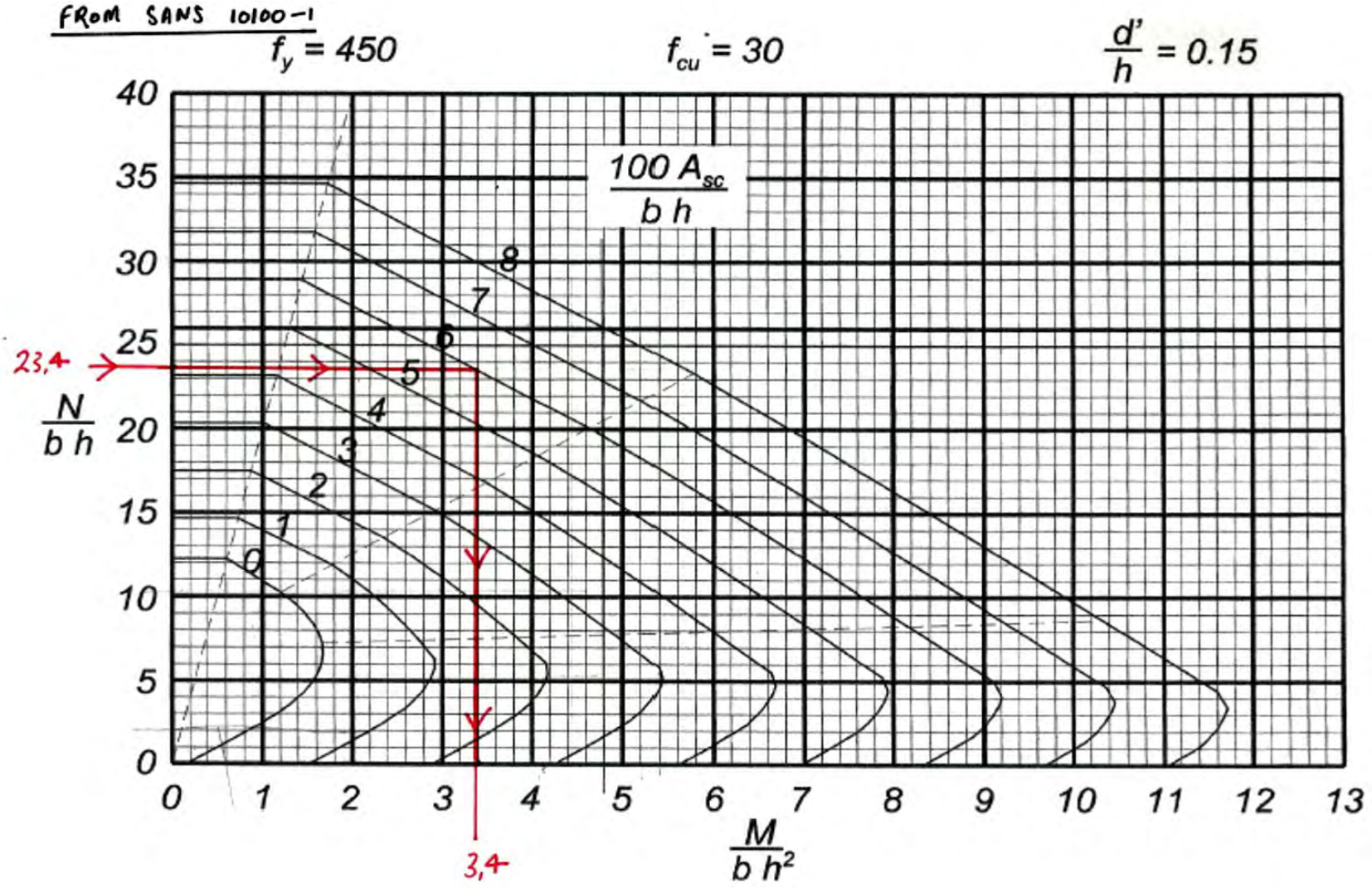
FROM SANS 10100-1
$f_y = 450$
$f_{cu} = 30$
$\frac{d'}{h} = 0.15$
$\frac{100\ A_{sc}}{b\ h}$
0
1
2
3
4
5
6
7
8
23,4
$\frac{N}{b\ h}$
40
35
30
25
20
15
10
5
0
0 1 2 3 4 5 6 7 8 9 10 11 12 13
3,4
$\frac{M}{b\ h^2}$

NOW MAX. M AT ULS:

$$M = \frac{3,4 \times (350 \times 350^2)}{10^6} = 146 \text{ kNm @ ULS}$$

TO PLOT MOMENT ON GRAPHS CONVERT BACK TO SLS:

146 kNm @ ULS		
DL - 2/3 = 97,33 kNm	LL - 1/3 = 48,67 kNm	ULS
$\frac{97,33}{1,2 \times 1,1}$ = 73,73 kNm	$\frac{48,67}{1,5 \times 1,1}$ = 29,50 kNm	SLS

MAX. MOMENT @ SLS = 73,73 + 29,50

= 103,23 kNm @ SLS →

CALCULATION FOR MAXIMUM MOMENT CAPACITY FOR 250 x 250 PC PILE:

- SIMILAR TO CALC AS 350 x 350 PILE.
- SAME NOTES, ASSUMPTIONS & FACTORS APPLY.

TYPICAL WORKING LOAD (250 SQUARE) = 1000 kN @ SLS
(FROM "FRANKI GUIDE" - 3RD ED.)

MAX. A_s = 6% (BS 5400 - PART 4 - 5.8.5 & SANS - 4.11.5.2)

$$\% A_s = \frac{100 A_s}{bh} = 6\%$$

$$\therefore A_s = \frac{6 \times 250^2}{100} = 3750\ mm^2$$

EQUIVALENT TO 8Y25 ($3928\ mm^2$) - VERY HIGH.

(SEE NOTES ON LOADING FROM 350 x 350 PILE)

1000 kN - SLS		
DL - 2/3 667 kN	LL - 1/3 333 kN	SLS
667 x 1,2 x 1 = 880,44 kN	333 x 1,5 x 1,1 = 549,45 kN	ULS

$$d' = 30 + \frac{25}{2} + 10 = 52,5\ mm$$

$$\frac{d'}{h} = \frac{52,5}{250} = 0,21$$ (use $\frac{d'}{h}$ = 0,20 design chart with f_y = 450 MPa & f_{cu} = 30 MPa)

$\sum N\ (ULS) = 880,44 + 549,45 = 1430\ kN$

$$\frac{N}{bh} = \frac{1430 \times 10^3}{250^2} = 22,88$$

FROM DESIGN CHART $\frac{M}{bh^2} = 3,1$

NOW MAX. MOMENT @ ULS :

$$M = \frac{3,1 \times 250 \times 250^2}{10^6} = 48,44\ kNm$$ @ ULS

48,44 kNm @ ULS

DL - 2/3 = 32,29 kNm	LL - 1/3 = 16,15 kNm	ULS
$\frac{32,29}{1,2 \times 1,1}$ = 24,5 kNm	$\frac{16,15}{1,5 \times 1,1}$ = 9,8 kNm	SLS

MAX MOMENT @ SLS = 24,5 + 9,8

= 34,3 kNm @ SLS

→

- VERY SMALL MOM. CAPACITY
- 250 SQUARE PILES VERY RARELY USED FOR BRIDGE FOUNDATIONS

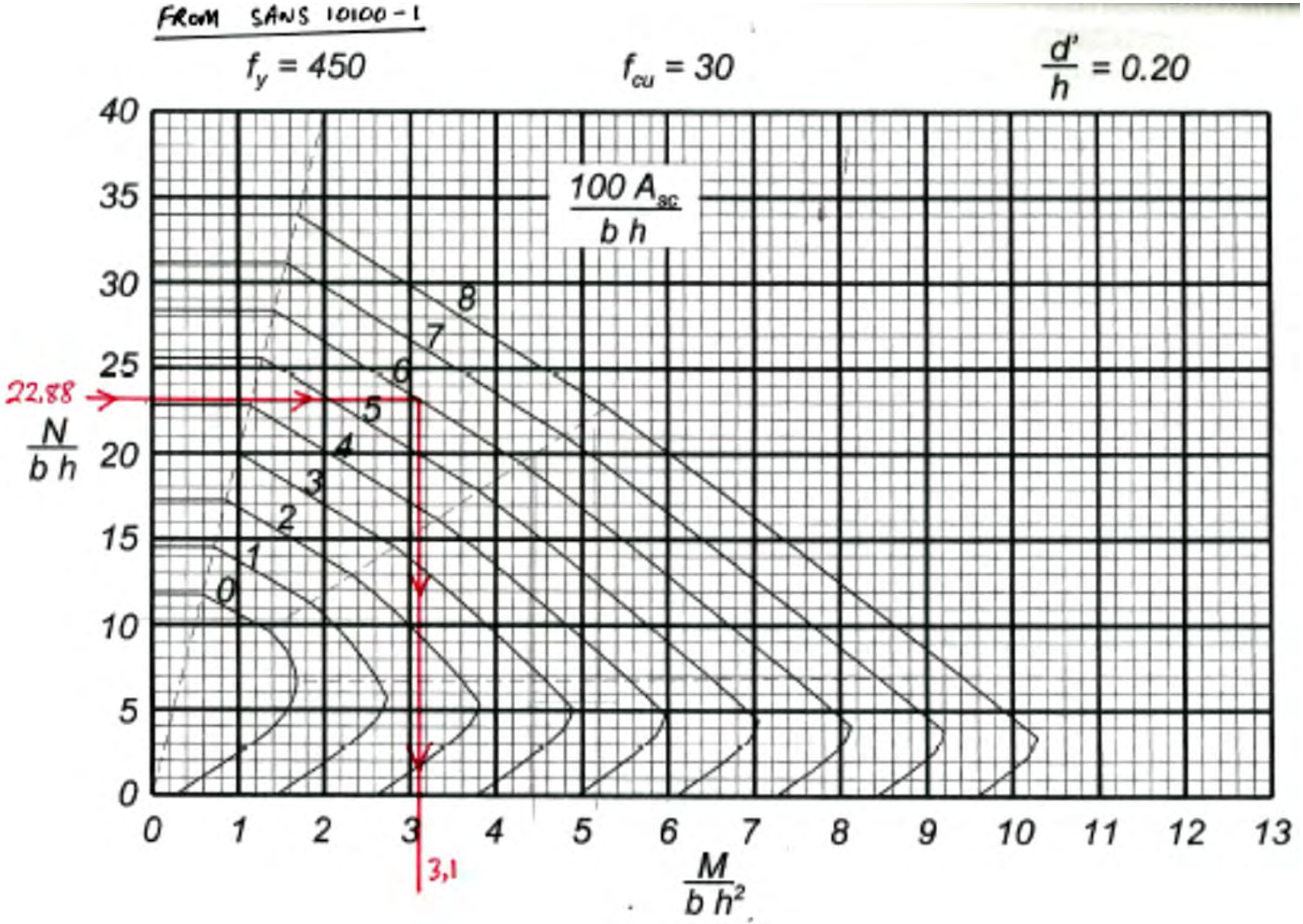
FROM SANS 10100 - 1
$f_y = 450$
$f_{cu} = 30$
$\frac{d'}{h} = 0.20$
$\frac{100\,A_{sc}}{b\,h}$
8
7
6
5
4
3
2
1
0
22,88
$\frac{N}{b\,h}$
3,1
$\frac{M}{b\,h^2}$
0 1 2 3 4 5 6 7 8 9 10 11 12 13
0 5 10 15 20 25 30 35 40

CALCULATION FOR MAXIMUM MOMENT CAPACITY FOR

600 mm ϕ PILE :

MAX A_s = 6% — (BS 5400 PART 4 & SANS)

WORKING LOAD = 1650 kN

1650 kN		
DL - 2/3 1100 kN	LL - 1/3 550 kN	SLS
1100 x 1.2 x 1.1 = 1452 kN	550 x 1.5 x 1.1 = 907,5 kN	ULS

ΣN = 1452 + 907,5 = 2359,5 kN @ ULS

$$\frac{N}{h^2} = \frac{2359,5 \times 10^3}{600^2} = 6,55$$

$\left(\frac{h_s}{h} = 0,90 \text{ & } f_{cu} = 30 \text{ MPa}\right)$ - use THIS CHART FROM CP110 - P3 - 1972 FOR CIRCULAR COLUMNS (see ATTACHED)

FROM CHART :

$$\frac{M}{h^3} = 4,833$$

$$M = \frac{4,833 \times 600^3}{10^6} = 1044 \text{ kNm @ ULS}$$

1044 kNm @ ULS		
DL - 2/3 = 696 kNm	LL - 1/3 = 348 kNm	ULS
$\frac{696}{1,2 \times 1,1}$ = 527,3 kNm	$\frac{348}{1,5 \times 1,1}$ = 211 kNm	SLS

MAX. MOMENT @ SLS = 527,3 + 211 = 738,3 kNm →

$A_c = \frac{\pi h^2}{4}$

A_{sc} = total area of reinforcement

f_{cu} 30
f_y 410
h_s/h 0·90

FROM CP 110 : PART 3 : 1972

Circular columns

Table D-2: Calculation of maximum moment capacity of 254 x 254 x 89 H-section

RESULT SUMMARY - 254x254x89 H-section				
Max moment under working load				
Length (m)	y-y axis (weak)	x-x axis (strong)		
m	kNm	kNm		
2 - 4.71	138,92	285,35		
5	138,92	248,43		
6	76,48	141,4		
7	21,54	55,75		
7,5	5,4	17,98		
INPUT-OUTPUT				
Length: (VARIABLE INPUT)	4	m		
	y-y axis (weak)	x-x axis (strong)		
Max Mu:	138,92	285,35	kNm	(Minimum of Mu1, Mu2 and Mu3)
Cu:	1169,55	kN		(0.3 x fy x A, British Steel Piling Handbook)
CALCULATIONS				
Assumed working load Cu	1169550	N		(0.3 x fy x A, British Steel Piling Handbook)
κ	0			M_{small}/M_{large}
Effective length factor K	2,1			(Contin @supp with lat restr. Lat & tor restr at tip)
w2	1,75			(1.75 + 1.05κ + 0.3κ^2)
Length	4000	mm		(VARIABLE)
Area	1,13E+04	mm^2		(SAISC Red Book)
E	2,00E+05	N/mm^2		(Assumed)
G	7,70E+04	N/mm^2		(SAISC Red Book)
J	1,04E+06	mm^4		(SAISC Red Book)
Cw	7,14E+11			(SAISC Red Book)
w1	0,6			$0.6 - 0.4(M_{small}/M_{large})$
Flange b/t	7,40			Class 1
Web b/t	19,05			Class 1
Yield stress fy	345	N/mm^2		(tf >16mm)
Cr (x-sect)	3508650	N		(0.9 x A x fy)
β	0,8500			(0.6 + 0.4λ ≤ 0.85)
	Weak Axis (y-y)	**Strong Axis (x-x)**		
r	65,2	112		(SAISC Red Book)
Ze	378000	1100000	mm^3	(SAISC Red Book)
I	4,83E+07	1,43E+08	mm^4	(SAISC Red Book)
Mre	119,07	346,5	kNm	(lat support, 0.9*Ze*fy)
Mcr (cantilever)	367,69	632,66	kNm	$\left(\frac{\pi}{KL}\sqrt{EI_yGJ\left(1+\frac{\pi^2EC_w}{(KL)^2GJ}\right)}\right)$
λ (K=1)	0,81	0,47		$\sqrt{\frac{f_y\left(\frac{KL}{r}\right)^2_{max}}{\pi^2E}}$
Cr (buckling)	2505232,24	3194742,51	N	$\left(0.9Af_y(1+\gamma^{2\times1.34})^{-\frac{1}{1.34}}\right)$
Ce	5958773,66	17641917,87	N	$\left(\frac{\pi^2EI}{L^2}\right)$
U1	0,75	0,64		$\left(\frac{\omega_1}{1-\frac{C_u}{C_e}}\right)$
Mu1 (x-sect)	138,92	285,35	kNm	$\left(\frac{C_u}{C_{r(x-sect)}}+\frac{U_1M_u}{M_{re}}=1\right)$
Mu2 (overall)	291,14	402,14	kNm	$\left(\frac{C_u}{C_{r(buckling)}}+\frac{U_1M_u}{M_{re}}=1\right)$
Mu3 (Lat torsional)	308,94	396,83	kNm	$\left(\frac{C_u}{C_{r(buckling)}}+\frac{U_1M_u}{M_{rcr\ (cantilever)}}=1\right)$

Table D-2: Calculation of maximum moment capacity of 356 x 10 pipe section

RESULT SUMMARY - 355.6x10 CHS			
355.6x10 CHS			
Length (m)	Max moment		
m	kNm		
2 - 7	201,1		
8	186,68		
INPUT-OUTPUT			
Length: (VARIABLE)	4	m	
Mu:	201,10	kNm	(Minimum of Mu1, Mu2 and Mu3)
Cu:	1144,5	kN	(0.3 x fy x A, British Steel Piling Handbook)
CALCULATIONS			
Area	1,09E+04	mm^2	(SAISC Red Book)
Ze	9,12E+05	mm^3	(SAISC Red Book)
I	1,62E+08	mm^4	(SAISC Red Book)
J	3,24E+08	mm^4	(SAISC Red Book)
fy	3,50E+02	N/mm^2	(Assumed)
Assumed working load Cu	1144500,00	N	(Based on 0.3 x fy x A, British Steel Piling Handbook)
Effective length factor K	2,1		(Contin @supp with lat restr. Lat & tor restr at tip)
κ	0		M_{small}/M_{large}
w2	1,75		(1.75 + 1.05κ + 0.3κ^2)
Length	4000	mm	(VARIABLE)
w1	0,6		$0.6 - 0.4(M_{small}/M_{large})$
Ce	2,00E+07	N	$\left(\frac{\pi^2 EI}{L^2}\right)$
Mre	287,28	kNm	(0.9*Ze*fy)
U1	0,64		$\left(\frac{\omega_1}{1-\frac{C_u}{C_e}}\right)$
Cr (x-section)	3,43E+06	N	(0.9 x A x fy)
Mu1 (x-section)	201,10	kNm	$\left(\frac{C_u}{C_{r(x-sect)}}+\frac{U_1 M_u}{M_{re}}\right.$
r	122	mm	(SAISC Red Book)
fe	1836,24	kN/mm^2	$\left(\frac{\pi^2 E}{\left(\frac{KL}{r}\right)^2_{max}}, \quad K=1\right)$
λ	0,44		$\left(\sqrt{\frac{f_y}{f_e}}\right)$
Cr (buckling)	3179475,01	N	$\left(0.9Af_y(1+\gamma^{2\times1.34})^{-\frac{1}{1.34}}\right)$
Mu2 (overall)	288,90	kNm	$\left(\frac{C_u}{C_{r(buckling)}}+\frac{U_1 M_u}{M_{re}}=1\right)$
Mcr (cantilever)	10633,13	kNm	$\left(\frac{\pi}{KL}\sqrt{EI_y GJ\left(1+\frac{\pi^2 EC_w}{(KL)^2 GJ}\right)}, \quad C_w=0\right)$
Mu3 (lateral torsional)	6805,57	kNm	$\left(\frac{C_u}{C_{r(buckling)}}+\frac{U_1 M_u}{M_{rcr\,(cantilever)}}=1\right)$

This Appendix provides the assumptions and basic calculations for the pile stresses for the example scenario in Chapter 4 and results shown in Chapter 5.

CALCULATION OF PILE STRESS – REF. TABLE 5-1

250 x 250 PC PILE:

$$\sigma = \frac{My}{I} = \frac{29 \times 125\ (\times 10^6)}{(3,255 \times 10^{-4}) \times 10^{12}} = 11,14\ MPa$$

MAX. PILE $\sigma = 0,4 f_{cu} = 0,4 \times 30 = 12\ MPa$

$\sigma = 11,14\ MPa < \sigma_{max} = 12\ MPa$ ∴ OK! (BUT ON HIGHER END)

H-PILE (STRONG AXIS):

$$\sigma = \frac{My}{I} = \frac{94 \times 10^6 \times 127}{(1,430 \times 10^{-4}) \times 10^{12}} = 83,48\ MPa$$ ∴ ok!

(f_y of STEEL (min) = 300 MPa)

H-PILE (WEAK AXIS):

$$\sigma = \frac{My}{I} = \frac{(31 \times 10^6)(127)}{(0,483 \times 10^{-4}) \times 10^{12}} = 81,51\ MPa < 300\ MPa$$ ∴ ok!

PIPE PILE:

$$\sigma = \frac{My}{I} = \frac{(104 \times 10^6)(178)}{(1,628 \times 10^{-4}) \times 10^{12}} = 113,71\ MPa < 300\ MPa$$ ∴ ok!

APPENDIX F – Derivation of Formulae for the Free and Fixed Headed Pile

Energy Method for Deflection Calculation

In the general case of a member subjected to bending (i.e. a beam):

$$W_{external} = U_{internal}$$

[Conservation of Energy: Work done by external forces equal to internal strain energy]

$$W_{external} = \frac{1}{2} F\Delta$$

[Area under force-displacement curve]

$$U_{internal} = \frac{1}{2}\int_L \frac{M_x^2}{EI} dx$$

[Area under stress-strain curve]

$$\therefore \frac{1}{2} F\Delta = \frac{1}{2}\int_L \frac{M_x^2}{EI} dx$$

$$\therefore F\Delta = \frac{1}{EI}\int_L M_x^2 dx$$

For a pinned cantilever:

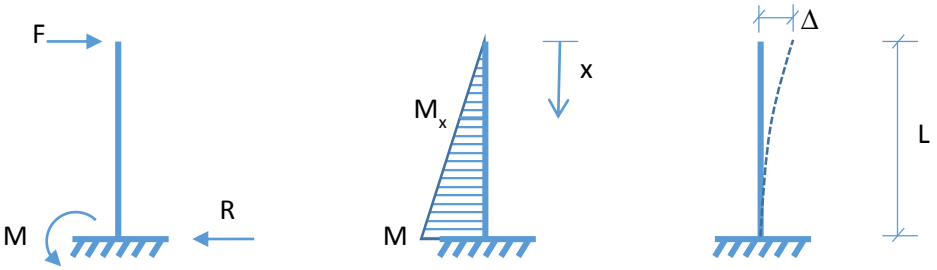

$$M_x = Fx \quad (x \leq L)$$

[Take moments of a top section at x]

$$F\Delta = \frac{1}{EI}\int_L M_x^2 dx$$

[see above]

$$\therefore F\Delta = \frac{1}{EI}\int_L (Fx)^2 dx = \frac{F^2 x^3}{3EI}\Big|_0^L = \frac{F^2 L^3}{3EI}$$

$$\therefore \Delta = \frac{F^2}{F}\frac{L^3}{3EI} = \frac{FL^3}{3EI}$$

For a fixed cantilever:

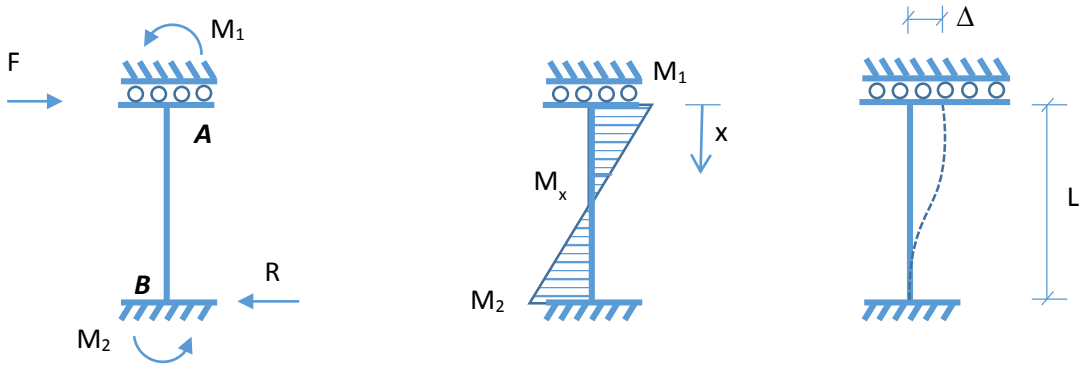

$$\sum F_x = 0 \qquad \text{[Equilibrium]}$$

$$\therefore F = R$$

$$M_1 = M_2 \qquad \text{[Assume, based on symmetry]}$$

$$\sum M_B = 0 \qquad \text{[Equilibrium]}$$

$$\therefore M_1 + M_2 - FL = 0$$

$$\therefore M_1 + M_2 = FL$$

$$\therefore 2M_1 = FL$$

$$\therefore M_1 = \frac{FL}{2}$$

$$\sum M_x = 0 \qquad \text{[Equilibrium]}$$

$$\therefore M_x = Fx - M_1 = Fx - \frac{FL}{2}$$

$$F\Delta = \frac{1}{EI}\int_L M_x^2 dx \qquad \text{[see above]}$$

$$\therefore F\Delta = \frac{1}{EI}\int_L \left(Fx - \frac{FL}{2}\right)^2 dx$$

$$\therefore F\Delta = \frac{1}{EI}\int_L \left(F^2x^2 - F^2Lx + \frac{F^2L^2}{4}\right) dx$$

$$\therefore F\Delta = \frac{1}{EI}\left(\frac{F^2x^3}{3} - \frac{F^2Lx^2}{2} + \frac{F^2L^2}{4}x\right)\Bigg|_0^L$$

$$\therefore F\Delta = \frac{1}{EI}\left(\frac{F^2L^3}{3} - \frac{F^2L^3}{2} + \frac{F^2L^3}{4}\right)$$

$$\therefore F\Delta$$

$$\therefore F\Delta = \frac{1}{EI}\left(\frac{4F^2L^3}{12} - \frac{6F^2L^3}{12} + \frac{3F^2L^3}{12}\right) = \frac{F^2L^3}{12EI}$$

$$\therefore \Delta = \frac{FL^3}{12EI}$$

DERIVATION OF PARTIALLY FIXED PILE CONDITION

δ at head of free-headed pile $= \frac{PL^3}{3EI}$

δ at head of fixed head pile $= \frac{PL^3}{12EI}$

Lets Assume some Average take place between "free" & "fixed" i.e. PARTIALLY FIXED CONDITIONS

$$\text{AVERAGE } \delta = \frac{\delta_{free} + \delta_{fixed}}{2}$$

$$\delta_{AVERAGE} = \frac{\frac{PL^3}{3EI} + \frac{PL^3}{12EI}}{2}$$

SOLVE:

$$\frac{PL^3}{3EI}\left(1 + \frac{1}{4}\right) = \frac{PL^3}{3EI}\left(\frac{5}{4}\right)$$

$$= \frac{5PL^3}{12EI} \times \frac{1}{2}$$

$$\delta_{AVERAGE} = \frac{5PL^3}{24EI}$$ ← PARTIALLY FIXED CONDITIONS

CALCULATION FOR THE EXPECTED RANGE OF MOVEMENT FOR THE BRIDGE DECK IN THE RESULTS SECTION (EXAMPLE). IT IS ASSUMED THAT THE BRIDGE DECK LOCATION IS IN EAST LONDON.

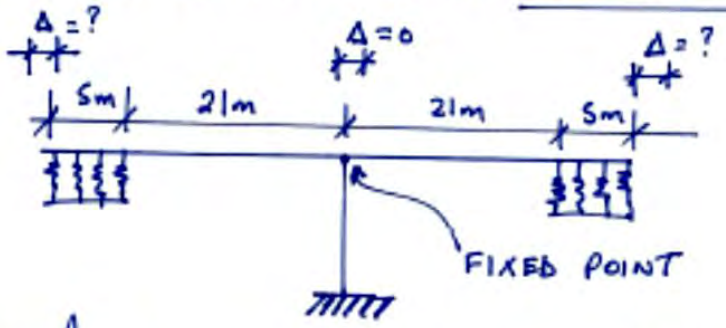

NOTE: AS PER THE LITERATURE THE APPROACH SLAB MUST BE CONSIDERE IN THE CALCULATION:

$\therefore \ell = 21m + 5m = 26m$

FROM FIGURE 20 OF TMH7 (P2) – MINIMUM SHADE AIR TEMPERATURE = −1,075°C

FROM FIG 21 OF TMH7 (P2) — MAXIMUM SHADE AIR TEMP = 49.00°C

FROM TABLE H OF TMH7 (P2) – MINIMUM EFFECTIVE BRIDGE TEMPERATURE = 1,00°C

FROM TABLE 12 OF TMH7 – MAX. EFF. BRIDGE TEMP. = 43,00°C

THEREFORE RANGE = 43 − 1

= 42°C

MOVEMENT RANGE $= (12 \times 10^{-6})(42)(26 \times 10^{3}) = 13,104\ mm$